Department of Theoretical Particle Physics

The Power of Perturbation Series

Author
Gabriele Spada

Supervisors
Prof. Marco Serone
Prof. Giovanni Villadoro

Thesis submitted in fulfillment of the requirements for the degree of Doctor of Philosophy

September 2018

Preface

The present PhD thesis is based on the following papers:

- M. Serone, G. Spada and G. Villadoro, "Instantons from Perturbation Theory," *Phys. Rev.* D **96** (2017) no.2, 021701 arXiv:1612.04376 [hep-th].
- M. Serone, G. Spada and G. Villadoro, "The Power of Perturbation Theory," JHEP **1705** (2017) 056 arXiv:1702.04148 [hep-th].
- M. Serone, G. Spada and G. Villadoro, "$\lambda\phi^4$ Theory I: The Symmetric Phase Beyond NNNNNNNNLO," JHEP **1808** (2018) 148 arXiv:1805.05882 [hep-th].
- M. Serone, G. Spada and G. Villadoro, In preparation.

The research performed by the author during his PhD studies has also led to the following article

- D. Ghosh, P. Paradisi, G. Perez and G. Spada, "CP Violation Tests of Alignment Models at LHCII," JHEP **1602** (2016) 178 arXiv:1512.03962 [hep-ph].

Contents

Chapter 1

Introduction

The vast majority of problems in quantum mechanics (QM) and quantum field theory (QFT) cannot be solved exactly and is usually addressed by means of perturbation theory, i.e. by expanding the equations around a solvable point in the parameter space (usually the free theory). A natural question then arises: Are the series thus obtained convergent? The answer is generically no. As originally pointed out by Dyson [5], in the context of quantum electrodynamics, perturbation series are typically asymptotic with zero radius of convergence. His reasoning, despite being heuristic, unveils a property which is common to the majority of QFTs and quantum mechanical systems. Dyson realized that in general we cannot expect the amplitudes of a theory to be described by functions $\mathcal{Z}(\lambda)$ of the coupling constant λ that are analytic at $\lambda = 0$. In fact, moving λ from a small positive to a small negative value usually makes the Hamiltonian of the system unbounded from below, completely altering the properties of the theory. In the path-integral language, if we write $\mathcal{Z}(\lambda)$ as

$$\mathcal{Z}(\lambda) = \int \mathcal{D}\phi \, G[\phi] \, e^{-S[\phi]/\lambda} \,,$$

with $S[\phi]$ being the Euclidean action, we see that $\lambda = 0$ is a singular point for the function: Taking λ to negative values makes the integrand exponentially enhanced hence making the path integral ill-defined. It is then natural to expect a zero radius of convergence of its Taylor expansion. The asymptotic character of perturbation theory is also suggested by a combinatorial argument: the number of Feynman diagrams at order n typically grows factorially as $n!$ [6, 7]. It was Lipatov [8] who showed, using the saddle-point method, that in scalar QFT the series coefficients c_n indeed grow factorially with the order $c_n \sim n!$. Similarly, the same factorial growth is found in quantum mechanics [9, 10], matrix models [11, 12] and topological strings [13], effectively making the perturbative expansion only an asymptotic series with zero radius of convergence.

There is a well-known resummation procedure due to Borel that allows to find a suitable analytic continuation of an asymptotic series: Basically it consists in taking the Laplace transform of the function obtained by resumming the original series after dividing their terms by a factorially growing coefficient. In special cases, such as the anharmonic oscillator in QM and ϕ^4 theories up to $d = 3$ space-time dimensions, the perturbative expansion turns out to be Borel resummable [14–17]. For the anharmonic oscillator it has been verified that the Borel resummed perturbative series converges to the exact result, available by other numerical methods. Perturbative series associated to more general systems and/or in higher space-time dimensions are typically non-Borel resummable, because of singularities in the domain of inte-

gration. These can be avoided by deforming the contour at the cost of introducing an ambiguity that is non-perturbative in the expansion parameter λ. The ambiguity is expected to be removed by including contributions from semiclassical instanton-like configurations (and all their corresponding series expansion), resulting in an expansion of the form

$$\mathcal{Z}(\lambda) = \sum_{n\geq 0} c_n \lambda^n + \sum_i e^{-A_i/\lambda} \sum_{n\geq 0} c_n^{(i)} \lambda^n$$

usually called transseries. Notice that the terms $e^{-A_i/\lambda}$ cannot be captured by perturbation theory, since their expansion in λ is identically zero. There has been considerable progress in recent years on these issues in the context of the theory of resurgence [18] (see e.g. refs. [19–21] for reviews and further references). A systematic implementation to generic QFT and QM is however not straightforward. A resurgent analysis requires a detailed knowledge of the asymptotic form of the perturbative coefficients, while typically only the leading large-order behaviour of the perturbative expansion might be accessed in generic QFT and QM [8, 22–24]. Besides, the knowledge of the coefficients of the perturbative series alone is not enough to guarantee that the reconstructed transseries reproduces the full answer. Some non-perturbative information is required, such as the knowledge of some analytic properties of the observable as a function of the expansion parameter. Most importantly, the practicality of transseries beyond the weak coupling regime is hindered by the need to resum the series expansion of all the semi-classical configurations that contribute, in general infinite in number.

In this work we will follow a different approach based on the generalization to path integrals of the usual steepest-descent method to evaluate ordinary integrals. For sufficiently regular functions Picard-Lefschetz theory teaches us how to decompose the initial contour of integration into a sum of steepest-descent trajectories (called Lefschetz thimbles, or simply thimbles). A geometric approach to the path integral from this perspective, as well as an excellent introduction for physicists to these ideas, has been given by Witten [25] (see also refs. [26, 27]). The theory of Lefschetz thimbles allows us to rigorously classify which saddle-point configurations contribute to a given physical observable and fixes the form of the transseries.

An interesting question to ask is under what conditions no non-trivial saddle point contributes, so that the whole result is given by the single perturbative series around the trivial saddle-point. In terms of Lefschetz thimbles, this corresponds to the simple situation in which the domain of integration of the path integral does not need any deformation being already a single Lefschetz thimble on its own. In those cases the transseries contains only the perturbative part and, as we will prove, it is Borel resummable to the exact result. This thesis is devoted to finding the answer to the above question in the case of scalar path integrals in $d \leq 3$ and to providing evidence with the explicit resummation of physical observables in many interesting systems. We summarize below the main novel results and outline the structure of the thesis.

Chapter 2. We briefly review the concepts of asymptotic series and Borel resummation and we introduce two methods for approximating the Borel function: the Padé approximants and the conformal mapping. The reader familiar with these concepts may skip this chapter altogether.

Chapter 3. We review the concept of Lefschetz-thimble decomposition for a class of one-dimensional integrals $Z(\lambda)$, viewed as prototypes of the path integrals. The properties of perturbation theory and the role of non-perturbative saddles can be easily understood in this context. We prove here that the saddle-point expansion of a thimble is always Borel resummable to the

exact answer. This result implies that when the decomposition of $Z(\lambda)$ involves trivially only one thimble, its ordinary perturbation theory is also Borel resummable to the whole result. We also show how non Borel resummable problems can be recast in terms of a more general family of Borel resummable problems for which the exact answer is recovered by a single perturbative series. We call this method "exact perturbation theory" (EPT).

Chapter 4. The Borel summability of thimbles is readily extended to multi-dimensional integrals and we discuss in some detail the non trivial generalization to path integrals in QM. In this way we are able to show that QM systems with a bound-state potential and a single non-degenerate critical point—the anharmonic oscillator being the prototypical example—are entirely reconstructable from their perturbative expansion. Namely, for any observable (energy eigenvalues, eigenfunctions, etc.) the asymptotic perturbation theory is Borel resummable to the exact result.[1] At least for the ground state energy, this remains true also for potentials with multiple critical points as long as the absolute minimum is unique. Potentials $V(x;\lambda)$ with more than one critical point are more problematic because not all observables are Borel resummable to the exact result and in general instantons are well-known to contribute. Unfortunately in most situations it is a challenging task to explicitly classify all saddle-points and evaluate the corresponding contributions (see e.g. ref. [28] for a recent attempt). In analogy to the one-dimensional integral we show how to bypass this problem by considering an alternative potential $\hat{V}(x;\lambda,\lambda_0)$ admitting always a Borel resummable perturbation theory in λ and coinciding to the original one for $\lambda_0 = \lambda$. The idea is to choose $\hat{V}$ as the sum of a tree-level and a quantum potential, with the former having only a single critical point. Since the thimble decomposition is controlled only by the saddle point of the tree-level part, the perturbative expansion of $\hat{V}$ (EPT) is guaranteed to be Borel resummable to the exact result. For any value of the coupling constant λ, EPT captures the full result. In contrast, the expansion from V requires in general also the inclusion of instanton contributions, we denote such expansion standard perturbation theory (SPT). We note that a virtue of EPT is that it works surprisingly well at strong coupling, where SPT becomes impractical. Using EPT, we can relax the requirement of having a single critical point in the original potential V, and arrive to the following statement: *In one-dimensional QM systems with a bound-state potential V that admits the $\hat{V}$ defined above, any observable can be exactly computed from a single perturbative series.* We illustrate our results by a numerical study of the following quantum mechanical examples: the (tilted) anharmonic potential, the symmetric double well, its supersymmetric version, the perturbative expansion around a false vacuum, and pure anharmonic oscillators. In all these systems we show that the exact ground state energy, computed by solving the Schrodinger equation, is recovered without the need of advocating non-perturbative effects, such as real (or complex) instantons. We will also show that the same applies for higher energy levels and the eigenfunctions.

Chapter 5. We extend the discussion to QFT, showing that arbitrary n-point correlation functions (Schwinger functions) are Borel reconstructable from their loopwise expansion in a broad class of Euclidean 2d and 3d scalar field theories. These includes basically all UV complete scalar field theories on $\mathbb{R}^d$ with the exception of those with continuously connected degenerate vacua in 2d. The Borel resummed Schwinger functions coincide with the exact

[1] As far as we know, the Borel resummability of observables other than the energy levels has not received much attention in the literature.

ones in a given phase of the theory. If phase transitions occur at some finite values of the couplings, the analysis is more subtle since the analytically continued Schwinger functions may not coincide with the physical ones in the other phase. We discuss these subtle issues for the two-dimensional ϕ^4 theory for which there is spontaneous symmetry breaking of the $\mathbb{Z}_2$ symmetry $\phi \to -\phi$, and we point out that Schwinger functions that are analytically continued from the unbroken to the broken phase correspond to expectation values of operators over a vacuum violating cluster decomposition. The rest of the chapter is devoted to the numerical study of the perturbation series of this theory, where resummation techniques are used for the first time to study the ϕ^4 theory away from criticality. For the unbroken phase of the theory we compute the perturbative series expansions up to 8-th order in the coupling constant of the 0-point and 2-point Schwinger functions. This requires the evaluation of Feynman diagrams up to nine and eight loops for the 0-point and the 2-point functions, respectively, that have been computed using numerical methods. We define, as usual, the physical mass M as the simple pole of the Fourier transform of the 2-point function (at complex values of the Euclidean momenta, corresponding to real Lorentzian momenta) and provide the perturbative series for M^2. Using well-defined resummation procedures we determine the vacuum energy and M for any coupling up to the critical point and we extract the latter as the point at which M vanishes. We also compute the critical exponents ν and η and find good agreement with the theoretically known values. We then emphasize the main differences and analogies between our resummation procedure and those already developed in the literature. Finally we focus on the the much less studied broken phase of the theory. In this phase the perturbative computations involve two types of vertices, cubic and quartic, and the resulting computation is technically more challenging. We show how to define a convenient scheme for the computations and we compute numerically all the diagrams for the 0-, 1-, and 2-point involving up to eight vertices. We also show some preliminary result of the resummation of the vacuum energy as will appear in ref. [4].

Chapter 2

Divergent Perturbation Series

In this chapter we review some basics facts about asymptotic series and introduce the concepts of optimal truncation and Borel resummation, providing some pedagogical examples. In Section 2.3 we present two methods for approximating the Borel function: Padé approximants and the conformal mapping. The latter is presented for both real and complex conjugated singularities.

2.1 Asymptotic Series

A formal power series

$$\sum_{n=0}^{\infty} Z_n \lambda^n \tag{2.1}$$

is said to be asymptotic to the function $Z(\lambda)$ if the remainder after $N+1$ terms of the series is smaller than the last retained term as $\lambda \to 0$, i.e.

$$Z(\lambda) - S_N(\lambda) = \mathcal{O}(\lambda^{N+1}) \,, \quad \text{as} \quad \lambda \to 0 \,, \tag{2.2}$$

where we defined the partial sums $S_N(\lambda)$ as the series truncated to the Nth order

$$S_N(\lambda) = \sum_{n=0}^{N} Z_n \lambda^n \,. \tag{2.3}$$

Notice that different functions can have the same asymptotic expansion (for instance when the difference is suppressed by a factor $e^{-\alpha/\lambda}$), and hence the coefficients of the asymptotic series alone do not uniquely fix the function $Z(\lambda)$. The condition (2.2) implies that the truncation of the series at any finite order provides a controlled approximation to $Z(\lambda)$. In the case of divergent asymptotic series, the partial sums $S_N(\lambda)$ first approach the correct value $Z(\lambda)$ and then, for sufficiently large N, they eventually diverge. Clearly there is a value for $N = N_{\text{Best}}$ that truncates the series in an optimal way, i.e. minimizing the remainder $\Delta_N = Z(\lambda) - S_N(\lambda)$. This procedure is called *optimal truncation*.

The accuracy obtained with this method depends on the behavior of the coefficients Z_n at large n. Suppose that for $n \gg 1$

$$Z_n \sim n! a^n n^c \,, \tag{2.4}$$

for some real parameters a and c,[1] then the optimal number of terms N_{Best} is approximately given by

$$N_{\text{Best}} \approx \frac{1}{|a\lambda|}\,, \tag{2.5}$$

as one can estimate using Stirling formula. The error is asymptotically given by

$$\Delta_{N_{\text{Best}}} \sim e^{-\frac{1}{|a\lambda|}}\,, \tag{2.6}$$

independently of c at leading order. This error is consistent with the intrinsic ambiguity related to asymptotic series discussed above. Keeping more than N_{Best} terms in the asymptotic series would lead to an increase in the error.

Example 2a. Consider the following function

$$Z(\lambda) \equiv \int_0^\infty dt\, e^{-t} \frac{1}{1+\lambda t}\,, \tag{2.7}$$

which has a branch cut for $\lambda \in (-\infty, 0)$. The Taylor expansion of $Z(\lambda)$ is given by $\sum_n^\infty n!(-1)^n\lambda^n$ which agrees with the asymptotic behavior (2.4) with parameters $a = -1$ and $c = 0$. As expected the radius of convergence of the series is zero because the expansion is performed at the singular point $\lambda = 0$. If we want to compute the value of $h(\lambda)$ using optimal truncation at, say, $\lambda = 1/10$, we know from eq. (2.5) that we can retain at most ten terms in the partial sum and the error can be estimated from eq. (2.6) as $e^{-10} \approx 5 \cdot 10^{-5}$. At smaller coupling we can retain more terms in the sum and the resulting accuracy is greater. ▲

2.2 Borel Resummation

A possible way to construct a function with asymptotic expansion of the form (2.1) is via Borel resummation. We define the Borel transform (also called Borel function)

$$\mathcal{B}(t) = \sum_{n=0}^{\infty} \frac{Z_n}{n!} t^n\,, \tag{2.8}$$

which is the analytic continuation of a series with non-zero radius of convergence.[2] In the absence of singularities for $t > 0$ the inverse Laplace transform

$$Z_B(\lambda) = \int_0^\infty dt\, e^{-t} \mathcal{B}(t\lambda) \tag{2.9}$$

defines a function of λ with the same asymptotic expansion as $Z(\lambda)$ and the series (2.1) is said to be Borel resummable. Since, as we mentioned, different functions can admit the same asymptotic series, certain properties of $Z(\lambda)$ and its behavior near the origin have to be assumed to prove that $Z_B(\lambda) = Z(\lambda)$.[3] These requirements are generically hard to verify. On the other

[1] The analysis that follows can easily be generalized for large-order behaviors of the kind $Z_n \sim (n!)^k a^n n^c$. In all the cases considered in this thesis the parameter k is equal to one.

[2] We assumed here that the coefficients Z_n have the large order behavior given by eq. (2.4).

[3] These assumptions have been given by Watson, see e.g. theorem 136, p.192 of the classic book [29], and subsequently improved by Nevanlinna, see ref. [30] for a modern presentation.

hand, in the specific cases where $Z(\lambda)$ is defined as an integral, one might be able to rewrite it directly in the form (2.9), so that the equality $Z_B(\lambda) = Z(\lambda)$ can be proved without the need of verifying the above assumptions. The latter is the approach taken in this work. When $Z_B(\lambda) = Z(\lambda)$ we say that the series (2.1) is Borel resummable to the exact result.

In the following we will be using a generalization of the Borel transform, due to Le Roy, obtained by defining

$$\mathcal{B}_b(\lambda) \equiv \sum_{n=0}^{\infty} \frac{Z_n}{\Gamma(n+1+b)} \lambda^n \,, \tag{2.10}$$

where b is an arbitrary real parameter. The function $Z_B(\lambda)$ now reads

$$Z_B(\lambda) = \int_0^\infty dt\, t^b e^{-t}\, \mathcal{B}_b(\lambda t) \,, \tag{2.11}$$

and clearly $\mathcal{B}_0(t) = \mathcal{B}(t)$. Borel-Le Roy transforms with different b can be related analytically as follows:

$$\begin{aligned} \mathcal{B}_b(t) &= t^{-b}\partial_t^n \left[t^{b+n} \mathcal{B}_{b+n}(t) \right] \,, \qquad n \in \mathbb{N}^+ \\ \mathcal{B}_{b+\alpha}(t) &= \frac{t^{-b-\alpha}}{\Gamma(\alpha)} \int_0^t dt' \, \frac{(t')^b\, \mathcal{B}_b(t')}{(t-t')^{1-\alpha}} \,, \qquad 0 < \alpha < 1 \,. \end{aligned} \tag{2.12}$$

Note that the position of the singularities of two Borel-Le Roy transforms is the same, which implies that Borel summability does not depend on b, though the nature of the singularities might.

The analytic structure of the Borel transform is connected to the large order behavior of the asymptotic series. For example the coefficient a in eq. (2.4) determines the position of the singularity closest to the origin ($\lambda t_\star = 1/a$). If $a < 0$ the series alternates in sign, the singularity is on the negative real axis of t and the series is Borel resummable in the absence of further singularities on the positive real axis. For $a > 0$ the closest singularity is on the real axis and the series is not Borel resummable. In this case a lateral Borel resummation can be defined by slightly deforming the integration contour of eq. (2.9) above or below the singularity. The resulting ambiguity in the choice of the path is of order $e^{-t_\star} = e^{-1/(a\lambda)}$, i.e. $\mathcal{O}(\Delta_{N_{\rm Best}})$. This ambiguity signals the presence of extra non-perturbative contributions to $Z(\lambda)$ not captured by $Z_B(\lambda)$. A systematic way of reconstructing the non-perturbative effects from the perturbative series is the subject of resurgence [18]. As we will see, the large-order behavior of the coefficients Z_n might more generally give rise to poles or branch-cut singularities of $\mathcal{B}_b Z(t)$ at complex values of t. The conclusion is the same as for the case $a < 0$.

Example 2b. The Borel transform of the asymptotic expansion for $Z(\lambda)$ in Example 2a is the geometric series

$$\mathcal{B}(t) = \sum_{n=0}^{\infty} (-1)^n t^n = \frac{1}{1+t} \,.$$

If we apply the inverse Laplace transform in eq. (2.9) we trivially get the definition of the original function: indeed the $Z(\lambda)$ considered in Example 2a was already written in the form (2.9). In this particular case we have $Z_B(\lambda) = Z(\lambda)$.
The same result can be obtained by using the Borel-Le Roy transform in eq. (2.10) with a non-vanishing b. Taking for instance $b = 2$, we get

$$\mathcal{B}_2(t) = \sum_{n=0}^{\infty} \frac{(-1)^n}{(n+2)(n+1)} t^n = t^{-2} \left[(1+t)\log(1+t) - t \right] \,,$$

where we factored out a t^{-2} which cancels against the t^2 in the integral (2.11). Notice that the Borel-Le Roy transform $\mathcal{B}_2 Z(\lambda t)$ has a logarithmic branch point at $t = -1/\lambda$, while $\mathcal{B}Z(\lambda t) = \mathcal{B}_0 Z(\lambda t)$ had a simple pole at that point. We can also check that the two are related by eq. (2.12). Indeed we have

$$\mathcal{B}_0(t) = \partial_t^{(2)} \left[t^2 \mathcal{B}_2(\lambda t)\right] = \partial_t^{(2)} \left[(1+t)\log(1+t) - t\right] = \frac{1}{1+t}\,.$$

▲

2.3 Approximation Methods for the Borel Function

The exact form of $\mathcal{B}(t)$ requires resumming the whole perturbative series. While this is feasible for the simplest examples (e.g. the ordinary functions we will consider in Chapter 3) it is clearly out of reach in the case of QM and QFT observables for which we have only access to a finite number of perturbative terms. It is then necessary to find a way to approximate $\mathcal{B}(t)$ before performing the integral (2.9). If we naively truncate the series (2.8) up to some order N and take the inverse transform term-wise we just get back the original truncated asymptotic expansion. The root of the problem is easy to understand. The large-order behavior (2.4) indicates that the radius of convergence of the series expansion (2.8) is $R = 1/|a|$. On the other hand, $\mathcal{B}(t)$ has to be integrated over the whole positive real axis, beyond the radius of convergence of the series. Obviously

$$\int_0^\infty dt\, e^{-t/\lambda} \sum_{n=0}^{\infty} B_n t^n \neq \sum_{n=0}^{\infty} B_n \int_0^\infty dt\, e^{-t/\lambda} t^n\,. \tag{2.13}$$

Any finite truncation of the series, for which sum and integration commute, would result in the right-hand side of eq. (2.13), i.e. back to the original asymptotic expansion we started from.[4]

There are two possible ways to overcome this difficulty: i) finding a suitable ansatz for $\mathcal{B}(t)$ by matching its expansion with the known perturbative coefficients or ii) manipulating the series to enlarge the radius of convergence over the whole domain of integration. In both cases, by knowing a sufficient number of perturbative orders in the expansion, one can approximate the exact result. We will adopt in the following the Padé-Borel approximants and the conformal mapping methods which are arguably the most used resummation techniques for cases i) and ii), respectively,[5] used to study the anharmonic oscillator in QM and the 2d ϕ^4 theory since refs. [31–35]. In the following we will always use both the methods as a consistency check, i.e. to make sure that the results are not artifacts of the chosen resummation method, however, depending on the number of perturbative terms available, we will privilege one method or the other. In the context of QM (Chapter 4), where the perturbative series can be easily computed up to very high orders, we will mostly use the Padé-Borel method while in the context of QFT (Chapter 5), where we have only a limited number of perturbative terms, we will mostly use the conformal mapping method. In the following two subsections we report some details of these widely used approximation methods, postponing to Section 5.3 our optimization procedures and error estimates for dealing with short perturbation series.

[4] Notice that the integral of the t^n term in eq. (2.13) is dominated by values of $t_0 \approx n\lambda$. As long as $n\lambda \lesssim 1/|a|$, the truncated series reliably computes the first terms in a λ-expansion. For $n\lambda \gtrsim 1/|a|$, the integral is dominated by values of t beyond the radius of convergence of the series, where its asymptotic nature and the fallacy of the expansion become manifest.

[5] We call it Padé-Borel method to emphasize that the approximant is applied to the Borel transform of a function, and not to the function itself.

2.3.1 Padé-Borel Approximants

Given the first $N+1$ terms of a series expansion of a function

$$B(\lambda) = \sum_{n=0}^{N} B_n \lambda^n + \mathcal{O}(\lambda^{N+1}) \,, \tag{2.14}$$

its Padé approximation consists in a rational function of order $[m/n]$

$$B^{[m/n]}(\lambda) = \frac{\sum_{p=0}^{m} c_p \lambda^p}{1 + \sum_{q=1}^{n} d_q \lambda^q} \,, \tag{2.15}$$

with $m+n=N$. The $m+n+1$ coefficients c_p and d_q are determined by expanding eq. (2.15) around $\lambda = 0$ and matching the result up to the λ^N term with eq. (2.14). The Padé approximation method can in principle be used directly to the observable of interest, rather than to its Borel transform. In so doing the results achieved are often less accurate. There is an intuitive explanation for that: Padé approximants are manifestly analytic at $\lambda = 0$, like the Borel functions $\mathcal{B}Z(\lambda)$. In contrast, the point $\lambda = 0$ of $Z(\lambda)$ is necessarily singular. Plugging the Padé approximant (2.15) for the Borel-Le Roy transform (2.10) in eq. (2.11) leads to an approximation of the observable given by

$$Z_b^{[m/n]}(\lambda) = \int_0^\infty dt\, t^b e^{-t} \mathcal{B}_b^{[m/n]}(\lambda t) \,. \tag{2.16}$$

The exact Borel function $\mathcal{B}_b(t)$ is generally expected to have a branch-cut singularity at $t = -1/a$, possible other singularities further away from the origin, and no singularities on the real positive axis. This behavior is typically reproduced by the $[m/n]$ Padé approximants when $m, n \gg 1$: most of the poles and zeros accumulate between the branch points, mimicking the presence of the branch-cut singularities (see for instance Figure 4.3 of Chapter 4). It is known[6] that a sequence of Padé approximants $[m/n]$ with $m, n \to \infty$ free of poles and zeros in a specific region containing the origin, converges uniformly to the analytic continuation of the Taylor series. This guarantees that when we have access to a very large number of perturbative terms, we can accurately reproduce the Borel function by means of sufficiently high-order Padé approximants. Moreover we can explicitly check the convergence of the procedure across the orders, making this method well suited in the case of the quantum mechanical examples of Chapter 4. At low orders, instead, the approximants often show spurious unphysical poles located on the positive real axis, or sufficiently close to it, which give rise to large numerical instabilities. This makes the application of the Borel-Padé method in the context of QFT less straightforward. In Section 5.3 we will explain in detail how we deal with such cases and we provide a method for the estimation of the error..

2.3.2 Conformal Mapping

The conformal mapping method [34, 35] is a resummation technique that uses in a key way the knowledge of the large order behavior (2.4). Suppose that $a < 0$, such that the closest singularity of the Borel function is on the negative real axis. After rescaling $t \to t/\lambda$ so that

$$Z_B(\lambda) = \frac{1}{\lambda^{1+b}} \int_0^\infty dt\, \lambda^b e^{-t/\lambda} \mathcal{B}_b(t) \,, \tag{2.17}$$

[6] A detailed discussion can be found for example in chapter 12 of [36].

the mapping is a clever change of variables of the form[7]

$$t = \frac{4}{|a|}\frac{u}{(1-u)^2}\,, \tag{2.18}$$

with inverse

$$u = \frac{\sqrt{1+|a|t}-1}{\sqrt{1+|a|t}+1}\,. \tag{2.19}$$

When we analytically continue $\mathcal{B}(t)$ in the complex plane, the transformation (2.18) turns into a conformal mapping of the plane into a disk of unit radius $|u| = 1$. In particular, under the mapping, the point at infinity in t and the singularity at $t = -1/|a|$ are mapped at $u = 1$ and $u = -1$, respectively. The branch-cut singularity $t \in [-1/|a|, -\infty]$ is mapped to the boundary of the disc $|u| = 1$. Any other point in the t-complex plane is mapped within the u-unit disc. The integral $t \in [0, \infty]$ turns into an integral in $u \in [0, 1]$. While the series expansion $\mathcal{B}_b(t)$ has radius $R = 1/|a|$ in t, assuming the absence of singularities away from the real axis, the series expansion of $\widetilde{\mathcal{B}}_b(u) \equiv \mathcal{B}_b(t(u))$ has radius $R = 1$ in u, namely it is convergent over the whole domain of integration. Setting for simplicity the Le Roy parameter $b = 0$, we can now rewrite

$$\begin{aligned} Z_B(\lambda) &= \frac{1}{\lambda}\int_0^\infty dt\, e^{-t/\lambda}\sum_{n=0}^\infty B_n t^n = \frac{1}{\lambda}\int_0^1 du\,\frac{dt}{du}e^{-t(u)/\lambda}\sum_{n=0}^\infty B_n t^n(u) \\ &= \frac{1}{\lambda}\int_0^1 du\,\sum_{n=0}^\infty \widetilde{B}_n\frac{dt}{du}e^{-t(u)/\lambda}u^n = \frac{1}{g}\sum_{n=0}^\infty \widetilde{B}_n\int_0^1 du\,\frac{dt}{du}e^{-t(u)/\lambda}u^n\,, \end{aligned} \tag{2.20}$$

where the exchange of the sum with the integral is now allowed. Indeed at large n the asymptotic behavior (2.4) makes the coefficients $\widetilde{B}_n$ polynomially bounded, the series in the next-to-last expression of eq. (2.20) has coefficients that are exponentially bounded (as $e^{-3n^{2/3}/(|a|\lambda)^{1/3}}$) uniformly in u, it is therefore possible to find an integrable function (e.g. a constant) that bounds the series and allows the application of the dominated convergence theorem. The mapping has converted the asymptotic but divergent series in λ into a convergent one. As can be seen from the form of eq. (2.18), the first $N+1$ terms in $\widetilde{B}_n$ are easily computed as linear combinations of the known $N+1$ terms in the original series B_n. At low orders the conformal mapping method is more reliable than the Padé-Borel one since it takes into account the large order behavior of the series (given as input with the position of the singularity) and it does not suffer from the numerical instabilities due to the spurious poles. Therefore it will be the preferred choice in the context of QFT. In Section 5.3 we will also introduce a procedure to estimate the error of the resummation.

We will sometimes encounter Borel functions for which the closest singularities do not lie on the real negative axis but are instead located at some complex conjugated values $t_\pm = \frac{1}{|a|}e^{\pm i\vartheta}$. In those cases we will use the more general change of variables

$$t = \frac{4}{|a|\pi}(\pi-\vartheta)^{1-\frac{\vartheta}{\pi}}\vartheta^{\frac{\vartheta}{\pi}}\frac{u}{(1+u)^2}\frac{(1-u)^{-2\frac{\vartheta}{\pi}}}{(1+u)^{-2\frac{\vartheta}{\pi}}}\,, \tag{2.21}$$

[7]The mapping (2.18) and its inverse (2.19) are often seen as mappings of the coupling constant λ into some other coupling $w(\lambda)$. Since the argument of the Borel function is the product $t\lambda$, one can equivalently redefine λ or t. We prefer the second choice because it makes more manifest the mapping as a change of variables in the integral.

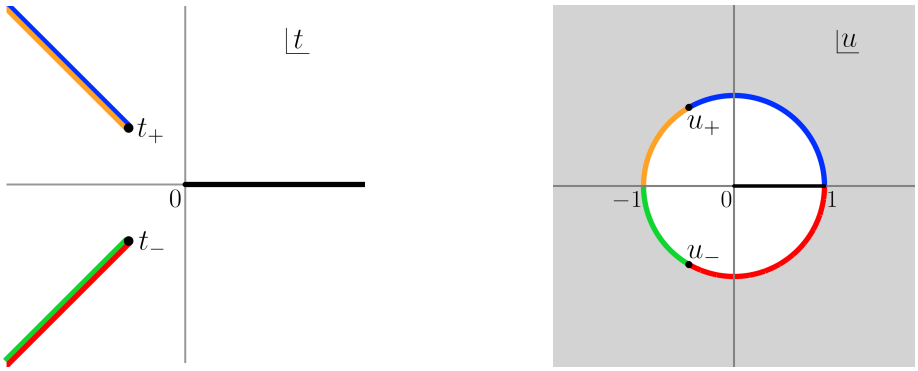

Figure 2.1: The change of variable (2.21) maps the cut t-plane (left panel) into the disk of unit radius $|u| = 1$ (right panel). The branch points $t_\pm$ are mapped into the points $u_\pm$; the real positive axis $t \in [0, +\infty]$ is mapped in the segment $u \in [0, 1]$; the rays connecting the branch points $t_\pm$ to the point at complex infinity are mapped to the arcs at the boundary of the disk as shown by the colors. In drawing this figure we picked $|a| = 1$, $\vartheta = 3\pi/4$.

which maps the singularities of the Borel transform into the unit circle as shown in Figure 2.1. The mapping in eq. (2.18) is recovered in the limit $\vartheta \to \pi$. Note that if the subleading singularities of the Borel function are not aligned with the leading ones, i.e. they do not lie on the rays $re^{\pm i\vartheta}$, $r \in [1/|a|, \infty]$, then with (2.21) they are mapped inside the unit circle and the radius of convergence of the series $\widetilde{\mathcal{B}}_b(u)$ decreases to some value $R < 1$ in u.

Chapter 3

Finite Dimensional Integrals (d=0)

In this chapter we apply Picard-Lefschetz theory to the zero-dimensional prototype of the path integral—i.e. a finite dimensional integral—where a step-by-step analytical study is possible. We start in Section 3.1 by explaining how to deform the contour of integration into a sum of Lefschetz thimbles. We then prove in Section 3.2 that the asymptotic expansion of each thimble is Borel resummable to the whole result. In Section 3.3 we introduce EPT for finite dimensional integrals, the modified perturbative expansion which allows us to recover the full non-perturbative answer from perturbation theory alone. We end in Section 3.4 describing how the large order behavior of the perturbative series is determined by the other saddle points.

3.1 Lefschetz-Thimble Decomposition

Consider the following integral

$$Z(\lambda) \equiv \frac{1}{\sqrt{\lambda}} \int_{-\infty}^{\infty} dx\, g(x)\, e^{-f(x)/\lambda}\,, \tag{3.1}$$

as a one-dimensional prototype of the path-integrals for QM and QFT. We assume that the functions $g(x)$ and $f(x)$, in general complex, are regular and the convergence of the integral for positive values of λ is determined only by $f(x)$.[1] In general g might also present a sufficiently regular dependence on λ. For simplicity, we take f and g to be entire functions of x, though more general cases could be considered.

The perturbative expansion of $Z(\lambda)$ around $\lambda = 0$ corresponds to the saddle-point approximation of the integral (3.1).[2] Since the function f in general has multiple saddle points and each saddle point has its own perturbative expansion, the exact result for $Z(\lambda)$ is recovered by a non-trivial combination of the various saddle-point contributions (properly resummed). We will review in this section the theory describing how to combine the various saddle-points, and discuss in the next one how to exactly resum each expansion.

The idea is to deform the integration contour into a sum of steepest descent paths of the saddle points. As first step we analytically continue the functions f and g in the complex plane

[1] We assume this to be true also for the analytic continuation of the integrand on the complex x-plane, which we will perform soon.

[2] Note that if $g(x)$ is brought to the exponent the saddle points of $f(x) - \lambda \log g(x)$ will be different. The associated saddle-point expansion, however, will not correspond to the original expansion in λ.

$z = x + iy$ and view eq. (3.1) as an open contour integral in z:

$$Z(\lambda) = \frac{1}{\sqrt{\lambda}} \int_{\mathcal{C}_x} dz\, g(z)\, e^{-f(z)/\lambda}, \tag{3.2}$$

where $\mathcal{C}_x$ is the real axis. We call z_σ the saddle points of $f(z)$, i.e $f'(z_\sigma) = 0$. As long as z_σ are isolated and non-degenerate, $f''(z_\sigma) \neq 0$, the contour of steepest-descent passing through z_σ is determined by a flow line $z(u)$ satisfying the first-order equations

$$\frac{dz}{du} = \eta \frac{\partial \overline{F}}{\partial \bar{z}}\,, \qquad \frac{d\bar{z}}{du} = \eta \frac{\partial F}{\partial z}\,, \quad \eta = \pm 1\,, \tag{3.3}$$

where $F(z) \equiv -f(z)/\lambda$ and u is the real line parameter. Unless $z(u) = z_\sigma$ for all u, a non-constant flow can reach z_σ only for $u = \pm\infty$. Using eq. (3.3) one has

$$\frac{dF}{du} = \frac{\partial F}{\partial z}\frac{dz}{du} = \eta \left|\frac{\partial F}{\partial z}\right|^2 . \tag{3.4}$$

The cycles with $\eta = -1$ and $\eta = +1$ are denoted respectively downward and upward flows, since $\mathrm{Re}\, F$ is monotonically decreasing and increasing in the two cases, as eq. (3.4) indicates. Following the notation of ref. [25][3] we denote by $\mathcal{J}_\sigma$ and $\mathcal{K}_\sigma$ the downward and upward flows passing through the saddle point z_σ. Equation (3.4) shows that $\mathrm{Im}\, F$ is constant on both $\mathcal{J}_\sigma$ and $\mathcal{K}_\sigma$. The downward flow $\mathcal{J}_\sigma$ coincides with the path of steepest-descent and when such path flows to $\mathrm{Re}\, F = -\infty$ it is called Lefschetz thimble, or thimble for short. By construction the integral over each thimble is well defined and convergent. When instead the steepest descent path hits another saddle point, the flow splits into two branches and an ambiguity arises. The corresponding integral is said to be on a Stokes line and, as we will see below, some care is required.

Given the absence of singularities on the complex plane, the contour $\mathcal{C}_x$ can be freely deformed to match a combination $\mathcal{C}$ of steepest descent paths keeping the integral (3.2) finite during the deformation:

$$\mathcal{C} = \sum_\sigma \mathcal{J}_\sigma n_\sigma\,. \tag{3.5}$$

By means of the Picard-Lefschetz theory the integer coefficients n_σ are given by

$$n_\sigma = \langle \mathcal{C}_x, \mathcal{K}_\sigma \rangle\,, \tag{3.6}$$

where $\langle \mathcal{C}_x, \mathcal{K}_\sigma \rangle$ denote the intersection pairings between the original contour $\mathcal{C}_x$ and the upward flows $\mathcal{K}_\sigma$ and we used the fact that $\mathcal{J}_\sigma$ and $\mathcal{K}_\sigma$ are dual to each other:

$$\langle \mathcal{J}_\sigma, \mathcal{K}_\tau \rangle = \delta_{\sigma\tau}\,. \tag{3.7}$$

The original integral (3.1) is then reduced to a sum of integrals along the thimbles $\mathcal{J}_\sigma$,

$$Z(\lambda) = \sum_\sigma n_\sigma Z_\sigma(\lambda)\,, \tag{3.8}$$

where

$$Z_\sigma(\lambda) \equiv \frac{1}{\sqrt{\lambda}} \int_{\mathcal{J}_\sigma} dz\, g(z)\, e^{-f(z)/\lambda}\,. \tag{3.9}$$

[3] We refer the reader to Section 3 of this paper for a more extensive introduction to Lefschetz thimbles.

Contrary to the naive expectation that the contour of integration should be deformed to pass through *all* (complex and real) saddles of f, only the subset of saddles with $n_\sigma \neq 0$ must be considered.

In the presence of a flow connecting two saddle points z_σ and z_τ, we have $\mathcal{J}_\sigma = \mathcal{K}_\tau$ and the corresponding intersection $\langle \mathcal{J}_\sigma, \mathcal{K}_\tau \rangle$ is not well defined. This problem can be avoided by taking λ to be complex, modifying in this way the flow curves, that implicitly depend on λ. The initial integral is then recovered in the limit $\mathrm{Im}\,\lambda \to 0$. When $Z(\lambda)$ is not on a Stokes line the intersection numbers n_σ in eq. (3.5) are unambiguous in such limit. On a Stokes line instead some of the n_σ are discontinuous and the decomposition (3.5) is different in the two limits $\mathrm{Im}\,\lambda \to 0^{\pm}$, yet the same $Z(\lambda)$ is recovered in the two cases.

Two choices of f are particularly interesting for the discussion of path integrals in QM and QFT: f purely imaginary (corresponding to the real-time path integral) and f real (corresponding to the Euclidean path integral). In the first case the integration cycle $\mathcal{C}_x$ is not a Lefschetz thimble (the imaginary part is not constant) and the decomposition (3.5) is non-trivial. On the contrary, in the second case f has at least one real saddle and $\mathcal{C}_x$ coincides with one or more steepest descent paths (being $\mathrm{Im}\,F = 0$). If the real saddle is unique, all others being complex, the real axis is a thimble and $\mathcal{C} = \mathcal{C}_x$. In presence of more real saddles $Z(\lambda)$ is on a Stokes line and the decomposition (3.5) requires an analytic continuation.

The quantum mechanical path integral generalization of this result implies an important difference between Minkoswki and Euclidean times. While in the former we expect in general a very complicated Lefschetz thimble decomposition (3.5) with an infinite number of saddles contributing, in the latter there is a class of theories where the original integration domain is already a thimble and eq. (3.5) is not necessary. For this reason we will focus on real functions f and correspondingly we will consider Euclidean path integrals.

In the following we illustrate the above discussion by considering two explicit examples, one for the Euclidean version (Example 3a) and one for the Minkowskian version (Example 3b) of our path-integral prototype (3.1).

Example 3a. We consider here the Euclidean case of a real function

$$f(x,m) = \frac{1}{2} m\, x^2 + \frac{1}{4} x^4\,, \qquad g(x) = 1\,, \tag{3.10}$$

which corresponds to the zero-dimensional reduction of the anharmonic oscillator for $m > 0$, the pure anharmonic oscillator for $m = 0$ and the symmetric double well for $m < 0$. The resulting function $Z(\lambda, m)$ is analytic in m and can be written as

$$Z(\lambda,m) = \begin{cases} \sqrt{\frac{m}{2\lambda}} e^{\frac{m^2}{8\lambda}} K_{\frac{1}{4}}\left(\frac{m^2}{8\lambda}\right) & m > 0\,, \\ \frac{\Gamma(1/4)}{\sqrt{2}}\, \lambda^{-1/4} & m = 0\,, \\ \sqrt{\frac{-m\pi^2}{4\lambda}} e^{\frac{m^2}{8\lambda}} \left[I_{-\frac{1}{4}}\left(\frac{m^2}{8\lambda}\right) + I_{\frac{1}{4}}\left(\frac{m^2}{8\lambda}\right)\right] & m < 0\,, \end{cases} \tag{3.11}$$

where K_n and I_n are the modified Bessel functions.

Consider first the case with $m > 0$, which, as we will see, is not on a Stokes line for λ real and positive. The function $f(z,m)$ has three saddle points: $z_0 = 0$, $z_\pm = \pm i\sqrt{m}$. For real λ the upward flows from the saddle z_0 hit the two saddles $z_\pm$. This can be avoided by giving a small imaginary part to λ as is shown in Figure 3.1 (first row) for positive (left) and negative (right)

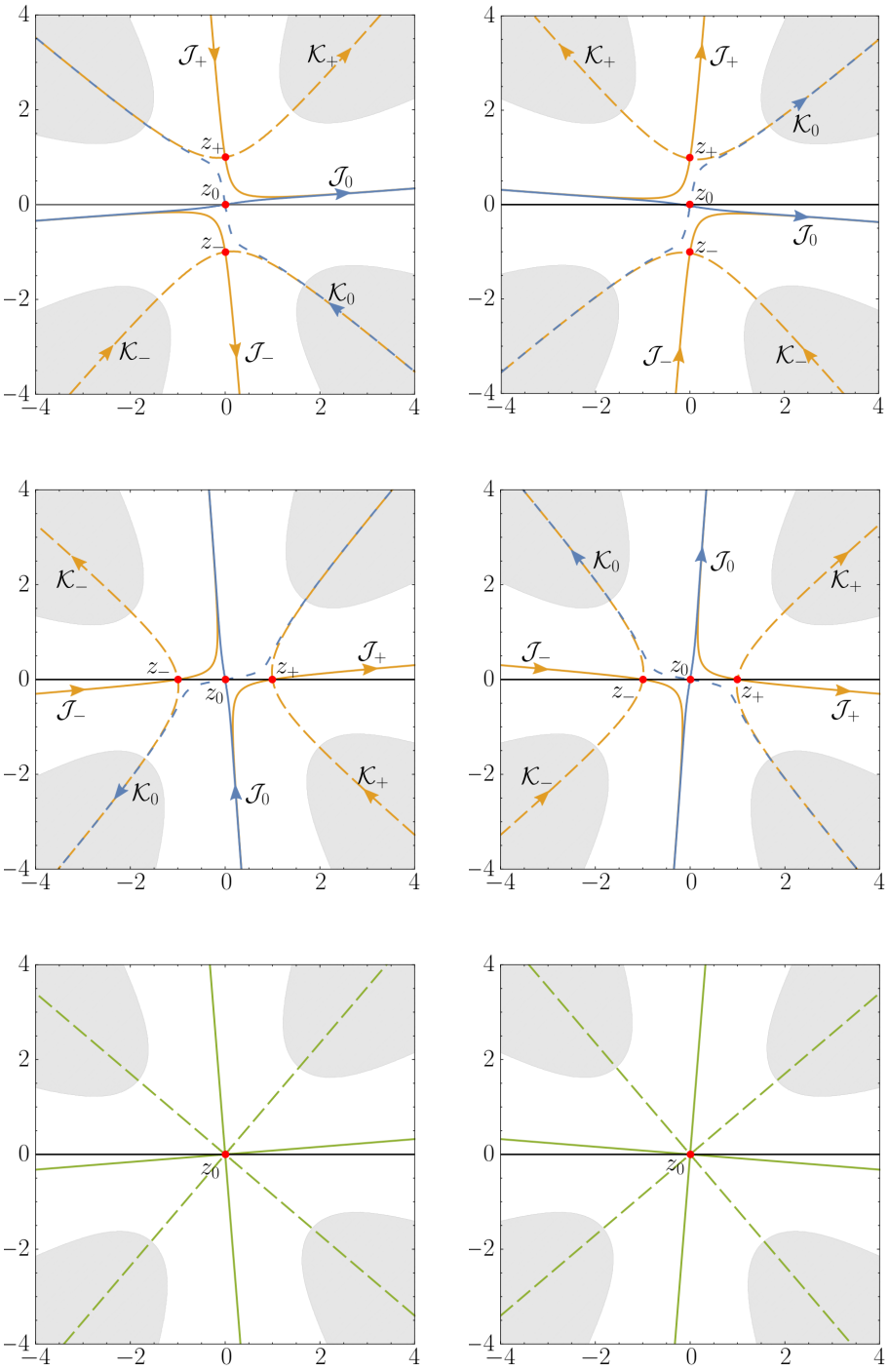

Figure 3.1: Downward and upward flows in the z plane associated to the functions $f(z,1)$ (upper panels), $f(z,-1)$ (middle panels) and $f(z,0)$ (lower panels) of Example 3a. The grey sectors correspond to the asymptotic regions where the integral diverges. The red points are the saddles of the functions $f(z,m)$. Continuous and dashed lines denote downward and upward flows, respectively. The lower panels correspond to the degenerate case, where multiple downward and upward flows depart from a saddle point. We have taken $\mathrm{Re}\,\lambda = 1$, $\mathrm{Im}\,\lambda > 0$ (left panels) and $\mathrm{Im}\,\lambda < 0$ (right panels).

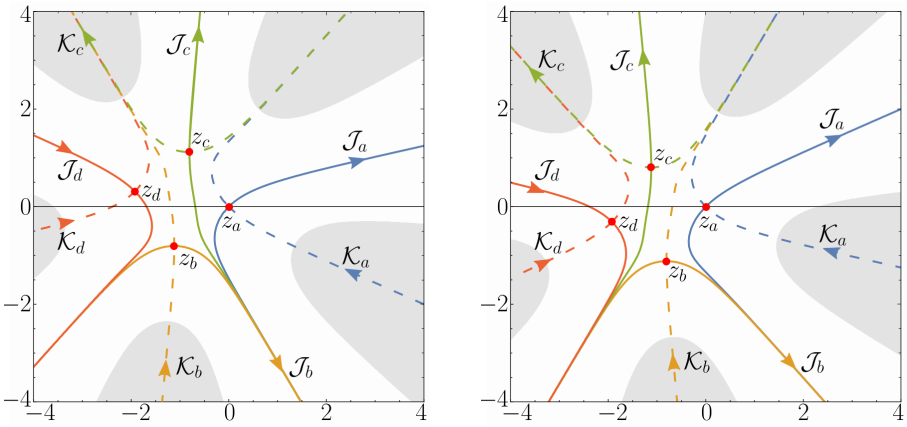

Figure 3.2: Downward and upward flows in the z plane associated to the function $f(z)$ of Example 3b. The grey sectors correspond to the asymtptotic regions where the integral diverges. The original integration path on the real axis lies at the boundary of two convergence regions, making the integral oscillatory rather than absolutely convergent. The red points are the saddles of the function $f(z)$. Continuous and dashed lines denote downward and upward flows, respectively. We have taken $\mathrm{Re}\,\lambda = 1$, $\mathrm{Im}\,\lambda > 0$ (left panel) and $\mathrm{Im}\,\lambda < 0$ (right panel).

values of $\mathrm{Im}\,\lambda$. The white regions are those where the integral is asymptotically convergent; by definition, the thimbles (continuous curves) start and end in these regions. The upward flows (dashed curves) instead start and end in the grey regions where the integrand diverges. Notice that the intersection numbers of the upward flows $\mathcal{K}_\sigma$ with the integration contour are the same in the two cases $\mathrm{Im}\,\lambda \lessgtr 0$ ($n_0 = 1$, $n_\pm = 0$). Therefore, the decomposition (3.5) is not ambiguous, $\mathcal{C}_x$ coincides with a single thimble and we are not on a Stokes line.

When $m < 0$ the integral is on a Stokes line for real positive λ, since the saddle points are all on the real axis ($z_0 = 0$, $z_\pm = \pm\sqrt{-m}$). As before the upward flows from z_0 hit the other two saddles $z_\pm$, but now the intersection numbers jump across $\mathrm{Im}\,\lambda = 0$ ($n_0 = \pm 1$, $n_\pm = 1$), as can be seen in Figure 3.1 (second row). Depending on the sign of $\mathrm{Im}\,\lambda$ the decomposition (3.5) reads

$$\begin{aligned} \mathcal{C}_+ &= \mathcal{J}_- - \mathcal{J}_0 + \mathcal{J}_+ \,, \qquad && \mathrm{Im}\,\lambda > 0 \,, \\ \mathcal{C}_- &= \mathcal{J}_- + \mathcal{J}_0 + \mathcal{J}_+ \,, \qquad && \mathrm{Im}\,\lambda < 0 \,. \end{aligned} \tag{3.12}$$

The integrals over the two paths $\mathcal{C}_\pm$ coincide when $\mathrm{Im}\,\lambda \to 0$, as manifest from the figure.

For $m = 0$ the only saddle point at $z_0 = 0$ is degenerate (i.e. $f''(0) = 0$) and multiple upward and downward flows depart from z_0 as illustrated in Figure 3.1 (third row). The decomposition rules (3.5) do not apply and analytic continuation of the parameter λ does not help. One possible way to use saddle point techniques is to define the case $m = 0$ as the limit $m \to 0$ of the previous cases, where the three saddle points $z_{0,\pm}$ collide. An alternative way will be described in Section 3.3. ▲

Example 3b. Consider now the Minkowskian case in which the function $f(x)$ is purely imaginary

$$f(x) = -i\left(\frac{x^2}{2} + \frac{x^3}{2} + \frac{x^4}{4} + \frac{x^5}{20}\right) , \qquad g(x) = 1 \,, \tag{3.13}$$

and the resulting integral (3.1) is oscillatory. The function $f(z)$ has two real saddle points, $z_a = 0$ and $z_d = -2$, and two complex ones, $z_b = -1 - i$ and $z_c = -1 + i$. For real λ we have

that the upward flow $\mathcal{K}_b$ coincides with the downward flow $\mathcal{J}_c$. This can be avoided by giving a small imaginary part to λ as is shown in Figure 3.2 for positive (left) and negative (right) values of $\operatorname{Im}\lambda$. Similarly to the case of Example 3a with $m > 0$ the intersection numbers of the upward flows $\mathcal{K}_\sigma$ with the integration contour are the same in the two cases $\operatorname{Im}\lambda \lessgtr 0$ and the decomposition (3.5) is unambiguously determined as

$$\mathcal{C} = \mathcal{J}_d + \mathcal{J}_b + \mathcal{J}_a \,. \tag{3.14}$$

Notice that in this case *all* the real saddles contribute together with *one* of two the complex saddles. This situation is clearly more difficult to handle than the Euclidean version since the decomposition is non-trivial even when original integral is not on a Stokes line. ▲

3.2 Borel Summability of Thimbles

We saw in Section 3.1 that the integral $Z(\lambda)$ can be decomposed into a sum of integrals over thimbles $Z_\sigma(\lambda)$. We will show now that each of these integrals admits an asymptotic expansion which is Borel resummable to the exact result.

Consider the following change of variable [37, 38]:

$$t = \frac{f(z) - f(z_\sigma)}{\lambda} \,. \tag{3.15}$$

Recalling eq. (3.4), we see that for any value of z along $\mathcal{J}_\sigma$ the variable t is real and non-negative. For each value of $t \neq 0$, there are two values $z_{1,2}(\lambda t) \in \mathcal{J}_\sigma$ satisfying eq. (3.15): one for each of the two branches of the downward flow. We take z_1 and z_2 to be along and opposite to the direction of the thimble. After this change of variable we get

$$Z_\sigma(\lambda) = e^{-f(z_\sigma)/\lambda} \int_0^\infty dt\, t^{-1/2}\, e^{-t} B_\sigma(\lambda t)\,, \quad B_\sigma(\lambda t) \equiv \sqrt{\lambda t}\left(\frac{g(z_1(\lambda t))}{f'(z_1(\lambda t))} - \frac{g(z_2(\lambda t))}{f'(z_2(\lambda t))}\right). \tag{3.16}$$

For small t's, we can expand $f(z) - f(z_\sigma) \propto z^2$ (recall that $f''(z_\sigma) \neq 0$) giving $f'(z_{1,2}(t)) \propto \sqrt{t}$ so that $B_\sigma(\lambda t)$ is analytic in the origin.[4] The reader may recognize eq. (3.16) as the Laplace transform of the Borel-Le Roy resummation formula (2.11) with

$$B_\sigma(\lambda t) = \mathcal{B}_{-1/2,\sigma}(\lambda t)\,. \tag{3.17}$$

In particular the coefficients of the expansion of $B_\sigma(\lambda)$ around the origin are related to those of $Z_\sigma(\lambda)$ by $B_\sigma^{(n)} = Z_\sigma^{(n)}\Gamma(n + 1/2)$. The function $B_\sigma(\lambda t)$ is analytic on the whole semipositive real t axis given the regularity of $f(z)$ and $g(z)$ and the absence of other saddle points for $f(z)$ along the thimble. This proves that the power series of $Z_\sigma(\lambda)$ is Borel resummable. Not only, but having been able to rewrite the integral directly in terms of a Borel transform of the associated asymptotic expansion, we are guaranteed that the Borel resummation reproduces the full function $Z_\sigma(\lambda)$.

The original integral (3.1) can then be computed using eq. (3.8) and Borel resummation of the perturbative expansion of the Z_σ's given in eq. (3.16). The contribution associated to the trivial saddle (i.e. the one with the smallest $f(z_\sigma)$) can be seen as the perturbative contribution

[4] Note that even if $f''(z_\sigma) = 0$ the function $B_\sigma(\lambda t)$ can still be defined in such a way to stay analytic in the origin by rescaling it for a different power of t. In particular, if $f(z(t)) - f(z_\sigma) \propto z^n$, with $n > 2$, we have $f'(z_{1,2}(t)) \propto t^{1-1/n}$.

to $Z(\lambda)$, while the other saddles can be interpreted as non-perturbative effects. When only one saddle contributes, the perturbative contribution is Borel resummable to the exact result. When more saddles contribute, the perturbative expansion, although Borel resummable, does not reproduce the full result. If $Z(\lambda)$ is on a Stokes line some of the perturbative expansions of the thimbles are not Borel resummable. This is due to singularities of the Borel function induced by the presence of other saddles in the steepest descent path ($f'(z_{1,2}(\lambda t)) = 0$ for $z \neq z_\sigma$).

Example 3c. We illustrate the results above in the case of the real function $f(x, m)$ defined in Example 3a. We start with the case $m > 0$ and, without loss of generality, set $m = 1$. The original integration path coincides with the thimble $\mathcal{J}_0$, the only one that contributes, and the perturbative expansion is expected to be Borel resummable to the exact result. The coefficients $Z^{(m=1)}_{\sigma=0,n}$ of the perturbative expansion of $Z(\lambda, 1)$ read

$$Z^{(1)}_{0,n} = \sqrt{2}(-)^n \frac{\Gamma(2n + \frac{1}{2})}{n!}\,. \tag{3.18}$$

For large n we have

$$Z^{(1)}_{0,n} = (-4)^n \frac{\Gamma(n)}{\sqrt{\pi}} \left(1 + \mathcal{O}\Big(\frac{1}{n}\Big)\right). \tag{3.19}$$

The Borel-Le Roy transform (2.10) with $b = -1/2$ gives

$$\mathcal{B}^{(1)}_{-1/2,0}(\lambda t) = \sqrt{\frac{1 + \sqrt{1 + 4\lambda t}}{1 + 4\lambda t}}\,, \tag{3.20}$$

which presents a branch-cut singularity in the t-plane at $\lambda t_\star = -1/4$ but it is regular on the positive real axis. By integrating over t one reproduces the exact result (3.11):

$$\int_0^\infty dt\, t^{-\frac{1}{2}} e^{-t} \mathcal{B}^{(1)}_{-1/2,0}(\lambda t) = \frac{1}{\sqrt{2\lambda}} e^{\frac{1}{8\lambda}} K_{\frac{1}{4}}\Big(\frac{1}{8\lambda}\Big) = Z(\lambda, 1)\,. \tag{3.21}$$

In this simple case we can also explicitly solve for the change of variable (3.15):

$$z_{1,2}(\lambda t) = \pm\sqrt{\sqrt{1 + 4\lambda t} - 1}\,, \tag{3.22}$$

and check the validity of eq. (3.17). The form of $\mathcal{B}^{(1)}_{b,0}$ depends on the value of b. For instance, the standard Borel function $\mathcal{B}^{(1)}_{0,0}$ associated to eq. (3.18) equals

$$\mathcal{B}^{(1)}_{0,0}(\lambda t) = \sqrt{\frac{8}{\pi}} \frac{K\Big(\frac{-1+\sqrt{1+4\lambda t}}{2\sqrt{1+4\lambda t}}\Big)}{(1 + 4\lambda t)^{1/4}}\,, \tag{3.23}$$

where $K(x)$ is the complete elliptic integral of the first kind. One can check that eq. (3.23) is in agreement with eq. (3.20) using the formula (2.12). We also see, as mentioned, that the position of the singularity of $\mathcal{B}^{(1)}_{0,0}$ and $\mathcal{B}^{(1)}_{-1/2,0}$ is the same.

The integral with $m < 0$ is more interesting because $Z(\lambda, m)$ has a non-trivial thimble decomposition and is on a Stokes line. As we discussed, this is avoided by taking complex values of λ. Depending on the sign of $\mathrm{Im}\,\lambda$ the two distinct decompositions in eq. (3.12) are

generated. Setting $m = -1$ for simplicity and factoring out $e^{-f(z_\sigma)/\lambda}$ from each $Z_\sigma^{(m=-1)}(\lambda)$, the coefficients of the perturbative expansions read

$$Z_{\pm,n}^{(-1)} = \frac{\Gamma\left(2n+\frac{1}{2}\right)}{n!}\,, \qquad Z_{0,n}^{(-1)} = iZ_{0,n}^{(1)}\,. \tag{3.24}$$

The Borel-Le Roy transform (2.10) with $b = -1/2$ gives

$$\mathcal{B}_{-1/2,\pm}^{(-1)}(\lambda t) = \sqrt{\frac{1+\sqrt{1-4\lambda t}}{2(1-4\lambda t)}}\,, \qquad \mathcal{B}_{-1/2,0}^{(-1)}(\lambda t) = i\mathcal{B}_{-1/2,0}^{(1)}(\lambda t)\,. \tag{3.25}$$

The Borel-Le Roy functions $\mathcal{B}_{-1/2,\pm}^{(-1)}$ have a branch-cut singularity in the t-plane at $t = 1/(4\lambda)$ and for real positive λ the asymptotic series with coefficients $Z_{\pm,n}^{(-1)}$ are not Borel resummable. However, the small imaginary part in λ needed to avoid the Stokes lines would also allow us to avoid the singularity that now moves slightly below or above the real t axis for $\operatorname{Im}\lambda$ respectively positive or negative. We are effectively performing a lateral Borel summation. After integrating over t we get

$$\begin{aligned} Z_{\pm}^{(-1)}(\lambda) &= \operatorname{sign}(\operatorname{Im}\lambda)\,\frac{ie^{\frac{1}{8\lambda}}}{2\sqrt{\lambda}}K_{\frac{1}{4}}\Big(-\frac{1}{8\lambda}\Big)\,, \\ Z_{0}^{(-1)}(\lambda) &= iZ_0^{(1)}(\lambda)\,. \end{aligned} \tag{3.26}$$

Using eq. (3.12), the sum of the three contributions in the limit $\operatorname{Im}\lambda \to 0$ gives

$$\sqrt{\frac{\pi^2}{4\lambda}}e^{\frac{1}{8\lambda}}\left[I_{-\frac{1}{4}}\left(\frac{1}{8\lambda}\right) + I_{\frac{1}{4}}\left(\frac{1}{8\lambda}\right)\right] = Z(\lambda,-1)\,. \tag{3.27}$$

Notice that the discontinuity of the intersection number $n_0 = -\operatorname{sign}(\operatorname{Im}\lambda)$ as $\operatorname{Im}\lambda \to 0$ fixes the ambiguity in the lateral Borel resummation of the perturbative series around the saddles $z_\pm$. ▲

3.3 Exact Perturbation Theory

We have seen in the previous sections how integrals of the form (3.1) can exactly be computed combining properly resummed saddle-point contributions. In particular, for real functions f, eq. (3.5) is trivial or not depending on the number of real saddles of f. We will explain in this section that the decomposition (3.5) in terms of thimbles can be modified. This implies that even when f has more real saddles we can trivialize eq. (3.5) so that $Z(\lambda)$ is reproduced by a saddle-point expansion around one (perturbative) saddle only. This observation will play a crucial role when considering QM, since the computation of the intersection numbers (3.6) is far from trivial in the path integral case.

The Lefschetz thimble decomposition associated to the integral (3.1) is governed by the saddle points of f and in particular it is independent of the prefactor $g(x)$. Define the function

$$\hat{Z}(\lambda,\lambda_0) \equiv \frac{1}{\sqrt{\lambda}}\int_{-\infty}^{\infty} dx\, e^{-\hat{f}(x)/\lambda}\hat{g}(x,\lambda_0)\,, \tag{3.28}$$

where

$$\hat{f}(x) \equiv f(x) + \delta f(x)\,, \qquad \hat{g}(x,\lambda_0) \equiv g(x)e^{\delta f(x)/\lambda_0}\,, \tag{3.29}$$

are regular functions of x that satisfy the same conditions as $f(x)$ and $g(x)$, in particular[5] $\lim_{|x|\to\infty} \delta f(x)/f(x) = 0$. The original integral is recovered by setting $\lambda_0 = \lambda$:

$$\hat{Z}(\lambda, \lambda) = Z(\lambda)\,. \tag{3.30}$$

From the point of view of the saddle-point expansion in λ at fixed λ_0, the function δf inside $\hat{f}$ is a "classical" modification of f, while the factor of δf in $\hat{g}$ is a "quantum" deformation. At fixed λ_0, the thimble decomposition of the integral (3.28) is determined by the downward and upward flows associated to the saddle points $z_{\hat{\sigma}}$ of $\hat{f}$ and not to the original saddles z_σ of f. By properly choosing the function δf, we can generally construct a function $\hat{f}$ with only one real saddle x_0 (for convenience chosen such that $\hat{f}(x_0) = 0$) that trivializes the thimble decomposition to $\mathcal{C} = \mathcal{C}_x$. While $Z(\lambda)$ may lie on a Stokes line, so that its perturbation theory is non-Borel resummable and requires extra non-perturbative contributions, the asymptotic expansion of $\hat{Z}(\lambda, \lambda_0)$ in λ at fixed λ_0 will be Borel-resummable to the exact result $\hat{Z}(\lambda, \lambda_0)$. Setting then $\lambda = \lambda_0$ allows us to derive the original function $Z(\lambda_0)$.

We call the series expansion of $\hat{Z}(\lambda, \lambda_0)$ in λ at fixed λ_0 "exact perturbation theory" (EPT), while we call the ordinary expansion of $Z(\lambda)$ "standard perturbation theory" (SPT). Note that in general SPT includes both perturbative and non-perturbative saddles.

Example 3d. We illustrate the method by reconsidering the Example 3a with $m = -1$, where the contour decomposition (3.12) required three different saddle-point contributions. Consider the choice

$$\delta f(x) = x^2\,, \tag{3.31}$$

so that

$$\hat{f}(x) = \frac{1}{2}x^2 + \frac{1}{4}x^4 = f(x, 1)\,, \qquad \hat{g}(x, \lambda_0) = \exp\Big(\frac{x^2}{\lambda_0}\Big)\,. \tag{3.32}$$

The thimble decomposition is now determined by $f(x, 1)$, in which case we know that $\mathcal{C}_x$ coincides with a thimble. The coefficients of the corresponding perturbative expansion read

$$\hat{Z}_n(\lambda_0) = \sqrt{2}(-)^n \frac{\Gamma(2n + \frac{1}{2})}{n!} {}_1F_1\Big(-n, \frac{1}{2} - 2n; -\frac{2}{\lambda_0}\Big)\,, \tag{3.33}$$

where ${}_1F_1(a, b; z)$ is the Kummer confluent hypergeometric function. At any fixed λ_0, the Kummer function for $n \gg 1/\lambda_0^2$ asymptotes to $\exp(-1/\lambda_0)$ and for large n we have

$$\hat{Z}_n(\lambda_0) \approx e^{-\frac{1}{\lambda_0}} (-4)^n \frac{\Gamma(n)}{\sqrt{\pi}} \left(1 + \mathcal{O}\Big(\frac{1}{n}\Big)\right)\,, \tag{3.34}$$

where the size of the $\mathcal{O}(1/n)$ subleading terms depends on λ_0. The Borel resummation of the perturbative series gives

$$\hat{\mathcal{B}}_{-1/2}(\lambda t, \lambda_0) = \sum_{n=0}^{\infty} \frac{\hat{Z}_n(\lambda_0)}{\Gamma(n + 1/2)} (\lambda t)^n\,. \tag{3.35}$$

Recovering the formula for the Borel transform from this equation is non-trivial. We can however use eq. (3.16) to get

$$\hat{\mathcal{B}}_{-1/2}(\lambda t, \lambda_0) = \mathcal{B}^{(1)}_{-1/2,0}(\lambda t)\; e^{\frac{\sqrt{1+4\lambda t}-1}{\lambda_0}}\,, \tag{3.36}$$

[5] It is possible that this condition might be relaxed to some extent. It would be interesting to further analyze this point and try to find necessary and sufficient conditions for $\delta f(x)$.

where $\mathcal{B}^{(1)}_{-1/2,0}$ is the Borel-Le Roy function associated to the $m = 1$ case, given in eq. (3.20). As expected, no singularities are present on the positive real t axis. By taking $\lambda_0 = \lambda$ and performing the integral over t one reproduces the exact result for $Z(\lambda, -1)$ given in eq. (3.11):

$$\hat{Z}(\lambda, \lambda) = \int_0^\infty dt\, t^{-\frac{1}{2}} e^{-t} \hat{\mathcal{B}}_{-1/2}(\lambda t, \lambda) = Z(\lambda, -1)\,. \tag{3.37}$$

▲

The above considerations are easily extended to more general functions $f(x)$. In particular, for polynomial functions of degree $2n$, independently of the location of the $2n-1$ saddle points and of the corresponding thimble decomposition associated to $f(z)$, we can always construct a function $\hat{f}(z)$, for example $\hat{f}(z) = z^2 + f^{(2n)}(0) z^{2n}/(2n)!$, which has only one real saddle point and a trivial thimble decomposition. Notice that the choice of allowed $\delta f(x)$ is arbitrary and all of them are equally good.

Interestingly enough, the method above provides also an efficient way to study degenerate cases with $f''(z_\sigma) = 0$, where perturbation theory is ill-defined. Instead of deforming the function $f(z)$, e.g. by adding a small quadratic term ϵz^2, and of analyzing the integral in the limit $\epsilon \to 0$, we can more simply consider an appropriate function $\delta f(z)$ that removes the degeneracy, bypassing the need of taking a limit.

Example 3e. Consider Example 3a with $m = 0$ and choose

$$\delta f(x) = \frac{x^2}{2}\,, \tag{3.38}$$

so that

$$\hat{f}(x) = \frac{1}{2}x^2 + \frac{1}{4}x^4 = f(x, 1)\,, \qquad \hat{g}(x, \lambda_0) = e^{\frac{x^2}{2\lambda_0}}\,. \tag{3.39}$$

Since this case corresponds to the previous one with $m = -1$ via the rescaling $\lambda_0 \to 2\lambda_0$, the Borel resummation of the perturbative expansion is simply given by $\hat{\mathcal{B}}_{-1/2}(\lambda t, 2\lambda_0)$, with $\hat{\mathcal{B}}_{-1/2}$ given in eq. (3.36). Taking $\lambda_0 = \lambda$ and performing the integral over t, one reproduces the exact result

$$\int_0^\infty dt\, t^{-\frac{1}{2}} e^{-t} \mathcal{B}_{-1/2} \hat{Z}(\lambda t, 2\lambda) = \frac{\Gamma(1/4)}{\sqrt{2}}\, \lambda^{-1/4}\,. \tag{3.40}$$

▲

3.4 The Asymptotic behavior from Semiclassics

The saddle-points, whether or not they contribute to the integral (3.1), dictate the large-order behavior of the series expansion of adjacent saddles. In QM this method has been first used[6] by Bender and Wu in ref. [10] and extended to QFT by Lipatov [8] (see also refs. [22–24] for early extensive studies). For the specific case of finite-dimensional integrals a more rigorous derivation can be found in refs. [37, 38], where an exact resurgent formula relating the asymptotic series of different saddles has been derived. It has been shown in ref. [37] that the leading large order behavior of the coefficients $Z_{\sigma,n}$ is governed by other saddles close to z_σ. More precisely, consider the integral (3.9) as a function of $\lambda = |\lambda| \exp(i\theta)$. The thimble $\mathcal{J}_\sigma(\theta)$ moves in the

[6] A similar method was already used in 1964, see ref. [39]. We thank Arkady Vainshtein for drawing our attention to his work.

complex z-plane as θ is varied. For the special values of θ where the thimble crosses other saddle points the integral is on a Stokes line. These saddles are called "adjacent" to z_σ. Among the adjacent saddles, we denote by z_{σ_0} the leading adjacent saddle as the one with the smallest value of $|f(z_{\sigma_0}) - f(z_\sigma)|$. Modulo an overall phase, the large-order behavior of $Z_{\sigma,n}$ is given by the lowest-order coefficient $Z_{\sigma_0,0}$ of the series associated to the leading adjacent saddle z_{σ_0} [37]:

$$Z_{\sigma,n} = \sum_{z_{\sigma_0}} Z_{\sigma_0,0} \frac{(n-1)!}{(f(z_{\sigma_0}) - f(z_\sigma))^n} \left(1 + \mathcal{O}\Big(\frac{1}{n}\Big)\right) , \tag{3.41}$$

where $Z_{\sigma_0,0} = g(z_{\sigma_0})/\sqrt{2\pi|f''(z_{\sigma_0})|}$ and the sum is present in case we have more than one saddle with the same minimal value of $|f(z_{\sigma_0}) - f(z_\sigma)|$. Equation (3.41) justifies and generalizes our working assumption (2.4) which was valid only for real values of $f(z_{\sigma_0}) - f(z_\sigma)$. Matching the two equations we get

$$a = \frac{1}{f(z_{\sigma_0}) - f(z_\sigma)} , \qquad c = -1 . \tag{3.42}$$

As we mentioned, the coefficient a dictates the location of the leading singularities (i.e. the ones closest to the origin) of the Borel function $\mathcal{B}Z(t)$. For real functions f with more than one saddle on the real axis the expansion around a minimum z_σ gives a real and positive, in agreement with the non-Borel summability of an asymptotic expansion on a Stokes line.[7] It is clear from eq. (3.41) that in general the Borel function can have leading singularities for complex values of its argument, as anticipated in Section 2.2.[8]

The n-dependence of the leading large-order behavior is governed by the function $f(z)$ and is independent of $g(z)$, the latter entering only in the determination of the overall normalization of the coefficients. For EPT this implies that at fixed λ_0, the n-dependence of the leading large order behavior of $\hat{Z}_n(\lambda_0)$ does not depend on λ_0. More precisely we have, using eq. (3.41),

$$\hat{Z}_n(\lambda_0) \approx \sum_{z_0} Z_{z_0,0} \frac{(n-1)!}{(\hat{f}(z_0) - \hat{f}(x_0))^n} \left(1 + \mathcal{O}\left(\frac{1}{n}\right)\right) , \qquad Z_{z_0,0} = e^{\frac{\delta f(z_0)}{\lambda_0}} \frac{g(z_0)}{\sqrt{2\pi|\hat{f}''(z_0)|}} , \tag{3.43}$$

where z_0 are the leading adjacent saddles associated to the (unique) real saddle x_0 and $Z_{z_0,0}$ is the leading order term of the series associated to z_0. Given the above choice of $\hat{f}(z)$, the factor $\hat{f}(z_0) - \hat{f}(x_0)$ in eq. (3.43) is always either complex or real negative, so that no singularities appear in the positive real t axis of $\mathcal{B}\hat{Z}(t)$. Equation (3.43) is valid at fixed λ_0 for parametrically large values of n. More specifically we need $n \gg 1$ and $n \gg 1/\lambda_0^2$ in order to suppress the contributions coming from the higher-order coefficient terms $Z_{z_0,1}$, $Z_{z_0,2}, \ldots$ associated to the leading adjacent saddle series $Z_{z_0,n}$. The large-order behavior (3.34) is immediately reproduced using eq. (3.43).

[7] The argument is valid also when the real saddle entering eq. (3.42) is not the leading adjacent one, in which case the singularity in the positive real t axis will still appear, though it will not be the closest to the origin.

[8] In the case of two complex conjugated singularities the large order behavior predicted by eq. (3.41) is $Z_{\sigma,n} \sim |a|^n \cos(n\vartheta)(n-1)!$ where $\vartheta = \operatorname{Arg} a$. This implies that the coefficient of the series at large order oscillate in sign with period $2\pi/\vartheta$.

Chapter 4

Path Integral of Quantum Mechanics (d=1)

We extend here the results obtained in the previous chapter to case of path integrals in QM. As a first step, we generalize in Section 4.1 the proof of Borel summability of thimbles to the multidimensional case. We then discuss in Section 4.2 the non-trivial generalization to path integrals in QM. In this way we are able to show that QM systems with a bound-state potential and a single non-degenerate critical point are entirely reconstructable from their perturbative expansion. In Section 4.3 we introduce EPT in QM which allows us to generalize the result by relaxing the requirement of a single critical point. In Section 4.4 we illustrate our results by a numerical study of the following quantum mechanical examples: the (tilted) anharmonic potential, the symmetric double well, its supersymmetric version, the perturbative expansion around a false vacuum, and pure anharmonic oscillators.

4.1 Higher Dimensional Integrals

The analysis of the one-dimensional integral (3.1) performed in Chapter 3 can be extended to n-dimensions. Interpreting the domain of integration as an n-dimensional cycle $\mathcal{C}_{\boldsymbol{x}} = \mathbb{R}^n$ in n complex dimensions (with coordinates $\boldsymbol{z}$), like in eq. (3.2), downward and upward flows can be defined generalizing eq. (3.3). For each saddle $\boldsymbol{z}_\sigma$, the Lefschetz thimble $\mathcal{J}_\sigma$ and its dual cycle $\mathcal{K}_\sigma$ are obtained by taking the union of all the down- and up- ward flows. As for the 1-dimensional case possible Stokes lines can be avoided by taking λ complex. After decomposing the cycle $\mathcal{C}_{\boldsymbol{x}}$ in terms of thimbles, like in eq. (3.5), we are left with the evaluation of integrals of the type

$$Z_\sigma(\lambda) = \lambda^{-n/2} \int_{\mathcal{J}_\sigma} d\boldsymbol{z}\, g(\boldsymbol{z})\, e^{-f(\boldsymbol{z})/\lambda}\,, \tag{4.1}$$

with f and g regular functions and such that the integral is convergent for any positive λ. By construction the function f has only one non-degenerate saddle $\boldsymbol{z}_\sigma$: $\boldsymbol{\nabla} f(\boldsymbol{z}_\sigma) = 0$ with $\det[\partial_i \partial_j f(\boldsymbol{z}_\sigma)] \neq 0$. Repeating the same steps as for the one-dimensional case and using known results from Morse theory, we can prove that the formal series expansion for $Z_\sigma(\lambda)$ around $\lambda = 0$ is Borel resummable to the exact result. Indeed performing the change of variables

$$t = \frac{f(\boldsymbol{z}) - f(\boldsymbol{z}_\sigma)}{\lambda}\,, \tag{4.2}$$

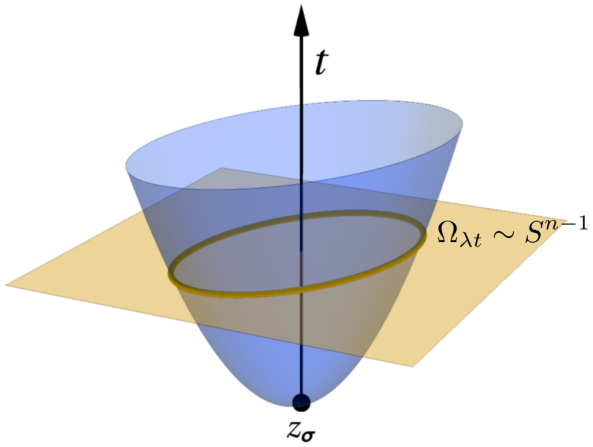

Figure 4.1: The support of integration $\Omega_{\lambda t}$ of the Borel function in n dimensions with topology S^{n-1} is the section of the thimble identified by the constraint (4.2).

we have (see also refs. [38, 40, 41])

$$\begin{aligned} Z_\sigma(\lambda) &= e^{-f(\boldsymbol{z}_\sigma)/\lambda} \int_0^\infty dt\, t^{n/2-1}\, e^{-t}\, B_\sigma(\lambda t)\,, \\ B_\sigma(\lambda t) &\equiv (\lambda t)^{1-n/2} \int_{\mathcal{J}_\sigma} d\boldsymbol{z}\, g(\boldsymbol{z})\, \delta[f(\boldsymbol{z}) - f(\boldsymbol{z}_\sigma) - \lambda t]\,. \end{aligned} \tag{4.3}$$

The integral in $B_\sigma(\lambda t)$ has support over the $(n-1)$-dimensional hypersurface $\Omega_{\lambda t}$, defined by the constraint $f(\boldsymbol{z}) = f(\boldsymbol{z}_\sigma) + \lambda t$ (see Figure 4.1). In the neighborhood of the minimum $\boldsymbol{z}_\sigma$ the hypersurface $\Omega_{\lambda t}$ has the topology of a compact $n-1$ dimensional sphere S^{n-1}.[1] Theorems from Morse theory (see e.g. ref. [42]) guarantee that this will continue to be true for any t as long as no other critical point of $f(\boldsymbol{z})$ is met, which is true for thimbles away from Stokes lines. Moreover, since $\boldsymbol{\nabla} f(\boldsymbol{z}) \neq \boldsymbol{0}$ for $\boldsymbol{z} \neq \boldsymbol{z}_\sigma$, it follows that the integral defining $B_\sigma(\lambda t)$ is finite for any value of $t > 0$. Similarly to the one-dimensional case, for $t \to 0$ one has $\boldsymbol{\nabla} f(\boldsymbol{z}) = \mathcal{O}(t^{1/2})$. Taking into account the λt dependence from the volume form we see that $B_\sigma(\lambda t)$ is analytic in the whole semipositive real axis including the origin. We conclude that the power series of $Z_\sigma(\lambda)$ in λ is Borel resummable to the exact result and $B_\sigma(t) = \mathcal{B}_{n/2-1} Z_\sigma(t)$. Depending on whether n is even or odd, the first relation in eq. (2.12) allows us to rewrite Borel and $b = -1/2$ Borel-Le Roy transforms as simple derivatives of the formula above, namely

$$\begin{aligned} \mathcal{B}_0 Z_\sigma(t) &= \partial_t^{k-1} \int_{\mathcal{J}_\sigma} d\boldsymbol{z}\, g(\boldsymbol{z})\, \delta[f(\boldsymbol{z}) - f(\boldsymbol{z}_\sigma) - t]\,, \qquad n = 2k\,, \\ \mathcal{B}_{-1/2} Z_\sigma(t) &= \sqrt{t}\, \partial_t^k \int_{\mathcal{J}_\sigma} d\boldsymbol{z}\, g(\boldsymbol{z})\, \delta[f(\boldsymbol{z}) - f(\boldsymbol{z}_\sigma) - t]\,, \qquad n = 2k+1\,. \end{aligned} \tag{4.4}$$

4.2 The Lefschetz Thimble Approach to the Path Integral

We are now ready to discuss path integrals in QM. Consider

$$\mathcal{Z}(\lambda) = \int \mathcal{D}x(\tau)\, G[x(\tau)] e^{-S[x(\tau)]/\lambda}\,, \tag{4.5}$$

[1] In one dimension S^{n-1} reduces to two points, which were denoted by z_1 and z_2 in eq. (3.16).

with τ the Euclidean time. The action S is of the form

$$S[x] = \int d\tau \left[\frac{1}{2}\dot{x}^2 + V(x)\right], \tag{4.6}$$

where the potential $V(x)$ is assumed to be an analytic function of x, with $V(x) \to \infty$ for $|x| \to \infty$, so that the spectrum is discrete. In analogy to the finite dimensional cases the functionals $S[x]$ and $G[x]$ are regular and such that the path integral is well-defined for any $\lambda \geq 0$. The measure $\mathcal{D}x$ includes a λ-dependent normalization factor to make $\mathcal{Z}(\lambda)$ finite. The integration is taken over real $x(\tau)$ configurations satisfying the boundary conditions of the observable of interest.

By definition the path integral is the infinite dimensional limit of a finite dimensional integral, namely eq. (4.5) means

$$\mathcal{Z}(\lambda) = \lim_{N\to\infty} \int \mathcal{D}^{(N)}x(\tau)\, G^{(N)}[x(\tau)] e^{-S^{(N)}[x(\tau)]/\lambda}, \tag{4.7}$$

where the limit is now explicit and $G^{(N)}[x(\tau)]$, $S^{(N)}[x(\tau)]$, $\mathcal{D}^{(N)}x(\tau)$, are discretized versions of the functionals G and S and of the path integral measure, which includes the factor $\lambda^{-N/2}$. Such limit can be twofold: The continuum limit, always present, and the infinite time limit, relevant for the extraction of certain observables. The former is not expected to generate problems in QM, since after having properly normalized the path integral all quantities are finite in this limit. The infinite time limit could instead be more subtle and we will discuss later when it may lead to troubles. For the moment we restrict our analysis to path integrals at finite time so that the limit in eq. (4.7) only refers to the continuum one.

Similarly to the finite dimensional case, the first step is to identify all the (real and complex) saddles $z_\sigma(\tau)$ (the solutions of the equations of motion) of the action $S[x]$ and to construct the analogue of the upward and downward flows from each $z_\sigma(\tau)$. Given the infinite dimensional nature of the path integral, the number of saddles is also infinite. In general a systematic analysis and computation of all the relevant flows and intersection numbers is impractical. In specific cases, however, only a few real saddle point solutions exist and we may hope to reconstruct the full answer from a finite set of saddle point expansions. In particular, if the equations of motion admit only one real solution, the domain of the integration (all real paths satisfying the boundary conditions) coincides with a thimble. We will now show that such path integral (and similarly any path integral over thimbles) admits a perturbation theory which is Borel resummable to the exact result.

The integral inside the limit in eq. (4.7) is finite dimensional and can now be treated as before, in particular we can rewrite it using eqs. (4.3) and (4.4) as

$$\begin{aligned} \mathcal{Z}(\lambda) &= \lim_{N\to\infty} e^{-\frac{S^{(N)}[x_0(\tau)]}{\lambda}} \int_0^\infty dt\, t^{-1/2} e^{-t} \mathcal{B}^{(N)}_{-1/2}\mathcal{Z}(\lambda t) \\ \mathcal{B}^{(N)}_{-1/2}\mathcal{Z}(\lambda t) &= \sqrt{\lambda t}\, \partial^N_{\lambda t} \int \mathcal{D}^{(N)}_{\lambda=1}x(\tau)\, G^{(N)}[x(\tau)]\, \delta[S^{(N)}[x(\tau)] - S^{(N)}[x_0(\tau)] - \lambda t], \end{aligned} \tag{4.8}$$

where for definiteness we discretized the path integral into a $2N+1$ dimensional one and $\mathcal{D}^{(N)}_{\lambda=1}x(\tau)$ is the discretized measure without the λ dependence (i.e. with $\lambda = 1$). The regularity of the functionals S and G and the absence of other real saddle points allow a choice of discretization for which the Borel-Le Roy function $\mathcal{B}^{(N)}_{-1/2}\mathcal{Z}(\lambda t)$ is finite and integrable for any N. In QM the absence of divergences in the continuum limit strongly suggests that the exchange

of the limit with the integral in the first line of eq. (4.8) can be performed safely. The function $\mathcal{B}^{(\infty)}_{-1/2}\mathcal{Z}(\lambda t)$ will then correspond to the Borel-Le Roy transform in the continuum limit, which will be integrable and will reproduce the full result $\mathcal{Z}(\lambda)$. As a check we verified the finiteness of $\mathcal{B}^{(\infty)}_{-1/2}\mathcal{Z}(\lambda t)$ at $\lambda t = 0$ (which reproduces the known results for the harmonic oscillator) as well as at any order in λt in polynomial potentials (see Appendix A).

We are then led to the following

Result 4A (Trivial Decomposition)**.** *If the action $S[x(\tau)]$ has only one real saddle point $x_0(\tau)$ satisfying the boundary conditions implicit in eq. (4.5), such that $\det S''[x_0(\tau)] \neq 0$, then no thimble decomposition is needed and the formal series expansion of $\mathcal{Z}(\lambda)$ around $\lambda = 0$, corresponding to the saddle point expansion of the path integral, is Borel resummable to the exact result.*

If the action $S[x]$ admits one real saddle only, in general it will admit several (or an infinite number of) complex saddles (or complex instantons). All these complex instantons, however, do *not* contribute to the path integral. Analogously to the finite-dimensional cases, whenever more than one real saddle point with finite action satisfying the boundary conditions of the path integral exists, the perturbative series generically will not be Borel resummable, as a result of the Stokes phenomenon.

Boundary conditions determine the number of real saddle points of S and hence are of crucial importance to check the validity of our working assumption. As a result the same theory may have some observables that are Borel resummable to the exact result and some for which the perturbative series requires the inclusion of non-perturbative effects. It might be useful to illustrate the point with an example. Consider a QM system with an (inverted) potential like the one depicted in Figure 4.2 and define

$$\mathcal{W}(\lambda, \beta, x_0) = \int_{x(\beta/2)=x(-\beta/2)=x_0} \mathcal{D}x(\tau)\, e^{-S[x(\tau)]/\lambda} = \sum_k |\psi_k(x_0;\lambda)|^2 e^{-\beta E_k(\lambda)}\,, \tag{4.9}$$

where $E_k(\lambda)$ and $\psi_k(x;\lambda)$ are the eigenvalues and the eigenfunctions of the system, respectively. Depending on x_0, the action S admits one or more real saddle points. For instance, for $x_0 > x_2$ only one real solution exist. For $x_0 < x_2$ depending on β one or more real solutions are allowed.

The partition function is related to $\mathcal{W}(\lambda, \beta, x_0)$ by

$$\mathcal{Z}(\lambda, \beta) = \int_{-\infty}^{\infty} dx_0\, \mathcal{W}(\lambda, \beta, x_0) = \sum_n e^{-\beta E_n(\lambda)}\,, \tag{4.10}$$

which corresponds to summing over all real periodic trajectories and it is not Borel resummable.

We now discuss the infinite β limit, which is relevant for the extraction of some observables such as the properties of the ground state (eigenvalue, eigenfunction, ...). Unlike the continuum limit, the large-β limit generically does not commute with the thimble decomposition. There are cases where the path integral admits more than one real saddle at finite β but only one survives at $\beta \to \infty$. There are other cases instead where only one real saddle exists for any finite β but the path integral lies on a Stokes line at $\beta = \infty$.

Consider for instance the ground state energy

$$E_0(\lambda) = -\lim_{\beta\to\infty} \frac{1}{\beta} \log \mathcal{Z}(\lambda, \beta)\,. \tag{4.11}$$

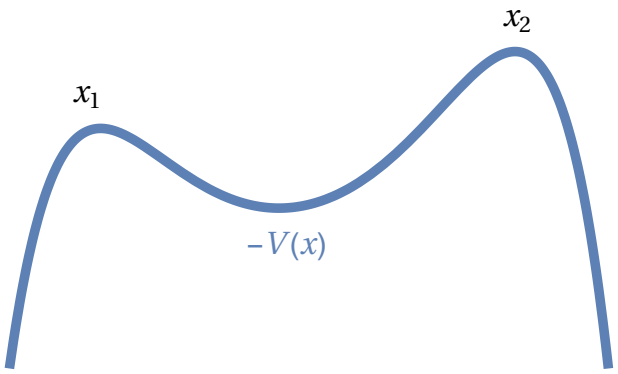

Figure 4.2: Sketch of a bounded (inverted) potential with more than one critical point.

For the example of tilted double-well potential discussed before, $\mathcal{Z}(\lambda, \beta)$ has multiple real saddles for any finite β, corresponding to solutions of the equations of motion with period β. Besides the trivial one, $x(\tau) = x_2$, the leading saddle corresponds to the solution $x(\tau) = x_1$, which is suppressed by a factor $e^{-\beta[V(x_1)-V(x_2)]/\lambda}$. Therefore in the limit $\beta \to \infty$ only the thimble associated to the true minimum gives a non-vanishing contribution. The perturbative series for E_0 is then Borel resummable to the full answer, though $\mathcal{Z}(\lambda, \beta)$ at finite β is not. This result is more manifest if we use the alternative formula

$$E_0(\lambda) = -\lim_{\beta\to\infty} \frac{1}{\beta} \log \mathcal{W}(\lambda, \beta, x_2)\,. \tag{4.12}$$

Since $\mathcal{W}(\lambda, \beta, x_2)$ has only one saddle ($x(\tau) = x_2$) for any β, the Borel summability of $E_0(\lambda)$ follows trivially from our analysis.[2]

The same discussion applies for any bound-state potential with a unique global minimum. When the minimum is not unique generically the perturbative series of E_0 is not Borel resummable because in the large β limit an infinite number of saddles with finite action are present, independently of the functional $\mathcal{W}$ used. This is also true if the degeneracy of the absolute minimum is lifted at the quantum level, i.e. $V(x_1) - V(x_2) = \mathcal{O}(\lambda)$, as it will become more clear below. We will discuss in more detail the properties of the Borel transform of E_0 for the different cases in Section 4.4.

The analysis is particularly simple for potentials $V(x)$ that have a single non-degenerate critical point (minimum). Without loss of generality we take it to be at the origin with $V(0) = 0$. Indeed, independently of the boundary conditions, there is always a single real saddle point both at finite and infinite β. Since our considerations apply for any allowed choice of the functional $G[x]$ in eq. (4.5) we are led to argue that perturbative series of any observable is Borel resummable to the exact result. By *any observable* we mean any path integral with regular boundary conditions and analytic functions of them, such as partition functions, energy eigenvalues, eigenfunctions, etc. In this way we recover in a simple and intuitive way known results [14, 15, 31] on the Borel summability of the energy spectrum of a class of anharmonic potentials and extend them to more general QM systems and observables.

[2] The Borel summability of $\mathcal{W}(\lambda, \beta, x_2)$ for any β and its explicit form (4.9) suggest that the same conclusion should hold for the rest of the spectrum.

4.3 Exact Perturbation Theory

Interestingly enough, the method of Section 3.3 can easily be extended to the QM path integral (4.5). Suppose we can split the potential $V = V_0 + \Delta V$ into the sum of two potentials V_0 and ΔV such that[3]

1. V_0 has a single non-degenerate critical point (minimum);
2. $\lim_{|x|\to\infty} \Delta V/V_0 = 0$.

Consider then the auxiliary potential

$$\hat{V} = V_0 + \frac{\lambda}{\lambda_0}\Delta V \equiv V_0 + \lambda V_1 \,, \tag{4.13}$$

where λ_0 is an arbitrary positive constant and define the modified path integral

$$\hat{\mathcal{Z}}(\lambda,\lambda_0) = \int \mathcal{D}x\; G[x]\; e^{-\frac{\int d\tau\, \Delta V}{\lambda_0}}\; e^{-\frac{S_0}{\lambda}} \,, \qquad S_0 \equiv \int d\tau \left[\frac{1}{2}\dot{x}^2 + V_0\right] . \tag{4.14}$$

Since $\hat{\mathcal{Z}}(\lambda,\lambda) = \mathcal{Z}(\lambda)$, the latter can be obtained by the asymptotic expansion in λ of $\hat{\mathcal{Z}}$ (EPT), which is guaranteed to be Borel resummable to the exact answer.

We can then relax the requirement of a single critical point and state our general result:

Result 4B (EPT)**.** *All observables in a one-dimensional QM system with a bound-state potential V for which points 1. and 2. above apply are expected to be entirely reconstructable from a single perturbative series.*

Generally the decomposition $V = V_0 + \Delta V$ is far from being unique. EPT is defined as an expansion around the minimum of V_0, which does not need to be a minimum (or a critical point) of the original potential V. The number of interaction terms present in EPT also depends on the particular decomposition performed and in general is higher than the number of interaction terms present in the original theory (SPT). Since the mass term we choose for V_0 might differ from the one of V, so will do the effective couplings of SPT and EPT. As long as conditions 1. and 2. above are fulfilled, any choice of EPT is equivalent to any other, though in numerical computations with truncated series some choices might be more convenient than others.

The leading large-order behavior of the coefficients associated to the asymptotic expansion of the ground state energy associated to $\hat{\mathcal{Z}}(\lambda,\lambda_0)$ can be deduced using the results of refs. [8, 22, 23] (see in particular Section II of ref. [23]). The large-order behavior of the ground state energy coefficients is governed by the action S_0 only. In analogy to the one-dimensional integral, the functional $G\exp(-\int \Delta V/\lambda_0)$ in eq. (4.14) governs only the overall n-independent size of the coefficients.

Note that so far we used non-canonical variables with the coupling constant λ playing the role of $\hbar$—the saddle-point expansion is the loopwise expansion. This means that in the canonical basis the potential $V(x)$ turns into $V(x;\lambda)$ defined as

$$V(x;\lambda) = \frac{V(\sqrt{\lambda}\,x)}{\lambda} \,. \tag{4.15}$$

On the other hand, the coupling constant dependence of a generic QM potential may not be of the form in eq. (4.15).

[3] The second condition may be too conservative, see also footnote 5.

Example 4a. The expansion in g for the potential

$$V(x;g) = x^2 + gx^4 + gx^6 \tag{4.16}$$

does not correspond to the loopwise parameter. Indeed, setting $\lambda = \sqrt{g}$, the terms $x^2 + \lambda^2 x^6$ satisfy eq. (4.15) while the term $\lambda^2 x^4$ is effectively a one-loop potential that should be included in the functional $G[x]$ of eq. (4.5). ▲

4.4 Quantum Mechanical Examples

In this section we study numerically some polynomial QM systems in SPT and EPT, providing extensive evidence of the results obtained in the previous sections.

The perturbative series in both SPT and EPT are obtained by using the `Mathematica` [43] package `BenderWu` of ref. [44] which is based on recursion relations among the perturbative coefficients first derived by Bender and Wu in refs. [10, 45]. We consider up to N orders in the perturbative expansion (for EPT we fix the auxiliary parameter λ_0 to a given value) and we approximate the Borel function with Padé approximants.[4] For definiteness we use the Borel-Le Roy function $\mathcal{B}_b\mathcal{Z}(\lambda)$ with $b = -1/2$, which numerically seems a convenient choice leading to more accurate Padé approximants. The numerical computation of the integral in eq. (2.11) gives the final result (evaluated for the value of the coupling $\lambda = \lambda_0$ in EPT).[5] In the following we will refer to the above procedure as the Padé-Borel method. The result obtained is then compared with other numerical methods such as the Rayleigh-Ritz (RR) method (see e.g. ref. [46] for some explicit realizations). For polynomial potentials of small degree an efficient implementation is as follows: One starts from the truncated basis $|k_0\rangle$, $k = 1, \ldots, N_{RR}$ of the harmonic oscillator eigenfunctions, and then computes the full Hamiltonian matrix $H_{kh} = \langle k_0|H|h_0\rangle$, which is almost diagonal. The approximate energy levels and eigenfunctions of the system are given by the eigenvalues and eigenvectors of H_{kh}. This method converges to the exact result very quickly. The accuracy depends on N_{RR} and on the energy level considered. The lower is the level, the higher is the accuracy.

We mostly focus on the energy eigenvalues $E_k(\lambda)$, though the eigenfunctions $\phi_k(x;\lambda)$ are also considered. Since the package [44] computes non-normalized wavefunctions, we define

$$\psi_k(x;\lambda) \equiv \frac{\phi_k(x;\lambda)}{\phi_k(x_0;\lambda)} \tag{4.17}$$

for some x_0 and compute

$$\Delta\psi_k(x;\lambda) = \frac{\psi_k^{\rm RR}(x;\lambda) - \psi_k^{\rm EPT}(x;\lambda)}{\psi_k^{\rm RR}(x;\lambda)}\,, \tag{4.18}$$

where for simplicity we omit the x_0 dependence in the $\psi_k(x;\lambda)$.

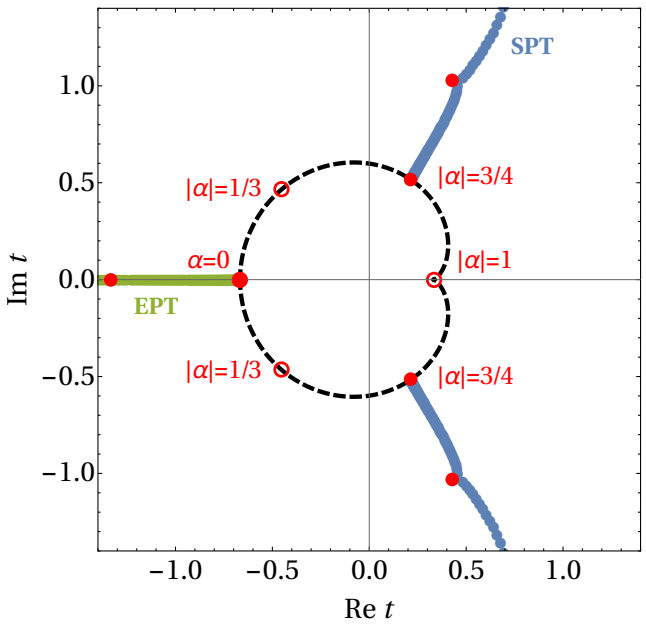

Figure 4.3: Location of the singularities in the Borel plane for the standard and exact perturbative series of $E_0(\lambda, \alpha)$ for the potential (4.19). The dashed line represents the location of the leading singularities as expected from eq. (4.20) with $|\alpha| \in [0, 1]$. The red bullets indicate the position of the first and second complex instantons for $|\alpha| = 3/4$. The regions where the simple poles of the Padé-Borel approximants accumulate are depicted in blue and green.

4.4.1 Tilted Anharmonic Oscillator

The first example we consider is the tilted anharmonic oscillator

$$V(x; \lambda) = \frac{1}{2}x^2 + \alpha\sqrt{\lambda}x^3 + \frac{\lambda}{2}x^4\,, \tag{4.19}$$

where α is a real parameter. For $|\alpha| < 2\sqrt{2}/3$, the potential has a unique minimum at $x = 0$. According to our results, SPT is then Borel resummable to the exact value for all the observables. For $2\sqrt{2}/3 \leq |\alpha| < 1$ some quantities, such as the ground state energy $E_0(\lambda, \alpha)$, are Borel resummable to the exact value while some are not, such as the partition function. The cases $|\alpha| = 1$ (symmetric double well) and $|\alpha| > 1$ (false vacuum) will be discussed in the next sections.

For definiteness, let us look at the ground state energy $E_0(\lambda, \alpha)$. The position of the leading singularities in the associated Borel plane is dictated by the value of the action $S[z_\pm]$ on the nearest saddle points, which for $|\alpha| < 1$ are complex instantons $z_\pm$ [23]:

$$\lambda t_\pm = \lambda S[z_\pm] = -\frac{2}{3} + \alpha^2 + \frac{1}{2}\alpha(\alpha^2 - 1)\left(\log\frac{1-\alpha}{1+\alpha} \pm i\pi\right). \tag{4.20}$$

This expectation is confirmed by a numerical analysis with Borel-Padé approximants (see Figure 4.3). The ground state energy coefficients $E_{0,n}(\alpha)$ for $n \gg 1$ oscillate with a period given by

[4] We also considered other approximation methods, such as the conformal mapping of refs. [34, 35]. While the results are consistent with those obtained using Borel-Padé approximants, the latter typically give a better numerical precision for $N \gg 1$. On the other hand, at small N the conformal mapping method is more reliable because of numerical instabilities of the Borel-Padé approximants.

[5] Results with $N = 100 \div 500$ are obtained within minutes÷hours with a current standard laptop.

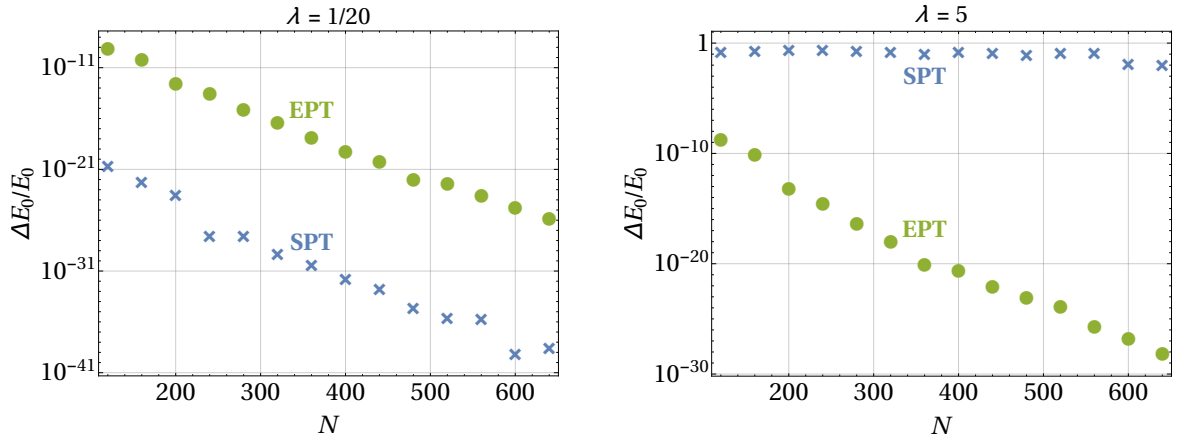

Figure 4.4: Comparison between the relative error $\Delta E_0/E_0$ in the computation of the ground state energy using Borel-Padé approximants of the series coming from eqs. (4.19) (SPT) and (4.21) (EPT) as a function of the number N of series coefficients retained. (Left panel) weak coupling $\lambda = 1/20$, (right panel) strong coupling $\lambda = 5$.

$2\pi/|\mathrm{Arg}\, t_\pm|$. As long as the coefficients oscillate, the observable is Borel resummable. The period is minimum at $\alpha = 0$, where the coefficients alternate, and grows with $|\alpha|$ until it becomes infinite at $|\alpha| = 1$ and Borel resummability is lost. In numerical evaluations at fixed order N the best accuracy is obtained at $\alpha = 0$. For $\alpha \neq 0$, at least $N > 2\pi/|\mathrm{Arg}\, t_\pm|$ orders are required to see the alternating nature of the series.

Even if $E_0(\lambda, \alpha)$ is Borel resummable for $|\alpha| < 1$ in SPT, EPT can be used to greatly improve the numerical results at strong coupling. Indeed, we can define a potential $\hat{V} = V_0 + \lambda V_1$ with

$$V_0 = \frac{1}{2}x^2 + \frac{\lambda}{2}x^4\,, \qquad V_1 = \alpha\frac{\sqrt{\lambda}}{\lambda_0}x^3\,, \tag{4.21}$$

so that the original one is recovered for $\lambda_0 = \lambda$.

The first terms in the perturbative SPT and EPT expansions read

$$\begin{aligned} E_0 =& \frac{1}{2} + \frac{3 - 11\alpha^2}{8}\lambda - \frac{21 - 342\alpha^2 + 465\alpha^4}{32}\lambda^2 + \frac{333 - 11827\alpha^2 + 45507\alpha^4 - 39709\alpha^6}{128}\lambda^3 + \dots \\ \hat{E}_0 =& \frac{1}{2} + \frac{3}{8}\lambda - \frac{21}{32}\lambda^2 + \Big(\frac{333}{128} - \frac{11\alpha^2}{8\lambda_0^2}\Big)\lambda^3 + \dots\,, \end{aligned} \tag{4.22}$$

which shows how EPT rearranges all the α-dependent terms in the perturbative expansion. For instance, the one-loop α^2-dependent term in SPT appears at three loops in EPT.

As we discussed, V_1 modifies the overall normalization of the large-order coefficients $\hat{E}_{0,n}(\lambda_0)$ with respect to the ones of the anharmonic oscillator $E_{0,n}(\alpha = 0)$ without altering their leading large-order n-dependence. The normalization at leading order is given by the exponential of the integral of V_1 evaluated at the nearest complex saddles

$$\exp\Big(-\alpha\frac{\lambda^{3/2}}{\lambda_0}\int_{-\infty}^{\infty} d\tau\, z_\pm^3[\tau]\Big) = e^{\pm i\pi\alpha/2\lambda_0}\,. \tag{4.23}$$

In analogy to the one-dimensional case outlined at the end of sect. 2, we expect for $n \gg 1$ and $n \gg 1/\lambda_0^2$,

$$\hat{E}_{0,n}\Big(\frac{\lambda_0}{\alpha}\Big) = E_{0,n}(\alpha = 0)\left[\cos\Big(\frac{\pi\alpha}{2\lambda_0}\Big) + \mathcal{O}\Big(\frac{1}{n}\Big)\right]\,, \tag{4.24}$$

k	$x=1/8$	$x=1/4$	$x=1/2$	$x=1$	$x=2$	$\Delta E_n/E_n$
Anharmonic						
0	$7\cdot10^{-24}$	$4\cdot10^{-23}$	$2\cdot10^{-22}$	10^{-21}	$8\cdot10^{-20}$	$3\cdot10^{-33}$
1	$3\cdot10^{-15}$	$2\cdot10^{-14}$	$7\cdot10^{-14}$	$5\cdot10^{-13}$	$3\cdot10^{-11}$	$4\cdot10^{-30}$
2	$2\cdot10^{-8}$	10^{-7}	$4\cdot10^{-6}$	$6\cdot10^{-7}$	$7\cdot10^{-6}$	$2\cdot10^{-27}$
Symmetric double well						
0	$5\cdot10^{-27}$	$3\cdot10^{-26}$	10^{-25}	$2\cdot10^{-25}$	$3\cdot10^{-24}$	$6\cdot10^{-34}$
1	$4\cdot10^{-18}$	$2\cdot10^{-17}$	10^{-16}	$6\cdot10^{-16}$	$2\cdot10^{-14}$	10^{-30}
2	$5\cdot10^{-11}$	$3\cdot10^{-10}$	$3\cdot10^{-9}$	$2\cdot10^{-9}$	10^{-8}	$5\cdot10^{-27}$

Table 4.1: Relative errors of the ratio of wave functions (4.18) and energies of the first three levels of the anharmonic and symmetric double well at $\lambda = 1$, evaluated at different points x using EPT with $N = 200$, and RR methods. In the anharmonic case EPT coincides with SPT. We have taken $x_0 = 1/16$ in eq. (4.17).

where

$$E_{0,n}(\alpha=0) = -\frac{\sqrt{6}}{\pi^{3/2}}\left(-\frac{3}{2}\right)^n \Gamma\left(n+\frac{1}{2}\right)\left[1+\mathcal{O}\left(\frac{1}{n}\right)\right]. \tag{4.25}$$

In particular, eq. (4.24) implies that the leading singularity of the Borel function is located at $t = -2/3$ as in the case of the anharmonic oscillator with $\alpha = 0$. This is numerically confirmed by the associated Borel-Padé approximants (see Figure 4.3). It is useful to compare the efficiency of SPT and EPT as a function of the number of terms N that are kept in the series expansion. These are reported in Figure 4.4 for weak and strong coupling values $\lambda = 1/20$, $\lambda = 5$, respectively, where ΔE_0 refers to the discrepancy with respect to $E_0^{\rm RR}$.

In agreement with expectation, at sufficiently weak coupling SPT performs better than EPT. The situation is drastically different at strong coupling, where SPT is essentially inaccurate for any N reported in Figure 4.4, while EPT has an accuracy that increases with the order.

At fixed number of perturbative terms, EPT works at its best for coupling constants $\lambda \sim \mathcal{O}(1)$. Like SPT, as λ increases the integral in eq. (2.11) is dominated by larger values of t (this is best seen by rescaling $t \to t/\lambda$) and hence more and more terms of the perturbative expansion are needed to approximate the Borel function. On the other hand, in analogy to the one-dimensional case (3.36)), the Borel function in EPT contains an additional exponential term coming from $\exp(-\int V_1)$. When $\lambda \ll 1$ the accuracy drops because the coefficients $\hat{E}_n(\lambda_0)$ are very large before reaching the regime when eq. (4.24) applies.

4.4.2 Symmetric Double-well

For $|\alpha| = 1$ the potential (4.19) turns into a symmetric double-well, with two degenerate minima. This is the prototypical model where real instantons are known to occur and the perturbative expansion around any of the two minima are known to be not Borel resummable. SPT requires the addition of an infinite number of real instantons to fix the ambiguities related to lateral Borel resummations and to reproduce the full result, see e.g. ref. [47] for a numerical study.

Shifting the x coordinate so that $x = 0$ is the maximum of the potential

$$V(x;\lambda) = \frac{\lambda}{2}\left(x^2 - \frac{1}{4\lambda}\right)^2, \tag{4.26}$$

we can perform an EPT by considering the auxiliary potential

$$V_0 = \frac{1}{32\lambda} + \frac{\lambda_0}{2}x^2 + \frac{\lambda}{2}x^4\,, \qquad V_1 = -\Big(1 + \frac{1}{2\lambda_0}\Big)\frac{x^2}{2}\,, \tag{4.27}$$

which has as effective couplings $\lambda/\lambda_0^{3/2}$ and $\lambda/\lambda_0(1 + 1/(2\lambda_0))$. This choice of EPT, where the minimum of V_0 is half way between the two minima of the double well, is such that the numerical Borel-Padé resummation is able to reconstruct the non-perturbative splitting between the first two levels at moderately small couplings, with a few hundred orders of perturbation theory. However, at fixed order N of perturbation theory and for very small couplings, the true vacua depart further and further from the minimum of V_0 and the corresponding EPT becomes even worse than the naive truncated series. In this regime a better choice would be to take the minimum of V_0 close to one of the true minima of the double well (although resolving non-perturbative effects in this regime becomes harder and, as expected, more terms of the perturbative expansion are required).

We start by considering the ground state energy $E_0(\lambda)$. The large order behavior of the series coefficients $\hat{E}_{0,n}(\lambda_0)$ in EPT for $n \gg 1$ and $n \gg 1/\lambda_0^2$ are given by

$$\hat{E}_{0,n}(\lambda_0) = \lambda_0^{\frac{1}{2}-\frac{3}{2}n}\, e^{-\sqrt{\lambda_0}\left(1+\frac{1}{2\lambda_0}\right)} E_{0,n}(\alpha = 0)\left[1 + \mathcal{O}\Big(\frac{1}{n}\Big)\right]. \tag{4.28}$$

As before, the exponential λ_0-dependent factor is obtained by evaluating the potential V_1, the second term in square brackets in eq. (4.27), at the leading complex instanton solutions $z_\pm$. The prefactor $\lambda_0^{\frac{1}{2}-\frac{3}{2}n}$ is instead due to the λ_0 dependence of the quadratic term in V_0.

By taking $N = 200, \lambda = \lambda_0 = 1/32$, we get $\Delta E_0/E_0 \approx 2{\cdot}10^{-5}$ and $\Delta E_1/E_1 \approx 2{\cdot}10^{-11}$. These accuracies are already several orders of magnitude smaller than the leading order one-instanton contribution

$$E_0^{\text{inst}} \approx \frac{2}{\sqrt{\pi\lambda}} e^{-\frac{1}{6\lambda}}\,, \tag{4.29}$$

which amounts to ≈ 0.031, or from the whole instanton contribution computed as the energy split between the ground state and the first excited level, which amounts to ≈ 0.024. For larger values of the coupling λ the accuracy of EPT improves very quickly. For instance, already at $\lambda = \lambda_0 = 1/25$, keeping $N = 200$ as before, $\Delta E_0/E_0 \approx 10^{-8}$ and $\Delta E_1/E_1 \approx 4 \cdot 10^{-14}$, way smaller than the leading one-instanton contribution ≈ 0.087 or of the whole instanton contribution, computed as above and ≈ 0.061. For $\lambda \geq 1$ SPT breaks down: one would need to resum the whole transseries given by the multi-instantons and their saddle-point expansions, which is very challenging. On the other hand EPT works very efficiently in this regime. At fixed order N, the error decreases as λ increases up to some value, beyond which the error slowly increases again. There is no need to consider too large values of N to get a reasonable accuracy, in particular in the strong coupling regime $\lambda \sim 1$. For instance, at $\lambda = 1$ and with $N = 2(4)$ orders, we get $\Delta E_0/E_0 \simeq 3\%(0.5\%)$ by using the conformal mapping method [34, 35] with coupling

$$w(\lambda) = \frac{\sqrt{1 + 3\lambda/2} - 1}{\sqrt{1 + 3\lambda/2} + 1}\,, \tag{4.30}$$

and Borel resumming the new series.

As far as we know, the convergence of series related to observables other than energy eigenvalues have been poorly studied. This has motivated us to analyze the series associated to the

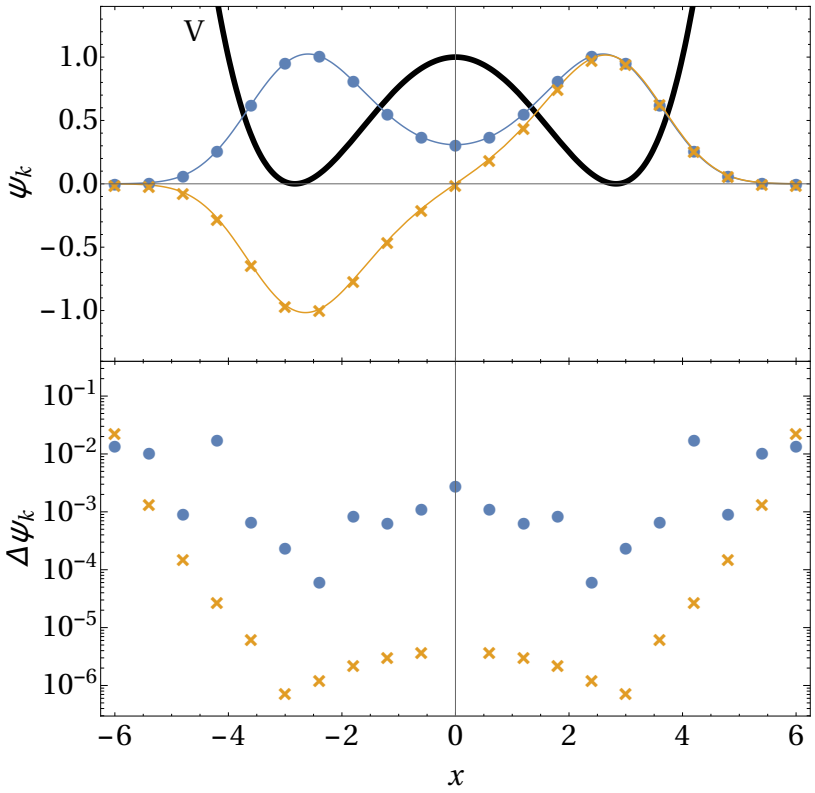

Figure 4.5: Comparison of the wavefunctions (normalized as in eq. (4.17) at $x_0 = 2\sqrt{2}$) for the first two levels of the symmetric double-well potential with $\lambda = 1/32$. Those computed in EPT with $N = 200$ are indicated by blue bullets (ground state) and orange crosses (first state) while the ones computed using the RR method are indicated by solid curves.

wave functions $\phi_k(x;\lambda)$. We report in table 4.1 the values of $\Delta\psi_k(x;\lambda)$ for the first three levels of the anharmonic oscillator, $\alpha = 0$ in eq. (4.19), and the symmetric double well (4.26), for some values of x at $\lambda = 1$. Given the exponential decay of the wave function, larger values of x are subject to an increasing numerical uncertainty and are not reported. The decrease in accuracy as the level number k increases is also expected, since both the RR methods and SPT/EPT require more and more precision. In all the cases considered the Borel-Padé approximants are free of poles in the real positive t axis. The results clearly indicate that EPT captures the full answer. For illustration in Figure 4.5 we plot $\psi_{0,1}$ and $\Delta\psi_{0,1}$ at $\lambda = 1/32$.

4.4.3 Supersymmetric Double Well

We now turn to the notable tilted double-well potential

$$V(x;\lambda) = \frac{\lambda}{2}\left(x^2 - \frac{1}{4\lambda}\right)^2 + \sqrt{\lambda}x\,. \tag{4.31}$$

This is the exact quantum potential that one obtains from the supersymmetric version of the double well when the fermionic variables are integrated out. As it is well known, the ground state energy $E_0 = 0$ to all orders in SPT due to supersymmetry. At the non-perturbative level, however, $E_0 \neq 0$ because supersymmetry is dynamically broken [48]. Due to the absence of perturbative contributions in SPT, the supersymmetric double-well is the ideal system where

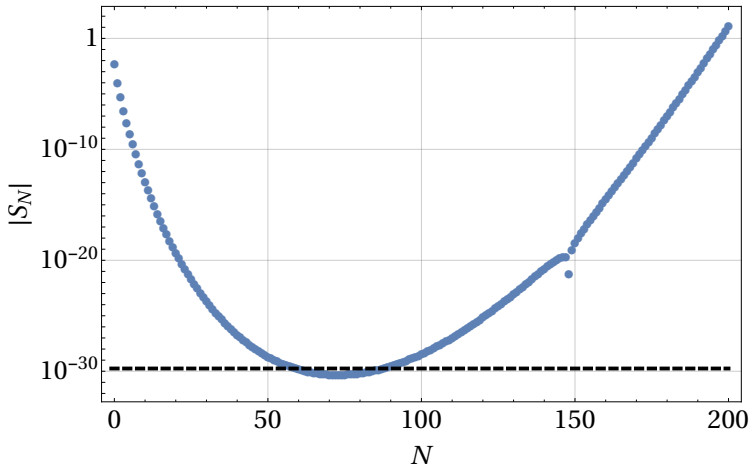

Figure 4.6: The partial sum (4.33) of APT for the potential (4.32) as a function of N for $\lambda = 1/200$. The black dashed line corresponds to the exact ground state energy as computed using RR methods.

to test EPT. It is also one of the simplest system where a perturbative expansion is Borel resummable (being identically zero), but the sum does not converge to the exact value.

Different authors have invoked complex instantons to reproduce E_0 [49, 50]. Their argument is essentially based on the observation that the entire quantum tilted potential (4.31) does not admit other real saddles that can contribute to the ground state energy. Note however that the perturbation theory in λ corresponds to the expansion around the saddle points of the classical action. Since the tilt in eq. (4.31) is quantum in nature, the saddle-points of this system are the same as the ones of the symmetric double-well. In particular, real instantons occur, meaning that the path integral is on a Stokes line. The instanton contributions to E_0 have been extensively studied in ref. [51], where the first nine terms of the perturbative series around the 1-instanton saddle have been computed using a generalized Bohr-Sommerfeld quantization formula [52]. As expected, this expansion agrees very well with the numerical calculation at small coupling, while it breaks down when λ approaches one since the perturbative expansion of more and more instantons need to be properly included.

Note that the expansion around the saddle-points of the full action corresponds to treat the whole potential (4.31) as classical. This means that the coefficient of the linear tilt is rescaled by a factor λ_0/λ to satisfy eq. (4.15). The resulting potential, which leads to an alternative perturbative expansion in λ (APT), reads

$$V_{\text{APT}} = \frac{\lambda}{2}\left(x^2 - \frac{1}{4\lambda}\right)^2 + \frac{\lambda_0}{\sqrt{\lambda}}x\,. \tag{4.32}$$

The original result is recovered by setting $\lambda = \lambda_0$. This expansion for the ground state energy is no longer supersymmetric, but according to the discussion in Section 3.2 is Borel resummable to the exact result. We show in Figure 4.6 the partial sums

$$S_N = \sum_{k=1}^{N} c_k \lambda^k \tag{4.33}$$

of the coefficients of APT as a function of N for $\lambda = 1/200$. The dashed line represents the exact ground state energy. While each term in perturbation theory is non-vanishing, cancellations

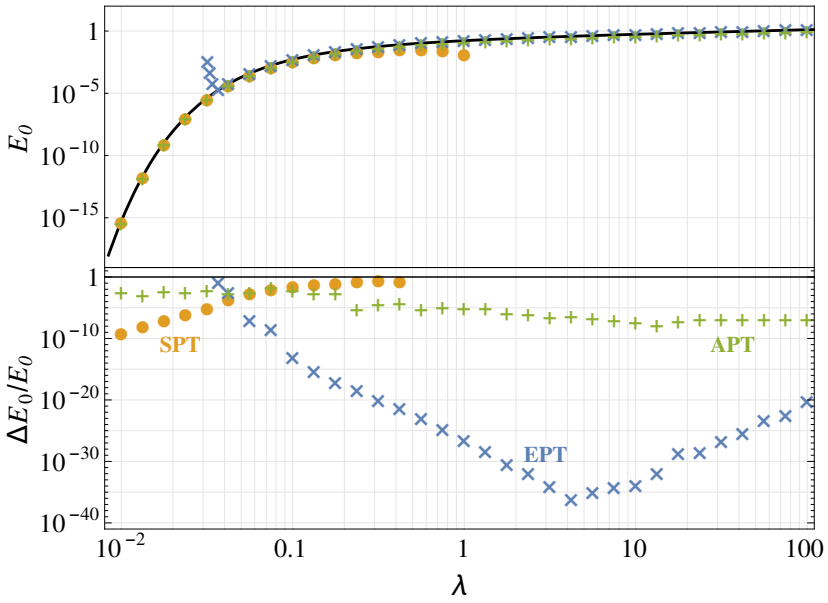

Figure 4.7: The ground state energy (top) and the relative error (bottom) as a function of the coupling λ for the supersymmetric double well (4.31). The blue [green] crosses refer to EPT [APT] from the potential (4.34) [(4.32)] with $N = 200$ series coefficients, the orange dots to SPT of ref. [51], with a truncated expansion up to the ninth order around the leading instanton. The black line corresponds to the exact result, computed by means of a Rayleigh-Ritz method.

make the size of the truncated sum to decrease until $N \approx N_{\text{Best}} = 74$, where it approaches the expected non-perturbative answer. For larger values of N the series starts diverging, though Borel resummation reconstructs the right value with a precision of $\mathcal{O}(10^{-3})$ using $N = 200$ terms. The feature appearing around $N = 150$ is due to the change of sign of the truncated sum. Indeed the sign of the coefficients c_k oscillates with a long period $\mathcal{O}(150)$ since at weak coupling the tilt of the double-well potential is small and complex singularities of the Borel plane are close to the real axis (see Figure 4.3).

Analogously to the previous cases we can also introduce an EPT for which all the observable are Borel resummable. For this purpose we consider the auxiliary potential

$$V_0 = \frac{1}{32\lambda} + \frac{\lambda_0}{2}x^2 + \frac{\lambda}{2}x^4\,, \qquad V_1 = \frac{x}{\sqrt{\lambda}} - \left(1 + \frac{1}{2\lambda_0}\right)\frac{x^2}{2}\,, \tag{4.34}$$

where V_1 includes the quantum tilt x and the quadratic x^2 term necessary to recover the original potential. The specific decomposition (4.34) turns out to be numerically convenient for moderately small and large couplings.

In Figure 4.7 we show a comparison between the various perturbative estimates of E_0 and the numerical RR one as a function of the coupling constant. As expected, at small coupling SPT provides the best estimate. In fact it encodes analytically the leading instanton effect providing the asymptotic value of E_0 at $\lambda \to 0$. However, already at moderately small couplings both APT and EPT are able to resolve the leading instanton effects with a good accuracy. At moderate and strong coupling the instanton computation quickly breaks down, while both APT and EPT work extremely well. In particular the accuracy of EPT strongly increases with λ up to $\lambda \sim 4$. For larger values of the coupling the accuracy drops, but it remains remarkable. For $\lambda \sim 10^2$

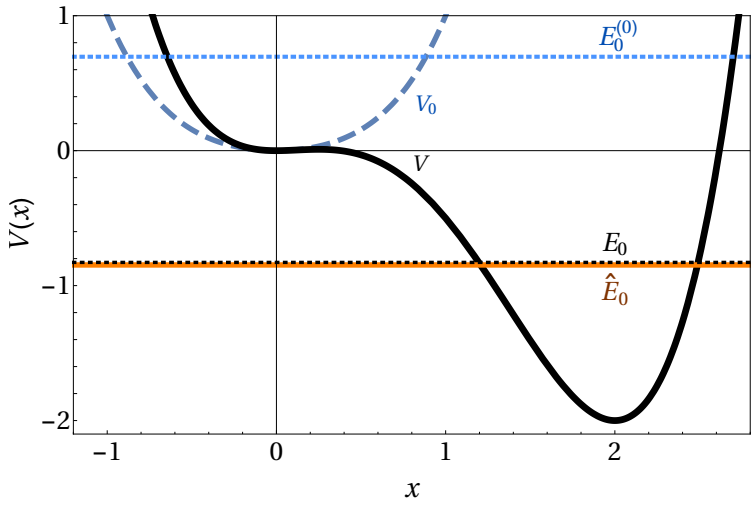

Figure 4.8: Plots of the potential (4.35) (solid black curve) and the associated potential V_0 in eq. (4.36) (dashed curve) with $\lambda = 1$. The dashed blue line corresponds to the ground state energy associated to V_0, the solid red and the dashed black ones are the ground state energy of the potential (4.35) obtained from EPT and RR methods, respectively.

we have an accuracy $\sim 10^{-20}$ with 200 orders of perturbation theory. It is amazing how a perturbative computation can work so efficiently at strong coupling!

4.4.4 False Vacuum

We now consider the potential (4.19) with $|\alpha| > 1$. In this case $x = 0$ is no longer the absolute minimum, and we are effectively expanding around a false vacuum. Clearly SPT is non-Borel resummable in this case, given the presence of other real instantons. The perturbative expansion around the false vacuum does not contribute at all to E_0, which, as we saw, is entirely reconstructed by the expansion around the true vacuum. Still the EPT around the false vacuum defined by the potential (4.21) is able to recover the (true) ground state energy.

In Figure 4.8 we show the shape of the original potential V for $\alpha = -3/2$

$$V(x;\lambda) = \frac{1}{2}x^2 - \frac{3}{2}\sqrt{\lambda}x^3 + \frac{\lambda}{2}x^4\,, \tag{4.35}$$

and the corresponding exact ground state energy $E_0 \approx -0.828$ at $\lambda = 1$. We also show the potential V_0 used in EPT

$$V_0 = \frac{1}{2}x^2 + \frac{\lambda}{2}x^4\,, \tag{4.36}$$

with the would-be ground state energy $E_0^{(0)} \approx 0.696$. Using EPT with $N = 280$ orders such value moves to $\hat{E}_0 \approx -0.847$. Although the accuracy is not comparable to that obtained in the previous cases, it is remarkable that one is able to compute the energy of the true vacuum starting from a perturbative expansion around a false vacuum.

4.4.5 Degenerate Saddle Points: Pure Anharmonic Oscillators

In this section we discuss how to use EPT to address the infinitely coupled systems described by potentials with degenerate saddle points. Consider for example the pure anharmonic oscillators

with potentials of the form

$$V(x) = 2^\ell x^{2\ell}\,, \qquad \ell \in \mathbb{N}^+\,. \tag{4.37}$$

The factor 2^ℓ is such that, modulo a trivial rescaling, the Hamiltonian is of the form $p^2+x^{2\ell}$ which is the conventional normalization used in the literature for this class of models. Pure anharmonic oscillators are intrinsically strongly coupled and can be obtained as the $\lambda \to \infty$ limit of their corresponding ordinary massive anharmonic oscillators after the rescaling $x \to \lambda^{-1/2(1+\ell)}x$. The potentials (4.37) are convex with a degenerate minimum at $x = 0$. In the absence of a quadratic mass term, perturbation theory cannot be used. The energy eigenvalues $E_k^{(2\ell)}$ of these systems have instead been studied using Rayleigh-Ritz methods (see e.g. ref. [53]), Thermodynamic Bethe Ansatz (TBA) [54] or a Wentzel Kramers Brillouin (WKB) approximation [55] (see also ref. [56] for a more modern perspective). In the WKB approximation one considers a series expansion in $1/k$, k being the quantum number level. It was found in refs. [55, 56] that the asymptotic series of the WKB expansion, where classical real trajectories in phase space are considered, does not reproduce the correct result. A better accuracy is achieved by adding in the WKB quantization formula the contribution of complex trajectories in phase space. However, there are an infinite number of them and a parametrically high accuracy could be obtained only by resumming all the infinite complex trajectories.

In terms of Lefschetz thimbles, the potentials (4.37) have a degenerate saddle for which our considerations do not apply. A possibility is to add a mass term ϵx^2 to eq. (4.37), compute the energy levels $E_k^{(2\ell)}(\epsilon)$ and extrapolate the result for $\epsilon \to 0$. By choosing $\epsilon > 0$ we are guaranteed that $E_k^{(2\ell)}(\epsilon)$ are Borel resummable for any ϵ and no (real or complex) non-perturbative contributions are expected. We have verified this expectation by computing the ground state energy $E_0^{(4)}(\epsilon)$ for the pure quartic oscillator for smaller and smaller values of ϵ (using the Padé-Borel method) and have found that the extrapolated value $E_0^{(4)}$ converges to the exact value.

The same result can be found with much greater accuracy and efficiency using EPT without taking any extrapolation. Consider the auxiliary family of potentials defined as

$$V_0 = \lambda^{\ell-1}2^\ell x^{2\ell} + \sum_{j=1}^{\ell-1} c_j \lambda^{j-1} x^{2j}\,, \qquad V_1 = -\frac{1}{\lambda_0}\sum_{j=1}^{\ell-1} c_j \lambda^{j-1} x^{2j}\,, \tag{4.38}$$

such that at $\lambda = \lambda_0 = 1$ the potential in eq. (4.37) is recovered. By a proper choice of the $\ell - 1$ coefficients c_j, V_0 has a unique non-degenerate minimum at $x = 0$ and perturbation theory is well-defined.

For the pure quartic case $\ell = 2$, by choosing $c_1 = 2$ in eq. (4.38) and by using only the first ten orders of EPT we get $E_0^{(4)} \simeq 1.060362$, which is more accurate than the value in Table 2 of ref. [56], obtained using 320 orders in the WKB expansion with the inclusion of the leading complex saddles. The accuracy is easily improved using more coefficients of the perturbative expansion. We have computed in this way the $E_k^{(2\ell)}$ for different values of ℓ and k, as well as the associated wave-functions $\psi_k^{(2\ell)}(x)$ for some values of x. In all cases we found excellent agreement between our results and those obtained with RR methods.

For illustration we report in Table 4.2 the accuracies for the energy levels of the first five states of the pure x^4 and x^6 oscillators computed comparing EPT to the results from RR methods. We used $N = 200$ orders of perturbation theory and in eq. (4.38) we chose $c_1 = 2$ for $\ell = 2$ and $c_1 = 4$, $c_2 = 2$ for $\ell = 3$. Notice the accuracy of $E_0^{(4)}$ up to 45 digits! At fixed N, similarly to the RR method, the accuracy decreases as the energy level and the power ℓ in

k	$E_k^{(4)}$	$\Delta E_k^{(4)}/E_k^{(4)}$	$E_k^{(6)}$	$\Delta E_k^{(6)}/E_k^{(6)}$
0	1.0603620904	$3 \cdot 10^{-45}$	0.5724012268	$2 \cdot 10^{-19}$
1	3.7996730298	$2 \cdot 10^{-44}$	2.1692993557	$3 \cdot 10^{-19}$
2	7.4556979379	$9 \cdot 10^{-37}$	4.5365422804	$9 \cdot 10^{-17}$
3	11.6447455113	$4 \cdot 10^{-36}$	7.4675848174	$7 \cdot 10^{-16}$
4	16.2618260188	$4 \cdot 10^{-36}$	10.8570827110	$2 \cdot 10^{-16}$

Table 4.2: Energy eigenvalues $E_k^{(2\ell)}$ and the corresponding accuracies $\Delta E_k^{(2\ell)}/E_k^{(2\ell)}$ of the first five levels of the pure anharmonic x^4 and x^6 potentials, computed using EPT with $N = 200$. Only the first ten digits after the comma are shown (no rounding on the last digit).

eq. (4.37) increase (in contrast to the WKB method where the opposite occurs) All the energy eigenvalues reported in Table 4.2 are in agreement with those reported in Table 1 of ref. [53], Table I and II of ref. [54] and Table 2 of ref. [56], in all cases computed with less precision digits than our results.[6] The accuracy of our results sensibly depend on the choice of the coefficients c_j in eq. (4.38). We have not performed a systematic search of the optimal choice that minimizes the errors, so it is well possible that at a fixed order N a higher accuracy than that reported in Table 4.2 can be achieved.

[6]Note however that the numerical computations based on the Rayleigh-Ritz methods remain superior for these simple potentials.

Chapter 5

Path Integral of Quantum Field Theory (d=2)

The aim of this chapter is to begin an extension of the above results in quantum field theory (QFT). We start in Section 5.1 by showing that arbitrary n-point correlation functions (Schwinger functions) are Borel reconstructable from their loopwise expansion in a broad class of Euclidean 2d and 3d scalar field theories. The Borel summability of Schwinger functions in this class of theories is deduced by using the same manipulations to the path-integral performed in the case of QM and by showing the absence of non-trivial positive finite actions solutions to the classical equations of motion. This is equivalent to establishing that the original path integral over real field configurations coincides with a single Lefschetz thimble. The ordinary loopwise expansion around the vacuum $\phi = 0$ can then be interpreted as the saddle point expansion over a Lefschetz thimble, hence Borel summability is guaranteed. In the presence of phase transitions the discussion is more subtle and the analytically continued Schwinger functions may not coincide with the physical ones in the other phase. We discuss these subtle issues for the two-dimensional ϕ^4 theory in Subsection 5.1.1, where we point out that Schwinger functions that are analytically continued from the unbroken to the broken phase correspond to expectation values of operators over a vacuum violating cluster decomposition.

The rest of the chapter is about the 2d ϕ^4 theory, described by the following Lagrangian density

$$\mathcal{L} = \frac{1}{2}(\partial_\mu \phi)^2 + \frac{1}{2} m^2 \phi^2 + \lambda \phi^4 \,. \tag{5.1}$$

The theory is super-renormalizable. Only the 0-point function and the momentum independent part of the 2-point functions are superficially divergent. The coupling constant λ is finite and there is no need of a field wave function renormalization, while counterterms are required for the vacuum energy and the mass term. The effective expansion parameter of the theory is the dimensionless coupling

$$g \equiv \frac{\lambda}{m^2} \,. \tag{5.2}$$

Using certain bounds and analytic properties of the Schwinger functions, the perturbation series of arbitrary correlation functions had already been rigorously proved to be Borel resummable, though only for parametrically small coupling constant and large positive squared mass, i.e. for $g \ll 1$ [16].

The RG flow of this theory is well-known. In the UV the theory becomes free, for any value of g and m^2. The flow of the theory in the IR depends on g and m^2. For $m^2 > 0$ and $0 \leq g < g_c$

the theory has a mass gap and the $\mathbb{Z}_2$ symmetry $\phi \to -\phi$ is unbroken. At a critical value of the coupling $g = g_c$ the theory develops a second-order phase transition [57, 58]. At the critical point the theory is a conformal field theory (CFT) in the same universality class of the 2d Ising model. Above g_c the theory is in the $\mathbb{Z}_2$ broken phase.

For $m^2 < 0$ and $0 < g < \widetilde{g}_c$ the theory has a mass gap and the $\mathbb{Z}_2$ symmetry is broken. At $g = \widetilde{g}_c$ the second-order phase transition occurs. The $\mathbb{Z}_2$ symmetry is restored for $\widetilde{g}_c < g < \widetilde{g}'_c$. At $g > \widetilde{g}'_c$, the theory returns to a broken phase. As we will see in Section 5.2 a simple duality [57] can be established between the $\mathbb{Z}_2$ unbroken and broken phases that allows, among other things, to relate the three critical values g_c, $\widetilde{g}_c$ and $\widetilde{g}'_c$.

5.1 Borel Summability in $d < 4$ Scalar Field Theories

In this section we show how the Borel summability of Schwinger functions in the $\lambda\phi^4$ theory can be more easily inferred and extended to a large class of scalar field theories (though in a less rigorous way than refs. [16, 17]) using a geometric approach borrowed by Picard-Lefschetz theory.

We start by considering the Euclidean path integral

$$F = \int \mathcal{D}\phi \, G[\phi] \, e^{-S[\phi]/\hbar} \,, \tag{5.3}$$

where we momentarily reintroduced $\hbar$, $S[\phi]$ is the Euclidean action

$$S[\phi] = \int d^d x \left[\frac{1}{2} (\partial\phi)^2 + V(\phi) \right] , \tag{5.4}$$

with $V(\phi)$ a generic polynomial potential bounded from below and $G[\phi]$ an arbitrary polynomial function of fields, product of local operators at different space-time points, corresponding to n-point Schwinger functions in the theory. In order to avoid the danger of having an ill-defined path integral $V(\phi)$ should not contain irrelevant couplings; we restrict to the case of super-renomalizable potentials to avoid complications from possible renormalons [41]. Hence in $d = 2$ $V(\phi)$ is a generic polynomial function bounded from below,[1] while in $d = 3$ it is a polynomial of degree up to four. For simplicity, we have omitted to write the space dependencies of G and of the resulting Schwinger functions F. A proper definition of F in general requires renormalization. The counterterms needed to reabsorb the divergences are subleading in a saddle point expansion in $\hbar$ and can be reabsorbed in the factor G, which clearly is no longer a polynomial in the fields.[2] The counterterms do not change the saddle point structure of $S[\phi]/\hbar$, as long as the convergence of the path integral at large field values is dictated by S, condition automatically satisfied in our case by the absence of marginal and irrelevant couplings.

Without lack of generality we can choose $\phi_0 = 0$ for the value of the absolute minimum of the classical potential (for the moment we assume that it is unique, we will discuss the case of degenerate minima afterwards) and normalize the path integral so that $S[0] = 0$. Out of the infinite integration variables of the path integral we now single out the one corresponding to the value of the action, namely we rewrite our path integral as [2, 38, 40, 41]

$$F = \int_0^\infty dt \, e^{-t} \int \mathcal{D}\phi \, G[\phi] \, \delta\big(t - S[\phi]/\hbar\big) = \int_0^\infty dt \, e^{-t} \mathcal{B}(\hbar t) \,, \tag{5.5}$$

[1] Most likely this is a conservative assumption and our considerations extend to more general potentials.

[2] For simplicity, we are assuming here that the saddle point expansion is well-defined for any field mode, namely $\det S'' \neq 0$. Whenever this condition is not met, the corresponding zero mode should be evaluated exactly.

viz. an integral over all possible values of the action $t = S/\hbar$ of the function $\mathcal{B}(\hbar t)$, which is a path integral restricted to the section of phase space with fixed action.[3] Note that the function $\mathcal{B}$ in eq. (5.5) is the Laplace transform of F and as such it corresponds to its Borel transform when expanded in $\hbar$. The manipulation above is legit as long as the change of variables $t = S[\phi]/\hbar$ is non-singular, i.e. as long as $S'[\phi] \neq 0$. Hence eq. (5.5) holds as long as there are no finite action critical points (aside from the trivial one $\phi_0 = 0$) for real field configurations. Following ref. [23], a generalization of Derrick's theorem [59] can be used to show that the action defined in eq. (5.4) does not have any non-trivial critical points with finite action. Analogously to the quantum mechanical case discussed in ref. [2], the combination of reality and boundedness of the action and the presence of a unique critical point makes the domain of integration of our path integral a single Lefschetz thimble away from Stokes lines. In this way Borel summability of the perturbative series to the exact result is guaranteed [2].[4] The above derivation is easily generalizable for multiple scalar fields.

If the minimum of the classical potential is not the global one, we generally have more than one finite action critical point (e.g. bounce solutions), the domain of integration of the path integral is on a Stokes line and correspondingly the perturbative series will not be Borel resummable. When the global minimum is not unique due to spontaneous symmetry breaking, by definition the action has multiple finite action critical points.[5] At finite volume, this would again imply that the domain of integration of the path integral is on a Stokes line and the perturbative series is non Borel resummable. In the infinite volume limit, however, all such vacua are disconnected from each other and the path integral should be taken in such a way that only one of such vacua is selected. This request is crucial to guarantee that correlation functions satisfy the cluster decomposition property. The vacuum selection is achieved by adding a small explicit symmetry breaking term in the action that removes the degeneracy, taking the infinite volume limit, and then removing the extra term (more on this in the next subsection). In the infinite volume limit we are now in the same situation as before with a single global minimum. The generalized Derrick's theorem forbids the existence of finite action solutions. The loopwise expansion around the selected vacuum $\phi^i = \phi^i_0$ can be interpreted as the saddle point expansion over a Lefschetz thimble and Borel summability is guaranteed. This argument does not apply to scalar theories with a continuous family of degenerate vacua in $d = 2$, because Derrick theorem does not hold in this case.[6] In particular, our results imply that 2d and 3d ϕ^4 theories with $m^2 < 0$, whose Borel resummability was not established before (see e.g. chapter 23.2 of ref. [60]), are in fact Borel resummable.

The discussion above applies in the absence of phase transitions. Whenever they occur at some finite values of the couplings, the analysis is more subtle because the infinite volume limit has to be taken with more care. In the following subsection we discuss in some detail the case of the ϕ^4 theory in $d = 2$ dimensions.

[3] The fact that $\mathcal{B}(\hbar t)$ is indeed a function of the product $\hbar t$ was shown explicitly in ref. [2].

[4] Derrick's argument about the absence of non-trivial critical points in scalar theories formally work also for non-integer dimensions. As such it could in principle be used as above to show the Borel summability of the ϵ-expansion. However, this reasoning would require a non-perturbative definition of the path integral of theories with non-integer dimensions, which is unknown to us.

[5] We do not discuss here the subtle case of degenerate vacua not related by symmetries.

[6] The connection between the absence of positive action critical points and the Borel summability of the perturbative series was proposed already in ref. [23], which also noted the intriguing relation between Borel summability and the existence of spontaneous symmetry breaking. However, the arguments of ref. [23] could not establish that the resummed series reproduce the exact result, while the Lefschetz thimble perspective allows us to fill this gap and to put on firmer grounds the conjecture of ref. [23].

5.1.1 Borel Summability and Phase Transitions in the ϕ^4 theory

We consider here

$$V(\phi) = \frac{1}{2}m^2\phi^2 + \lambda\phi^4\,, \tag{5.6}$$

with $m^2 > 0$, $\lambda > 0$ in $d = 2$ dimensions. We can set $\hbar = 1$, since the loopwise expansion is equivalent to the expansion in $g = \lambda/m^2$. For small enough g the theory has a mass gap and the Schwinger functions are expected to be analytic in the coupling. The situation becomes more delicate at and beyond the critical point $g \geq g_c$ where the theory undergoes a second order phase-transition [57, 61]. The latter typically suggests the presence of non-analyticities of n-point functions around the critical point. On the other hand, the r.h.s. of eq. (5.5) could be well defined for any g, suggesting that the Schwinger functions could be smooth even beyond g_c. Consider for example the 1-point function $\langle\phi\rangle$, order parameter of the $\mathbb{Z}_2$ symmetry breaking. Since the path integral is an odd function of ϕ, $\langle\phi\rangle$ is obviously identically zero, and thus analytic and Borel summable, for any value of g. For $g < g_c$, $\langle\phi\rangle = 0$ is the correct result, but for $g > g_c$ the theory is in a $\mathbb{Z}_2$ broken phase and it fails to reproduce the correct value of the order parameter $\pm v \neq 0$.

The apparent paradox is explained by recalling that vacuum selection in presence of spontaneous symmetry breaking requires the introduction of an explicit $\mathbb{Z}_2$ symmetry breaking term ϵ which should be turned off only *after* the infinite volume limit is taken.[7] Phase transitions show up as non-analiticities of the correlation functions F after the $V \to \infty$ and $\epsilon \to 0$ limits are taken. We should consider the theory in a finite volume V and modify the action as, for example,

$$S_{V,\epsilon}[\phi] = S_V[\phi] + \epsilon \int_V d^2x\, \phi(x)\,, \tag{5.7}$$

and define the correlation functions as

$$F_{\rm SSB} \equiv \lim_{\epsilon\to 0} \lim_{V\to\infty} F_\epsilon(V)\,, \tag{5.8}$$

where, crucially, the limit $\epsilon \to 0$ is taken after the infinite volume one. In our arguments about Borel summability of scalar theories with a classically unique global minimum neither V nor ϵ entered in the discussion, since we had $V = \infty$ and $\epsilon = 0$ to start with. The Schwinger functions F that are reconstructed by Borel resummation in this way would correspond to take the limits in the opposite way:

$$F \equiv \lim_{V\to\infty} \lim_{\epsilon\to 0} F_\epsilon(V)\,. \tag{5.9}$$

For $g \geq g_c$ we expect that $F \neq F_{\rm SSB}$ as a result of the non commutativity of the two limits. In particular, for the one-point function we would have

$$\begin{aligned} \langle\phi\rangle_{\rm SSB} &= v \lim_{\epsilon\to 0^\pm} \text{sign}\,(\epsilon)\,, \\ \langle\phi\rangle &= 0\,, \end{aligned} \tag{5.10}$$

where v is the non-perturbative value of the order parameter.

Resummation of the perturbative series for F in the presence of an explicit breaking term is not straightforward (there is actually no need to consider finite volume, since this limit should

[7] In textbook perturbative treatments of spontaneous symmetry breaking such procedure is not necessary because we select "by hand" the vacuum around which to expand our fields according to the minima of the classical (or perturbative effective) potential.

be taken first). Denoting by $|\pm\rangle$ the two vacua in the $\mathbb{Z}_2$ breaking phase, in the absence of the proper $\epsilon \to 0$ limit selecting either the vacuum $|+\rangle$ or $|-\rangle$, for $g \geq g_c$ the vacuum is a linear combination of the form

$$|\alpha\rangle = \cos\alpha|+\rangle + \sin\alpha|-\rangle\,. \tag{5.11}$$

The condition $\langle\phi\rangle = 0$ fixes $\alpha = \pi/4$ in eq. (5.11), but it is useful to keep it generic in what follows. The Schwinger functions F for $g \geq g_c$ correspond then to correlation functions around the vacuum $|\alpha\rangle$. As well-known, such vacua violate cluster decomposition (see e.g. the end of section 19.1 of ref. [62]). This can easily be seen by considering for instance the large distance behavior of the connected two-point function $\langle\phi(x)\phi(0)\rangle_c$:

$$\lim_{|x|\to\infty} \langle\alpha|\phi(x)\phi(0)|\alpha\rangle_c = \sum_{n=\pm} \langle\alpha|\phi(0)|n\rangle\langle n|\phi(0)|\alpha\rangle - \langle\alpha|\phi(0)|\alpha\rangle^2 = \sin^2(2\alpha)v^2\,, \tag{5.12}$$

which does not vanish for $\alpha = \pi/4$ (while it does for $\alpha = 0, \pi/2$, as expected).

Summarizing, Borel resummation of perturbation theory around the unbroken vacuum, when applied beyond the phase transition point and without explicit breaking terms, reconstructs the correlation functions F in the wrong vacuum where cluster decomposition is violated. The correlation functions F do not coincide with the ordinary ones, $F_{\rm SSB}$, in the broken phase in any of the two vacua $|\pm\rangle$.

We will mostly focus our attention on the simplest Schwinger functions, the 0- and the 2-pt functions. The presence of a phase transition can still be detected by looking at the mass $M(g)$ as a function of the coupling and defining g_c as $M(g = g_c) = 0$. Since the vacua $|\pm\rangle$ are degenerate, the vacuum energy Λ, computed in the $|\alpha\rangle$ vacuum through resummation for $g \geq g_c$, is expected to coincide with the vacuum energy in any of the two $\mathbb{Z}_2$ broken vacua.

The interpretation of the resummed mass gap $|M|$ for $g \gtrsim g_c$ is more subtle and we postpone the discussion of this region in ref. [4]. In all the plots we present in Section 5.5, the region with $g > g_c$ is shaded to highlight the $\mathbb{Z}_2$ unbroken phase $0 \leq g \leq g_c$, where our computations should not present any subtleties.

5.2 Renormalization and Chang Duality

The superficial degree of divergence δ of a connected Feynman graph $\mathcal{G}$ in 2d scalar theories without derivative interactions is simply given by

$$\delta(\mathcal{G}) = 2L - 2I = 2 - 2V\,, \tag{5.13}$$

where L is the number of loops, I the number of internal lines, V the number of vertices and the last expression follows from $I = L + V - 1$. The only superficially divergent graphs are therefore those with 0 and 1 vertex. The former correspond to the divergence of normalization of the free-theory path integral, while the latter correspond to diagrams with loops from contraction of fields in the same vertex. It follows that 2d theories without derivative interactions can be renormalized simply by normal ordering. In particular in the ϕ^4 theory superficial divergences only occur in the 0-point function from $V = 0$ and $V = 1$ graphs (the 2-loop "8"-shaped graph), and in the momentum independent part of the 2-point function with $V = 1$ (1-loop tadpole propagator graph). Correspondingly, only the vacuum energy and the mass term require the introduction of the counterterms $\delta\Lambda$ and δm^2. We choose δm^2 such that it completely cancels the contribution coming from the tadpole diagram (see Figure 5.1). In dimensional regularization,

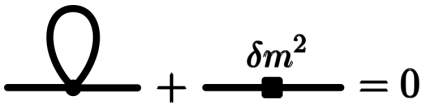

Figure 5.1: The divergent one-loop diagram is exactly canceled by the mass counterterm. Within this scheme we can forget all the diagrams with lines that start and end at the same quartic vertex, their contribution being zero.

with $d = 2 - \epsilon$, it reads

$$\delta m^2 = -\frac{6\lambda}{\pi\epsilon} + \frac{3\lambda}{\pi}\left(\gamma_E + \log\frac{m^2}{4\pi}\right) + \mathcal{O}(\epsilon)\,, \tag{5.14}$$

where γ_E is the Euler's constant. We choose $\delta\Lambda$ such that it completely cancels the one and two-loop divergencies described above, so that $\Lambda = \mathcal{O}(g^2)$. The presence of these counterterms makes all n-point Schwinger functions finite to all orders in perturbation theory. The scheme above is a modified version of the minimal subtraction scheme and coincides with the normal ordering, which is commonly used in other calculations of the ϕ^4 theory. This makes possible a direct comparison of scheme-dependent quantities such as the value of the critical coupling g_c (see Section 5.6).

As pointed out by Chang [57] a simple duality can be established between the theories with positive and negative squared mass terms (see also ref. [63] for a nice recent discussion) which in the following will be identified respectively with the Lagrangian densities $\mathcal{L}$ and $\mathcal{L}'$. Neglecting for simplicity the vacuum energy counterterms, we have

$$\mathcal{L} = \frac{1}{2}(\partial\phi)^2 + \frac{1}{2}m^2\phi^2 + \lambda\phi^4 + \frac{1}{2}\delta m^2\phi^2\,, \qquad m^2 > 0\,,\ \lambda > 0\,, \tag{5.15}$$

$$\mathcal{L}' = \frac{1}{2}(\partial\phi)^2 - \frac{1}{4}\widetilde{m}^2\phi^2 + \lambda\phi^4 + \frac{1}{2}\delta\widetilde{m}^2\phi^2\,, \qquad \widetilde{m}^2 > 0\,,\ \lambda > 0\,, \tag{5.16}$$

where the counterterm $\delta\widetilde{m}^2$ is also chosen in the normal ordering scheme—i.e. in dimensional regularization it is determined by an equation analogous to (5.14) where m^2 is replaced by $\widetilde{m}^2$. We can then add and subtract the term $\delta\widetilde{m}^2\phi^2/2$ to $\mathcal{L}$ to obtain

$$\mathcal{L} = \frac{1}{2}(\partial\phi)^2 + \frac{1}{2}\left(m^2 + \frac{3\lambda}{\pi}\log\frac{m^2}{\widetilde{m}^2}\right)\phi^2 + \lambda\phi^4 + \frac{1}{2}\delta\widetilde{m}^2\phi^2\,, \tag{5.17}$$

where we used eq. (5.14) and its analogous for $\delta\widetilde{m}^2$ to express the finite difference $\delta m^2 - \delta\widetilde{m}^2$. The Lagrangian $\mathcal{L}$ is then equivalent to the Lagrangian $\mathcal{L}'$ provided that

$$m^2 + \frac{3\lambda}{\pi}\log\frac{m^2}{\widetilde{m}^2} = -\frac{1}{2}\widetilde{m}^2\,, \tag{5.18}$$

or, equivalently expressed in terms of the dimensionless couplings $g = \lambda/m^2$ and $\widetilde{g} = \lambda/\widetilde{m}^2$,

$$\log g - \frac{\pi}{3g} = \log\widetilde{g} + \frac{\pi}{6\widetilde{g}}\,. \tag{5.19}$$

The equations above express the duality between one description in which the theory is quantized around the $\mathbb{Z}_2$-invariant vacuum state and one description in which the theory is quantized

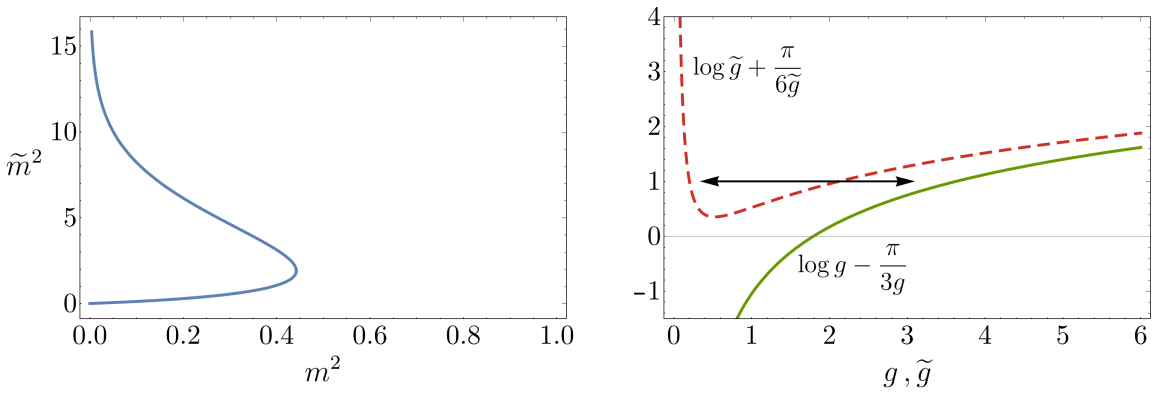

Figure 5.2: Chang duality expressed as the relation between the masses in eq. (5.18) for $\lambda = 1$ (left panel) and as the graphical solution of eq. (5.19) for the effective couplings g and $\widetilde{g}$ (right panel).

around a $\mathbb{Z}_2$-breaking vacuum. The dual description exists for all $g \geqslant g_\star$, with the point $g_\star$ determined by

$$g_\star = \frac{\pi}{3W(2/e)} \approx 2.26\,, \tag{5.20}$$

where $W(z)$ is the Lambert function. As can be inferred by looking at the right panel of Figure 5.2, for each value of g above $g_\star$ there are two solutions of eq. (5.19) in $\widetilde{g}$, one of which becomes weakly coupled and the other strongly coupled for $g \gg g_\star$. We will refer to this two solutions as the *weak* and *strong branch* of the duality. Keeping track of the vacuum energy terms in the above derivation one finds that the following finite vacuum energy term

$$\Delta\Lambda = \frac{1}{8\pi}(\widetilde{m}^2 - m^2) + \frac{1}{8\pi} m^2 \log\frac{m^2}{\widetilde{m}^2} + \frac{3\lambda}{16\pi^2}\left(\log\frac{m^2}{\widetilde{m}^2}\right)^2\,, \tag{5.21}$$

must be included in $\mathcal{L}'$ in order to have a complete match of the two theories.

The duality was originally used by Chang [57] to show that the theory with positive squared mass undergoes a phase transition. At small g we can use perturbation theory to argue that the $\mathbb{Z}_2$ symmetry is unbroken and $\langle\phi\rangle = 0$, while at strong coupling $g \gg g_\star$ we can use the perturbation theory of the weak branch of the dual description to argue that the $\mathbb{Z}_2$ symmetry is spontaneously broken and $\langle\phi\rangle \neq 0$. Hence, as we increase the coupling g from 0 to ∞, we will cross at some point a critical value of the coupling g_c at which the vacuum expectation value of ϕ becomes non-vanishing. This argument proves the existence of a phase transition in the two-dimensional ϕ^4 theory, which, by the theorems of Simon and Griffiths [58], cannot be of first order. It is in fact of second order, as supported by Monte Carlo simulations [64–66], as well as by computations using DLCQ [67], density matrix renormalization group [68], matrix product states [69], and the Hamiltonian truncation [63, 70–72]

5.3 Numerical Determination of the Borel Function and Error Estimate

Since the series we will obtain in QFT are rather short in comparison to the ones in QM and, furthermore, they will be subject to numerical uncertainties, we need to develop a bit more the methods we introduced in Section 2.3 in order to get sensible results. The goal of this section

is to systematize and optimize the approximation of the Borel functions in the case of short perturbation series and, at the same time, to introduce procedures to estimate the error of the resummation. The strategy we adopt is based on the apparent convergence of the result and the stability of the latter with respect to the variation of some spurious parameter. For instance, we will use the sensitivity of the Borel resummed $F(g)$

$$F_B(g) = \frac{1}{g^{1+b}} \int_0^\infty dt\, t^b e^{-t/g} \mathcal{B}_b(t)\,, \tag{5.22}$$

with respect to the Le Roy parameter b. The exact function $F_B(g)$ is clearly independent of b, but a dependence will remain in approximations based on truncated series. As we will see, such dependence can be used both to improve the accuracy of the numerical approximation and to estimate its error. In the following subsections we give a detailed description of our methods, allowing the interested reader to reproduce our results.[8]

5.3.1 Conformal Mapping

We further develop here the conformal mapping method of Subsection 2.3.2 for the Borel transform of the function $F(g)$.[9] In order to improve the convergence of the u-series and at the same time to have more control on the accuracy of the results, we introduce, in addition to the Le Roy parameter b, another summation variable s [74] and write

$$\begin{aligned} F_B(g) &= \frac{1}{g} \int_0^\infty dt \left(\frac{t}{g}\right)^b e^{-t/g} \sum_{n=0}^\infty \frac{F_n}{\Gamma(n+b+1)} t^n = \frac{1}{g^{b+1}} \int_0^1 du\, \frac{dt}{du} e^{-t(u)/g} \frac{t^b(u)}{(1-u)^{2s}} \sum_{n=0}^\infty \widetilde{B}_n^{(b,s)} u^n \\ &= \frac{1}{g^{b+1}} \sum_{n=0}^N \widetilde{B}_n^{(b,s)} \int_0^1 du\, \frac{dt}{du} e^{-t(u)/g} \frac{t^b(u) u^n}{(1-u)^{2s}} + R^{(N)}(g) \equiv F_B^{(N)}(g) + R^{(N)}(g)\,, \end{aligned} \tag{5.23}$$

where $R^{(N)}$ is the error associated to the series truncation and $\widetilde{B}_n^{(b,s)}$ are the coefficients of the Taylor expansion of the function $\widetilde{\mathcal{B}}_{b,s}(u) \equiv (1-u)^{2s} \widetilde{\mathcal{B}}_b(u)$. The convergence of the series above ensures that $\lim_{N\to\infty} R^{(N)} = 0$. The use of the modified function $\widetilde{\mathcal{B}}_{b,s}$ allows us to better parametrize Borel functions with an arbitrary polynomial behavior at infinity. At fixed order N, for $g \to \infty$ the integral in eq. (5.23) is dominated by the region $u \simeq 1$. It is immediate to see that in this limit each term in the series behaves similarly, and we have $F_B(g) \sim g^s$ for $g \to \infty$. Although the exact observable $F(g)$ is independent of the resummation parameters b and s, a proper choice of s, the one that will more closely resemble the actual behavior of $F(g)$ at large g, can improve the accuracy of the truncated series.

The values of the parameters b and s to use in the resummation are determined by maximizing the convergence of the series and minimizing the sensitivities to b and s. More specifically, we identify a sensible region in the (b, s) parameter space and choose the values b_0 and s_0 that minimize the following quantity:

$$\Delta F_B^{(N)} = \sum_{i=s,b} (\partial_i F_B^{(N)})^2 + \left(|F_B^{(N)} - F_B^{(N-1)}| - |F_B^{(N-1)} - F_B^{(N-2)}| \right)^2 . \tag{5.24}$$

[8] Most of the results based on these resummation techniques in the literature are not very detailed, making hard to reproduce the results (see ref. [73] for a recent notable exception in the context of the ϵ-expansion).

[9] The expansion parameter is denoted here as g instead of λ.

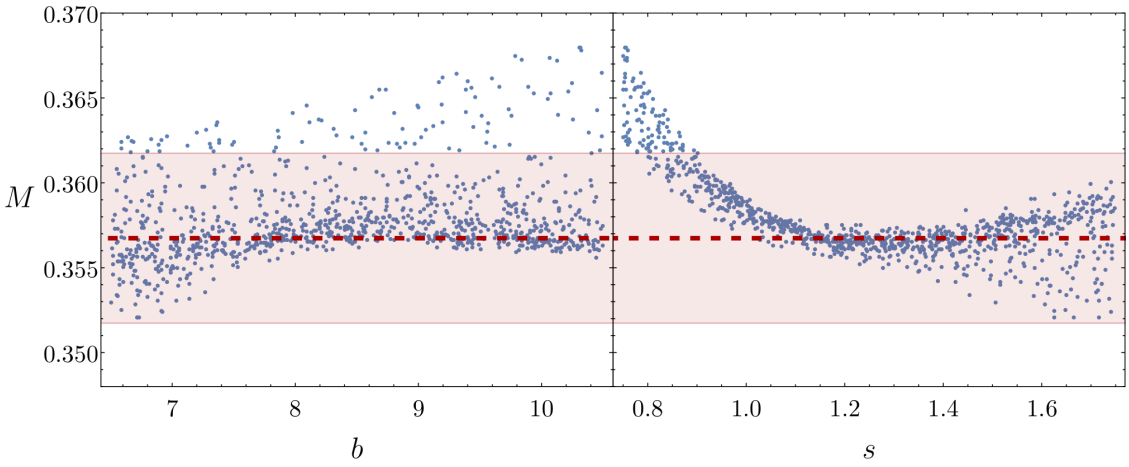

Figure 5.3: Estimate of the error in the resummation of the physical mass M in the $\mathbb{Z}_2$-symmetric phase of the theory at coupling $g = 2$. The blue points are the values of $F_{B,k}^{(N=8)}$ as function of the parameters s and b. The red dashed line is the central value of the resummation obtained for $s_0 = 5/4$, $b_0 = 17/2$. The red band is the final error on the resummation computed as in (5.25).

The first term in eq. (5.24) measures the sensitivity of the observables to b and s, while the second term measures how fast the series is converging. In order not to disfavor an oscillatory convergence of $F_B^{(N)}$ to a monotonic one, we compute the difference of the differences rather than the simple differences among different loop orders. Eq. (5.24) is computed at order N for different values of g. For both the mass and the vacuum energy the values of $s_0^{(N)}$ and $b_0^{(N)}$ do not sensitively depend on the value of g (s_0 shows also a mild dependence on N, as expected, given its interpretation in terms of the large coupling behavior of the observable) so we can fix them once and for all for each observable considered. The central value of our final estimate is given by $F_B^{(N)}(s_0^{(N)}, b_0^{(N)})$. The final error is taken as follows:

$$\mathrm{Err}_{\mathrm{CM}}\, F_B^{(N)} = \left(\frac{1}{\Delta s} + \frac{1}{\Delta b}\right) \frac{1}{K} \sum_{k=1}^{K} \left| F_{B,k}^{(N)} - F_B^{(N)} \right| + |F_B^{(N)} - F_B^{(N-1)}|\,, \tag{5.25}$$

where the first term in the above equation takes into account both the residual dependence of the resummation on the parameters (s, b) and the uncertainty in the knowledge of the coefficients (which is however subdominant). It is obtained by generating a set of $K = 200$ evaluations $F_{B,k}^{(N)}$ in which the parameters $s_k \in [s_0 - \Delta s, s_0 + \Delta s]$ and $b_k \in [b_0 - \Delta b, b_0 + \Delta b]$ are randomly generated with a flat distribution and the coefficients of the series are varied with a gaussian distribution around their central value and with a standard deviation equal to the reported error. The contribution to the final error is then computed as the mean of the differences between $F_{B,k}^{(N)}$ and the central value $F_B^{(N)}$ (in absolute value) weighted by the factor $(1/\Delta s + 1/\Delta b)$, thus reproducing a sort of discrete derivative in the parameter space. We find this method more robust than a simple estimate based on the derivatives of $F_B^{(N)}$ w.r.t. s and b, which tends to underestimate the error on very flat distributions. In the following we set $\Delta s = 1/2$ and $\Delta b = 2$. In Figure 5.3 we report as an example the points $F_{B,k}^{(N=8)}$ for the physical mass at coupling $g = 2$ together with a red band representing the error computed by eq. (5.25). We should emphasize that the error estimate above is subject to some arbitrariness and, as such, it should be seen in a statistical sense as roughly giving one standard deviation from the mean.

As mentioned mentioned in Subsection 2.3.2, there is an important assumption underlying the conformal mapping method. All other singularities of the Borel function $\mathcal{B}(t)$ beyond the one at $t = 1/|a|$ should be located on the negative real t-axis, so that they are all mapped at the boundary of the u-unit disc. Possible singularities away from the negative t-axis would be mapped inside the u-unit disc, reducing the radius of convergence of the u series and invalidating eq. (2.20) and the analysis that follows. These singularities would arise from classical solutions to the ϕ equation of motion with both a real and an imaginary component. The absence of such solutions has been proved in the 1d ϕ^4 theory (the quartic anharmonic oscillator) but not in the 2d or 3d ϕ^4 theories. Using the conformal mapping to our truncated series, we do not see instabilities related to the possible presence of such singularities. This justifies, a posteriori, the plausibility of the assumption.

5.3.2 Padé-Borel Approximants

The Padé-Borel method relies on fewer assumption than the conformal mapping method and thus it is a better choice in the study of Borel functions for which the analytic properties are unknown. However, at low orders in perturbation theory, the method is hindered by the presence of spurious poles on (or very close to) the positive real axis, which give rise to numerical instabilities. At a given order $[m/n]$, the location of the poles depends on b and dangerous poles might be avoided by a proper choice of this parameter. If there is no sensible choice of b that remove them all, the approximant $[m/n]$ is disregarded. For the remaining approximants we proceed as follows. At fixed b and order N, we can have at most $N + 1$ different estimates given by $[0/N], [1/(N-1)], \ldots, [N/0]$. Each of them has a different behavior as $g \to \infty$: $\mathcal{B}_b^{[m/n]}(g) \sim g^{m-n}$. Suppose the exact Borel function approaches a power like behavior of the form $\mathcal{B}(g) \sim g^s$ as $g \to \infty$, leading to $F_B(g) \sim g^s$ in the same limit. If we knew s, it would be clear that the best Padé-Borel approximant would be given by rational functions of order $[(N+[s])/2, (N-[s])/2)]$, with $[s]$ being the integer value closest to s (and with the appropriate even or odd N). As N varies, we would expect that the value of $\mathcal{B}^{[(N+[s])/2,(N-[s])/2)]}(t)$ as $t \to \infty$ would be fairly stable and asymptote the value of $\mathcal{B}(t)$ as $t \to \infty$. When s is unknown, like in our case, the Padé-Borel approximant with the asymptotic behavior closest to the would-be correct one can be found by comparing the $t \to \infty$ limit of Padé-Borel approximants with the same value of $m - n$ as N varies, and take the series that shows the stablest results [33]. This procedure can be done scanning over different values of the parameter b or for the selected value of b, as explained below. In both cases, the procedure gives always the same answer for the optimal value of $m - n$ to take. Once $m - n \equiv s_0$ is fixed, we can consider all the Padé-Borel approximants $[(s_0+n)/n]$ for different values of n that are free of dangerous poles. We then take the highest approximant $[(s_0 + n_{\max})/n_{\max}]$ as our best approximation to the Borel function.[10] The value of s_0 selected as above is always consistent with the one obtained using the conformal mapping, as explained in subsection 2.3.2, providing a good consistency check.

The possible presence of spurious poles makes inadequate to fix the parameter b by a scanning procedure like in the conformal mapping case. It can however be chosen by knowing the large order behavior of the coefficients (5.38). If we take the parameter b of the Borel-Le Roy transform equal to the one analytically determined in eq. (5.40), then the Gamma function of the large order behavior is exactly canceled, so that the leading singularity of the Borel function at

[10] If $s_0 + 2n_{\max}$ equals $N - 1$, rather than N, we are effectively not using the g^N coefficient of the series. The latter can however be used to compute $[(s_0 + n_{\max})/(n_{\max} + 1)]$ or $[(s_0 + n_{\max} + 1)/n_{\max}]$ approximants to test the stability of the result.

$t = 1/a$ is expected to be close to a simple pole[11] and should be more easily reproduced by Padé-Borel functions that can only have pole singularities. If such value of b gives rise to an unstable approximant, we move away from this value until a stable approximant is found at $b = b_0$. We then take the Padé-Borel approximant $F_{b_0}^{[(s_0+n_{\max})/n_{\max}]} \equiv \hat{F}_{n_{\max}}$ as our best choice.

The error estimate (subject again to some arbitrariness) is taken as follows:

$$\mathrm{Err}\, \hat{F}_{n_{\max}} = |\partial_{\log b} \hat{F}_{n_{\max}}|_{b_0} + |\hat{F}_{n_{\max}} - \hat{F}_{n_{\max}-1}| + \Delta^{(s_0+2n_{\max})} \,. \tag{5.26}$$

The term $\Delta^{(s_0+2n_{\max})}$ represents the contribution of the error in the knowledge of the perturbative coefficients. It is determined by generating a set of 100 random coefficients with a gaussian distribution, with mean and standard deviation as given in eqs.(5.30) and (5.37). We correspondingly get an approximate gaussian distribution for the 100 output values of $\hat{F}_{n_{\max}}$ and identify $\Delta^{(s_0+2n_{\max})}$ as the standard deviation of this output distribution. The factor $\Delta^{(s_0+2n_{\max})}$ is typically sub-dominant with respect to the other error terms.

The conformal mapping method generally gives more accurate results than Padé-Borel approximants. Moreover, the presence of spurious poles hinders a systematic use of the latter. We have mostly used Padé-Borel approximants as a consistency check of the results found using the conformal mapping. An exception is given in section 5.5.2 where, in order to extract the critical exponent ν, we resum the inverse of the logarithmic derivative of the physical mass. In that case the conformal mapping gives poor results and Padé-Borel approximants are preferred.

5.4 Perturbative Coefficients for the Symmetric Phase

The renormalization scheme adopted is particularly useful for perturbative computations, since a large set of diagrams—those involving self-contractions—is identically zero (their contribution in a different scheme can be reproduced by a proper shift of the mass). In the following we focus on the 0- and the 2-point functions. Multi-loops computations present two obvious challenges: i) classifying the topologically distinct graphs and computing their multiplicities, ii) evaluating the loop integrals. In the ϕ^4 theory point i) can be addressed with a number of tools (e.g. FORM, FeynArts, QGRAF, ...) but we find that it is possible to perform brute force Wick contractions with a simple Mathematica code up to the order g^6. In order to overcome memory limitations and reach the order g^8 we use the method described in ref. [75]. A non-trivial check of the topologies and multiplicities of the Feynman diagrams is performed in the one-dimensional ϕ^4 theory by verifying that the integration of the diagrams reproduces the perturbative series of the quantum mechanical anharmonic oscillator, which can easily be computed to very high orders with the recursion relations by Bender and Wu [10, 45].

An analytic approach to point ii) is possible but quite challenging, so we opt for a numerical evaluation of the loop integrals. To this purpose it is convenient to write the Feynman diagrams in configuration, rather than momentum, space. The tree-level two-point function reads

$$G_0(x) = \frac{1}{2\pi} K_0(mx) \,, \tag{5.27}$$

where $x = \sqrt{x_\mu x_\mu}$ and K_n is the modified Bessel function. For large x, $K_0(x) \propto e^{-x}/\sqrt{x}$ and such exponential decay of G_0 makes a configuration space approach quite suitable to a numerical evaluation. We perform the integration of the diagrams in polar coordinates using the Monte Carlo VEGAS algorithm [76] as implemented in the `python` module `vegas`. Since the number of

[11] The singularity is not exactly a pole because of the $1/k$ corrections in eq. (5.38).

g	g^2	g^3	g^4	g^5	g^6	g^7	g^8
0	1	1	3	6	19	50	204

Table 5.1: Number of topologically distinct 1PI 0-pt diagrams without self-contractions.

different topologies rapidly increases with the order, calculating diagram by diagram becomes unpractical and summing up the diagrams seems a better approach. However, summing up many diagrams, and thus evaluating more complicated integrals, leads to a less precise estimate of the integral. For these reasons we find convenient to split the diagrams in bunches (ranging from 5 to 40 diagrams each) in such a way to have a balance between the number of evaluations and the final precision obtained. Typically the number of points used in the Monte Carlo integration for each bunch is 10^9 at order g^8, which roughly delivers a precision of 10^{-5} in the estimate of the integral. Since order by order different diagrams contribute with the same sign the precision improves in the final sum. We checked the numerical convergence of the integrals when the number of points is increased.

5.4.1 Vacuum Energy

We compute the vacuum energy up to order g^8, which corresponds to evaluate one-particle irreducible (1PI) graphs with up to nine loops. The number of topologically distinct graphs (in the chosen scheme) as a function of g is reported in table 5.1. For illustration, up to order g^4, these are

$\Lambda = -12$  $g^2 + 288$  $g^3 +$ (5.28)

$-\Big(2304$ 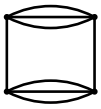 $+ 2592$ 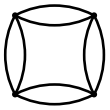 $+ 10368$  $\Big) g^4 + \mathcal{O}(g^5)\,,$ (5.29)

where the numbers indicate the multiplicities of the different topologies.

Evaluating all Feynman diagrams leads to our final expression for the perturbative expansion of Λ up to g^8 order:

$$\begin{aligned}\frac{\Lambda}{m^2} = &-\frac{21\zeta(3)}{16\pi^3}\,g^2 + \frac{27\zeta(3)}{8\pi^4}\,g^3 - 0.116125964(91)\,g^4 + 0.3949534(18)\,g^5 \\ &- 1.629794(22)\,g^6 + 7.85404(21)\,g^7 - 43.1920(21)\,g^8 + \mathcal{O}(g^9)\,.\end{aligned} \tag{5.30}$$

The numbers in parenthesis indicate the error in the last two digits due to the numerical integration. The coefficients proportional to g^2 and g^3 are computed analytically.[12]

5.4.2 Physical Mass

The mass gap can be defined directly from the 2-pt function as $M = -\lim_{x\to\infty} \log(\langle\phi(x)\phi(0)\rangle)/x$. Equivalently, it can be computed from the smallest zero of the 1PI two-point function for complex values of the Euclidean momentum (corresponding to the real on-shell momentum in Minkowski space):

$$\widetilde{\Gamma}_2(p^2 = -M^2) \equiv 0\,, \tag{5.31}$$

[12] We thank A.L. Fitzpatrick for having pointed out to us that the g^3 coefficient can be analytically computed.

g	g^2	g^3	g^4	g^5	g^6	g^7	g^8
0	1	2	6	19	75	317	1622

Table 5.2: Number of topologically distinct 1PI 2-pt diagrams without self-contractions.

where

$$\widetilde{\Gamma}_2(p^2) = \int d^2x\, e^{ip\cdot x}\, \Gamma_2(x) = p^2 + m^2 + \mathcal{O}(g^2) \tag{5.32}$$

is the Fourier transform of the configuration space 1PI two-point function $\Gamma_2(x)$, that has no correction of $\mathcal{O}(g)$ in the chosen scheme. We are interested to get an expansion of M^2 in powers of g of the form

$$M^2 = m^2(1 + \sum_{k=2} a_k\, g^k) \equiv m^2 + \delta\,. \tag{5.33}$$

Plugging eq. (5.33) in eq. (5.31) gives

$$0 = \widetilde{\Gamma}_2(-M^2) = \widetilde{\Gamma}_2(-m^2 - \delta) = \sum_{n=0} \frac{\widetilde{\Gamma}_2^{(n)}(-m^2)}{n!}(-\delta)^n\,, \tag{5.34}$$

where the Taylor coefficients can be computed directly as follows

$$\widetilde{\Gamma}_2^{(n)}(-m^2) \equiv \left[\frac{d}{dp^2}\right]^n \widetilde{\Gamma}_2(p^2)\Big|_{p^2=-m^2} = \frac{2\pi}{(-2m)^n}\int_0^\infty dx\, x^{n+1} I_n(mx)\Gamma_2(x)\,, \tag{5.35}$$

where in the integral x is the modulus of x^μ and $I_n(x)$ is the modified Bessel function of first kind. We then compute the series expansions

$$\widetilde{\Gamma}_2^{(n)}(-m^2) = m^{2-2n}\left(b_0^{(n)} + \sum_{k=2} b_k^{(n)}\; g^k\right), \qquad b_0^{(n)} = \delta_{n,1}\,, \tag{5.36}$$

and plug them in eq. (5.34) to find the series (5.33). The values of the coefficients $b_k^{(n)}$ necessary to get the series (5.33) up to $\mathcal{O}(g^8)$ are reported in Table B.1 in the appendix. We need to compute $\widetilde{\Gamma}_2^{(0)}$ up to $\mathcal{O}(g^8)$, $\widetilde{\Gamma}_2^{(1)}$ up to $\mathcal{O}(g^6)$, $\widetilde{\Gamma}_2^{(2)}$ up to $\mathcal{O}(g^4)$ and $\widetilde{\Gamma}_2^{(3)}$ to $\mathcal{O}(g^2)$. The order g^8 in the two-point function is equivalent to eight loops in perturbation theory. The number of topologically distinct non-vanishing graphs for $\Gamma_2(x)$ (in the chosen scheme) as a function of g is reported in table 5.2. For instance, up to order g^3, we have

$\Gamma_2 = -96$ $g^2 + \Big[1152$  $+ 3456$  $\Big] g^3 - \Big[41472$  $+ 13824$ 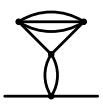

$+82944$  $+ 41472$ 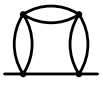 $+ 82944$  $+ 27648$ 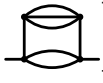 $\Big] g^4 + \mathcal{O}(g^5)\,,$

where the numbers indicate the multiplicities of the different topologies.

The final expression for the perturbative expansion of M^2 up to g^8 order is the following:

$$\begin{aligned}\frac{M^2}{m^2} = 1 - \frac{3}{2}\,g^2 + \left(\frac{9}{\pi} + \frac{63\zeta(3)}{2\pi^3}\right) g^3 - 14.655869(22)\, g^4 + 65.97308(43)\, g^5 + \\ - 347.8881(28)\, g^6 + 2077.703(36)\, g^7 - 13771.04(54)\, g^8 + \mathcal{O}(g^9)\,.\end{aligned} \tag{5.37}$$

Order	3	4	5	6	7	8
R_Λ	2.5059	0.9808	1.0051	0.9941	0.9931	0.9946
R_M	1.0040	0.9531	0.9113	0.9076	0.9158	0.9284

Table 5.3: Comparison between the ratio of ratios of the series for Λ and M^2 with their asymptotic values as given by eq. (5.38).

As for the vacuum energy, the numbers in parenthesis indicate the statistical errors due to the numerical integration. The coefficients up to order g^3 have been computed analytically. We have also computed the connected two-point function $G_2(x) \equiv \langle \phi(x)\phi(0) \rangle$ in configuration space for various values of x. This requires of course the evaluation of additional Feynman diagrams, connected but not 1PI. The knowledge of $G_2(x)$ as a function of x allows us to directly compute, in the critical regime, the exponent η, see Subsection 5.5.3. At fixed order g^n, the numerical computation of connected Schwinger functions is more demanding than the 1PI ones, because more integrals have to be performed, due to the presence of the external lines. For this reason, we have computed $G_2(x)$ up to order g^6. We report in table B.1 in the appendix the coefficients of the series expansion for some selected values of x.

5.4.3 Large Order Behavior

It is well known that the large order behavior of the perturbative expansion of n-point Schwinger functions G_n in certain QFTs, including 2d and 3d ϕ^4 theories, can be determined by looking at the semi-classical complex instanton configurations [8, 22–24]. In particular, ref. [77] worked out the details for the $d = 2$ and $d = 3$ $O(N)$ vector models (see also ref. [78] for a recent analysis of next-to-leading large order behavior in the 2d and 3d ϕ^4 theories). The coupling expansion for the Fourier transform of n-point functions at zero momentum $G_n = \sum_k G_n^{(k)} g^k$ behaves, for $k \gg 1$, as

$$G_n^{(k)} = c_n a^k \Gamma(k + b_n + 1)\Big(1 + \mathcal{O}(k^{-1})\Big)\,. \tag{5.38}$$

In eq. (5.38), a is an n-independent constant, proportional to the inverse of the classical action evaluated at the complex leading instanton configuration, while b_n and c_n are n-dependent parameters that require a detailed analysis of small fluctuations around the instanton configuration. The coefficient a can only be determined numerically, since the leading instanton solution is not known analytically. For $N = 1$, the case of interest, we find

$$a = -0.683708...\,, \tag{5.39}$$

in agreement with the results of ref. [77]. The parameter b_n can be determined analytically and for the 2d ϕ^4 theory ref. [77] finds

$$b_n = \frac{n}{2} + 1\,. \tag{5.40}$$

ref. [77] also determined the coefficient c_n, but since this expression is scheme-dependent, we will consider ratios of coefficients so that the dependence on this parameter will cancel out.

The parameters a and b_n play an important role when Borel resumming the perturbative series. From eq. (5.38) we see that the leading singularity of the Borel transform of G_n sits, for any n, at

$$t = -\frac{1}{a}\,. \tag{5.41}$$

g_c	ν	η	κ
2.807(34)	0.96(6)	0.244(28)	0.29(2)

Table 5.4: The values of the critical coupling g_c, the critical exponents ν, η and the 2-point function normalization κ at the critical point as defined in eq. (5.45), found in this work. The exact values of the exponents are $\nu = 1$ and $\eta = 1/4$ [79].

The knowledge of the position of this singularity allows us to use the conformal mapping method.

The large-order estimate (5.38) allows us to see how much our truncated series for Λ and M^2 differ from their asymptotic behavior. The closer the series is to its asymptotics, the better the resummation methods are to reconstruct non-perturbative results. To this aim let us define the ratios

$$r^{(k)}_{n,\text{asym}} = \frac{G^{(k)}_n}{G^{(k-1)}_n}\,, \qquad r^{(k)}_{\Lambda} = \frac{\Lambda^{(k)}}{\Lambda^{(k-1)}}\,, \qquad r^{(k)}_{M} = \frac{M^{2(k)}}{M^{2(k-1)}}\,, \tag{5.42}$$

where $\Lambda^{(k)}$ and $M^{2(k)}$ are the $\mathcal{O}(g^k)$ coefficients of the series expansions (5.30) and (5.37), and the ratio of ratios

$$R_\Lambda \equiv \frac{r^{(k)}_{0,\text{asym}}}{r^{(k)}_{\Lambda}}\,, \qquad R_M \equiv \frac{r^{(k)}_{2,\text{asym}}}{r^{(k)}_{M}}\,. \tag{5.43}$$

We report in table 5.3 R_Λ and R_M for different values of k. It is remarkable how close are the two series to their asymptotic estimates, already for low values of k. These results should be contrasted to the claimed poor convergence to the asymptotics in the ϵ-expansion, see e.g. table VI of ref. [73].[13]

5.5 Results for the Symmetric phase

We report in this section the results obtained by resumming the perturbative series as explained in Section 5.3. We compute the vacuum energy Λ and the physical mass M of the elementary field excitation ϕ as a function of the coupling constant g and we determine the critical value of the coupling g_c (defined as $M(g_c) = 0$) where the theory is expected to have a second-order phase transition. By resumming a proper function of M we compute the critical exponent ν, defined as

$$M(g) \propto |g_c - g|^\nu, \quad g \to g_c\,. \tag{5.44}$$

The exponent η is extracted directly by its definition as the power-like decay of the two-point function at the critical point, where the theory is a CFT:

$$\langle \phi(x)\phi(0)\rangle_{g=g_c} = \frac{\kappa}{|x|^\eta}\,. \tag{5.45}$$

We also compute the non-perturbative renormalization constant κ appearing in eq. (5.45), required to properly match the fundamental field ϕ with the 2d Ising magnetization operator σ. For the convenience of the reader, we report in Table 5.4 the values of g_c, ν, η and κ and in Figure 5.4 Λ and M as a function of g. These are the most important numerical results of the section. From now on we set for simplicity $m^2 = 1$.

[13] We notice, however, that ref. [73] compares individual coefficients and not their ratios.

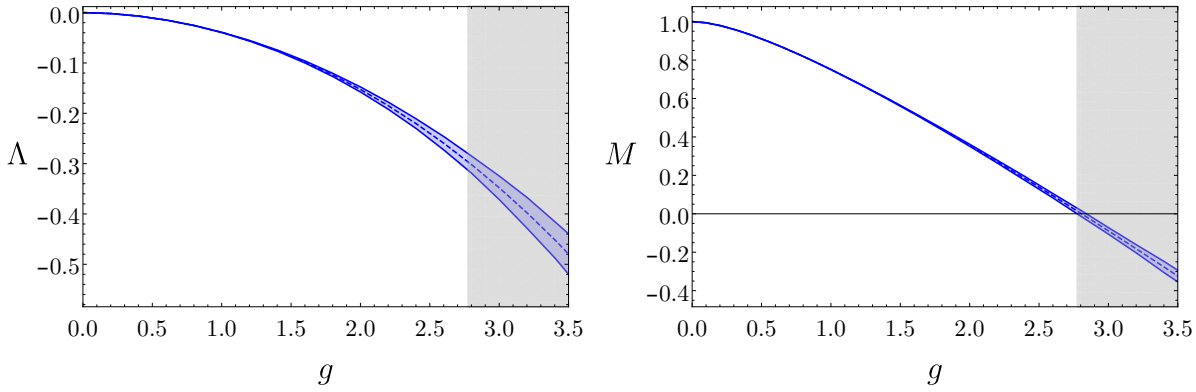

Figure 5.4: The vacuum energy Λ (left) and the mass gap M (right) as a function of the coupling constant g obtained by Borel resumming the perturbative series using the coefficients up to the g^8 order. The values reported of Λ and M for $g > g_c \approx 2.8$, where a phase transition occurs, refer to the extrapolation using the Borel resummed function.

5.5.1 Vacuum Energy

In the 2d ϕ^4 theory, regularized using a normal ordering prescription, the vacuum energy Λ is finite and calculable to all orders in perturbation theory. The perturbative expression for Λ up to order g^8 (i.e. nine loops) is reported in eq. (5.30). We show in the left panel of Figure 5.5 $\Lambda(g)$ in the weak coupling regime. The asymptotic nature of perturbation theory is manifest by comparing ordinary untruncated perturbation theory (blue dashed line) with optimal truncation of perturbation theory (red dotted line). In the former one keeps all the available perturbative coefficients independently of the value of g, while in the latter the number of terms that are kept in the series expansion changes as g varies, and decreases as g increases. Indeed, according to the large-order behavior (5.38), at fixed g the minimum error in the series expansion is obtained by keeping $N_{\text{Best}} \sim 1/(|a|g) \sim 1.5/g$ terms. For $g \lesssim 0.2$ optimal truncation and untruncated perturbation theory coincides and well approximate the Borel resummed result (black line). For $g \gtrsim 0.2$ untruncated perturbation theory breaks down, while optimal truncation, by removing more and more coefficients in the perturbative expansion, reproduces quite well the Borel resummed result up to $g \approx 0.4$, though with an increasingly unsuppressed error of order $\exp(-N_{\text{Best}})$. For $g \gtrsim 0.4$, N_{Best} is so low that optimal truncation becomes unreliable. We conclude that the region $g > 0.4$ is inaccessible in perturbation theory. The value of g where optimal truncation and untruncated perturbation theory differ depends on the order g^N reached and *decreases* as N *increases*. Increasing N by computing more and more terms in the perturbative series would result in a better and better accuracy at small coupling, but would not change the range of applicability of perturbation theory, which is always $g \lesssim 0.4$, independently of N.

In the right panel of Figure 5.5 we go at strong coupling and report the value of $\Lambda(g = 1)$ as a function of the number of coefficient terms used in the conformal mapping method. The resummation parameters used are $(s^{(5)} = 9/4,\, b^{(5)} = 9)$, $(s^{(6)} = 5/2,\, b^{(6)} = 13/4)$, $(s^{(7)} = 5/2,\, b^{(7)} = 11/2)$, $(s^{(8)} = 5/2,\, b^{(8)} = 37/4)$. The improvement as N increases is evident.

In the left panel of Figure 5.6 we plot $\Lambda(g)$ computed using the conformal mapping at order $N = 5, 6, 7, 8$. As N increases, Λ tends to bend more towards negative values. The convergence of the result is evident, with the $N = 7$ and $N = 8$ results overlapping with each other and indistinguishable in the figure.

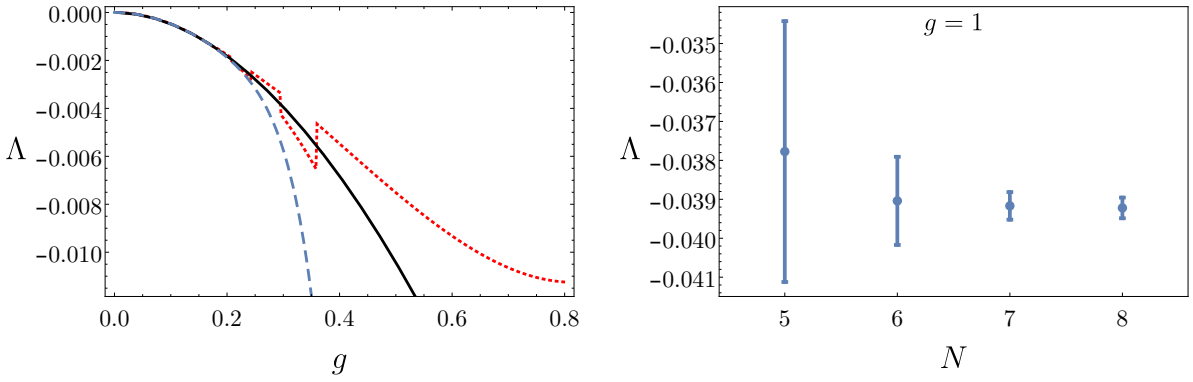

Figure 5.5: (Left panel) The vacuum energy Λ as a function of the coupling constant g obtained by ordinary perturbation theory up to the g^8 order (blue dashed line), optimal truncation (red dotted line) and Borel resummation using conformal mapping (black solid line). Notice how optimal truncation gives accurate predictions up to $g \lesssim 0.4$, in contrast to blind perturbation theory that breaks down for smaller values of the coupling $g \lesssim 0.2$. For $g \gtrsim 0.4$ the optimal truncation estimate breaks down, since we run out of perturbative terms. Errors are not reported to avoid clutter. (Right panel) Central value and error of $\Lambda(g = 1)$ as a function of the g^N terms kept in the conformal mapping resummation technique.

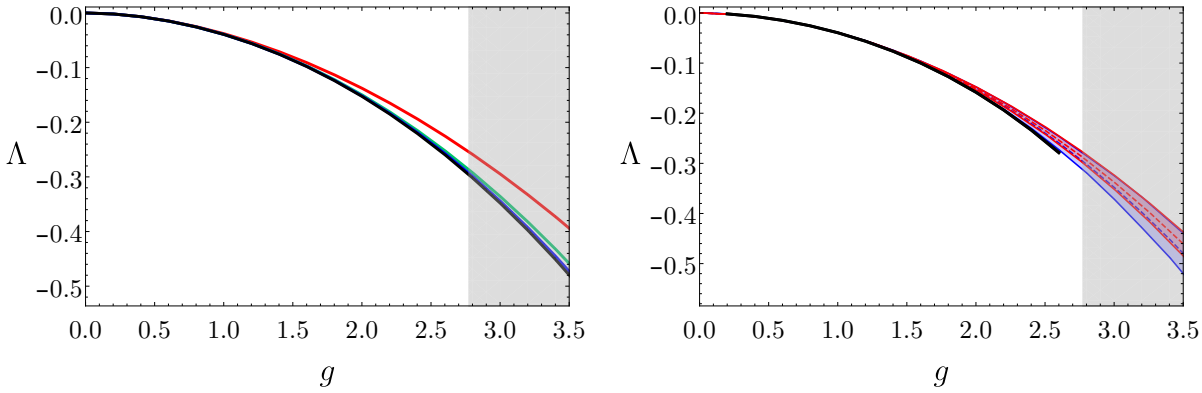

Figure 5.6: (Left panel) The vacuum energy Λ as a function of the coupling constant g using conformal mapping at different orders: $N = 5$ (red line), $N = 6$ (green line), $N = 7$ (blue line), $N = 8$ (black line). Errors are not reported to avoid clutter. The $N = 7$ and $N = 8$ lines are indistinguishable. (Right panel) Comparison between the results obtained using conformal mapping at $N = 8$ (light blue), Padé-Borel approximants (light red) and the results of ref. [80] (black).

In the right panel of Figure 5.6 we compare the conformal mapping at $N = 8$ with the Padé-Borel method and the results of ref. [80]. In order to avoid dangerous poles, in the Padé-Borel method we have removed the vanishing $\mathcal{O}(g^0)$ and $\mathcal{O}(g)$ coefficients from the series and effectively resummed $\Lambda(g)/g^2$. The approximant shown is [3/3] with $b = -3/4$. All the results are consistent with each other, with the results of ref. [80] consistently at the lower border of our error band for $g \gtrsim 2$, as probably expected, given the N-dependence shown in the left panel of Figure 5.6.

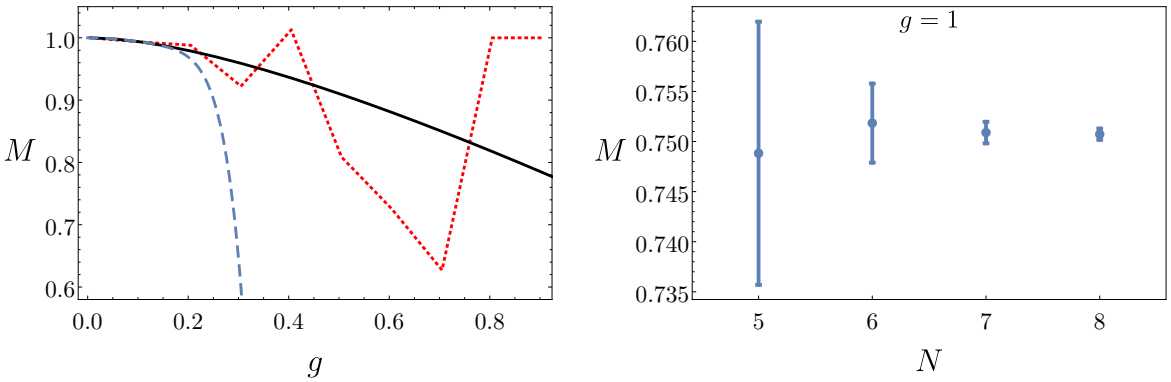

Figure 5.7: (Left panel) The physical mass M as a function of the coupling constant g obtained by ordinary perturbation theory up to the g^8 order (blue dashed line), optimal truncation (red dotted line) and Borel resummation using conformal mapping (black solid line). Notice how optimal truncation gives accurate predictions up to $g \lesssim 0.3$, in contrast to blind perturbation theory that breaks down for smaller values of the coupling $g \lesssim 0.15$. Errors are not reported to avoid clutter. (Right panel) Central value and error of $M(g = 1)$ as a function of the number of loops N kept in the conformal mapping resummation technique.

5.5.2 Physical Mass

The perturbative expression for M^2 up to order g^8 (i.e. eight loops) is reported in eq. (5.37). In the left panel of Figure 5.7 we show $M(g)$ in the weak coupling regime. The asymptotic nature of perturbation theory is manifest by comparing ordinary untruncated perturbation theory (blue dashed line) with optimal truncation of perturbation theory (red dotted line). For $g \lesssim 0.15$ optimal truncation and untruncated perturbation theory coincides and well approximate the Borel resummed result (black line). For $g \gtrsim 0.15$ untruncated perturbation theory breaks down while optimal truncation reproduces quite well the Borel resummed result up to $g \approx 0.3$, again with a quickly increasing error as N_{Best} decreases. For $g \gtrsim 0.3$ optimal truncation becomes unreliable. We conclude that the region $g > 0.3$ is inaccessible in perturbation theory.

In the right panel of Figure 5.7 we report the value of $M(g = 1)$ as a function of the number of coefficient terms used in the conformal mapping method. The resummation parameters used are $(s^{(5)} = 6/5,\ b^{(5)} = 4)$, $(s^{(6)} = 1,\ b^{(6)} = 4)$, $(s^{(7)} = 6/5,\ b^{(7)} = 6)$, $(s^{(8)} = 5/4,\ b^{(8)} = 17/2)$. The improvement as N increases is evident.

In the left panel of Figure 5.8 we plot $M(g)$ computed using the conformal mapping method at order $N = 5, 6, 7, 8$. The convergence of the result is evident, with the $N = 7$ and $N = 8$ results overlapping and indistinguishable in the figure.

In the right panel of Figure 5.8 we compare the conformal mapping at $N = 8$ with the Padé-Borel method and the results of ref. [80]. The approximant shown is $[4/3]$ with $b = 1$. All the results are nicely consistent with each other in the whole range of couplings shown.

5.5.3 Critical Regime

The critical coupling g_c where the second-order phase transition occurs is determined as

$$M(g_c) = 0\,. \tag{5.46}$$

We report in the left panel of Figure 5.9 the value of g_c using conformal mapping at different

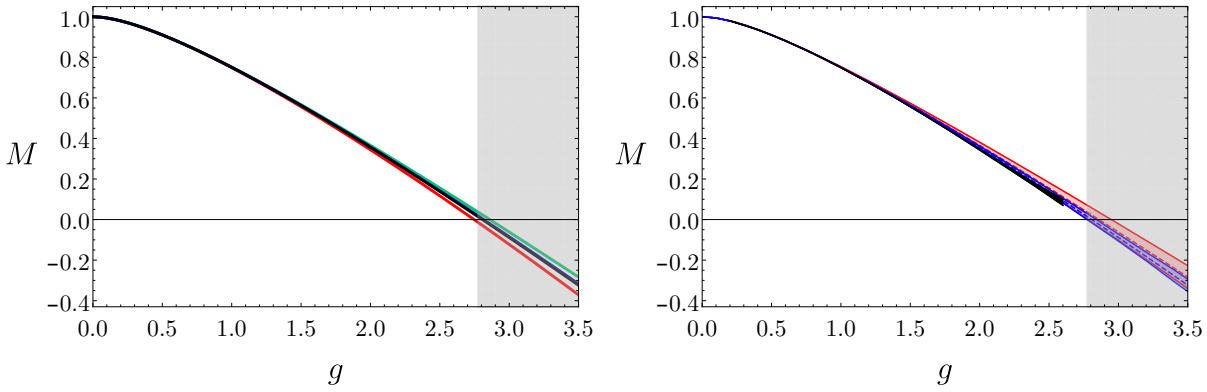

Figure 5.8: (Left panel) The physical mass M as a function of the coupling constant g using conformal mapping at different orders: $N = 5$ (red line), $N = 6$ (green line), $N = 7$ (blue line), $N = 8$ (black line). Errors are not reported to avoid clutter. The $N = 7$ and $N = 8$ lines are indistinguishable. (Right panel) Comparison between the results obtained using conformal mapping at $L = 8$ (light blue), Padé-Borel approximants (light red) and the results of ref. [80] (black).

orders. Our final estimate is given by

$$g_c = 2.807(34)\,. \tag{5.47}$$

We now turn to the determination of the critical exponents ν and η. The exponent ν, defined in eq. (5.44), is known to be exactly equal to 1 in the 2d Ising model, which is in the same universality class of the critical 2d ϕ^4 theory. In some sense, we have tacitly used before the information $\nu = 1$ in deciding to resum M instead of, say, M^2 or some other function of M. As a matter of fact, the accuracy of the results significantly depend on which mass function one decides to resum and the best choice should be given by the function that approaches the critical point smoothly, and has a simple zero at $g = g_c$, i.e. $M(g)$. This expectation is fully confirmed by our analysis. Since the Borel resummed mass is an analytic function of the coupling, by resumming $M(g)$ we would automatically, but somewhat trivially, obtain $\nu = 1$.

A possible way to determine ν (and g_c) is obtained by resumming the combination

$$L(g) \equiv \frac{2g^2}{g\partial_g \log M^2}. \tag{5.48}$$

Close to the critical point, for $g \to g_c^-$, we have

$$L(g) = \frac{g_c}{\nu}(g - g_c) + \mathcal{O}\Big((g_c - g)^2\Big)\,, \tag{5.49}$$

and ν can be extracted as

$$\nu = \frac{g_c}{\partial_g L}\bigg|_{g=g_c}. \tag{5.50}$$

In Figure 5.9 we report $L(g)$ as a function of g obtained by a [4/2] Padé-Borel approximant, the maximal approximant of the form $[m + 2/m]$ for $L(g)$ that has an expansion up to $O(g^6)$. The conformal mapping technique does not give good results for $L(g)$, probably because the coefficients in the series expansion of $L(g)$ differ more from the asymptotic values (5.38) due to the manipulation of taking the inverse of a logarithmic derivative, and this results in a poor accuracy.

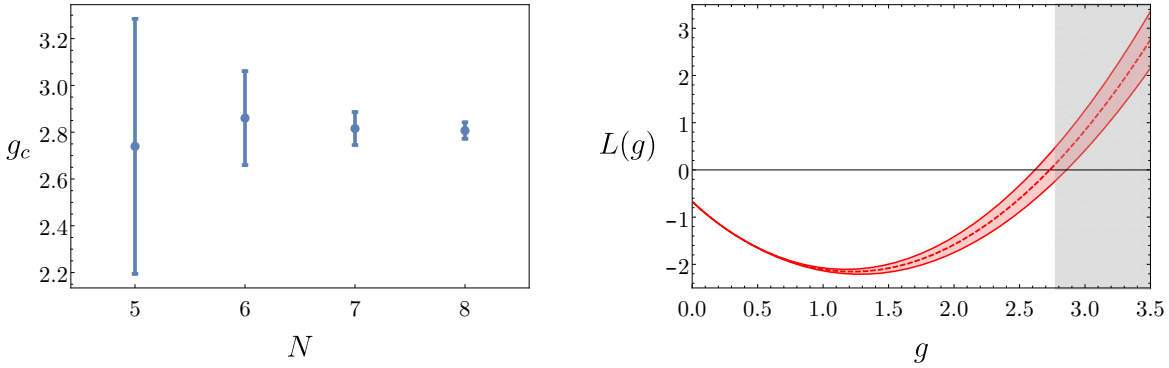

Figure 5.9: (Left panel) Central value and error of g_c as a function of the number of loops N kept in the conformal mapping resummation technique. (Right panel) The inverse of the logarithmic derivative of the physical mass M as a function of the coupling constant g using a [4/2] Padé-Borel approximant. This expression allows us to determine the critical exponent ν, as explained in the main text.

The values of the critical coupling and ν obtained from $L(g_c) = 0$ and eq. (5.50) are

$$g_c = 2.73(12)\,, \qquad \nu = 0.96(6)\,. \tag{5.51}$$

The result for g_c is consistent with that obtained in eq. (5.47) by resumming M, but it has a larger uncertainty, so we take as our best estimate the result (5.47).

The exponent η is defined in eq. (5.45). As well-known, the field $\phi(x)$ at criticality flows to the magnetization field σ of the two-dimensional Ising model and one has $\eta = 2\Delta_\sigma = 1/4$. We provide a perturbative estimate of η as follows: we define a normalized two-point function

$$T(x, \bar{x}) \equiv \frac{\langle \phi(x)\phi(0)\rangle}{\langle \phi(\bar{x})\phi(0)\rangle} \tag{5.52}$$

where $\bar{x}$ is an arbitrary fixed value. We then calculate $T(x, \bar{x})$ from the Borel resummed two-point function $\langle \phi(x)\phi(0)\rangle$ and evaluate it at g_c. In this way, η is given by

$$\eta = -\frac{\log T(x, \bar{x})}{\log(|x|/|\bar{x}|)}\,. \tag{5.53}$$

In Figure 5.10 we plot the results obtained for the ratio of eq. (5.53) as a function of $\log(|x|/|\bar{x}|)$ for different values of x at $g = g_c$. We use the value of g_c as determined in eq. (5.47) and we fix $|\bar{x}| = 1/100$. The points are compatible with a constant giving

$$\eta = 0.244(28)\,. \tag{5.54}$$

The uncertainty obtained by varying the critical coupling g_c within its error is subleading. The base-point $\bar{x}$ has been chosen as the point for which the correlator $\langle \phi(\bar{x})\phi(0)\rangle$ at $g = g_c$ has the smallest error, thus minimizing the errors on $T(x, \bar{x})$. In practice choosing a different $\bar{x}$ has only a very small effect on the determination of η, with the central value estimate always being well within the reported error. Because of the uncertainty Δg in g_c, the two-point function would still have an exponential suppression roughly of order $\exp(-M(\Delta g)|x|)$. Requiring $M(\Delta g)|x| \ll 1$, so that the exponential factor does not spoil our determination of η, leads to a bound $|x| < 1$ in the selection of points.

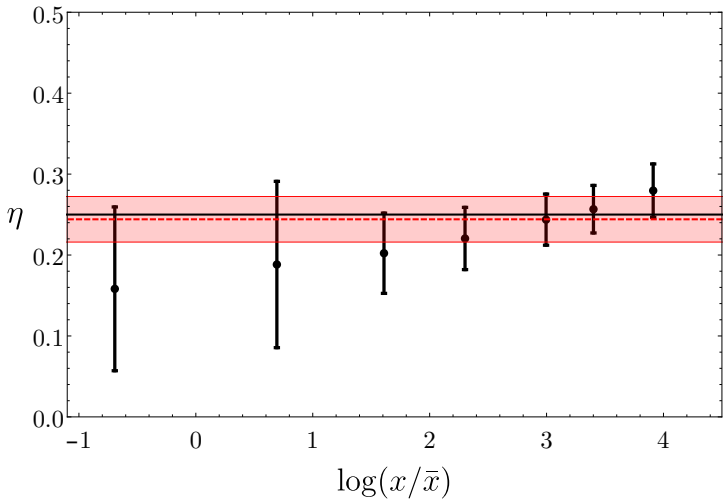

Figure 5.10: The slope coefficient $-\log[T(x,\bar{x})]/\log(|x|/|\bar{x}|)$ of the normalized 2 point function computed by Borel resumming the series at $g = g_c$, as a function of $\log(|x|/|\bar{x}|)$. At the critical point it is supposed to be constant in x and equal to the critical exponent η. The black solid line represents the theoretically known value $\eta = 1/4$.

Once the exponent η is known, we can also extract the two-point function normalization κ using eq. (5.45):

$$\kappa = |x|^{\eta}\langle\phi(x)\phi(0)\rangle_{g=g_c} \tag{5.55}$$

by taking the mean of the values at different x. We obtain $\kappa = 0.29(2)$ where the reported error takes into account both the uncertainty in the determination of the exponent η and the uncertainty in the resummation.

5.6 Comparison with Other Approaches

The critical value of the coupling g_c in the 2d ϕ^4 theory has been determined using a variety of approaches, such as lattice Monte Carlo, lattice matrix product states, Hamiltonian truncations and variants of the resummation of perturbation theory (supplemented by lattice) performed in this work. Most of these approaches, including our work, are based on an ordinary covariant quantization and normal ordering regularization, making possible a direct comparison of a scheme-dependent quantity like g_c. A comparison with approaches using other quantization or regularization schemes, such as the light-cone Hamiltonian truncation methods of refs. [81, 82], requires a careful mapping of the parameters and will not be considered (see ref. [83] for a recent attempt in this direction).

We report in table 5.5 the most recent results for g_c using various methods. The Hamiltonian truncation results in refs. [80, 85] and [84] are based on the study of the $\mathbb{Z}_2$ unbroken and broken phases, respectively. The lattice analysis in ref. [69] is based on a tensor network with matrix product states. ref. [69] reports two values for g_c, denoted by I and II in the table: in I g_c is defined as the value where the energy of the first excited state vanishes, while II is obtained by looking at the value where $\langle\phi\rangle$ vanishes, starting from the $\mathbb{Z}_2$ broken phase. ref. [66] is based on a Monte Carlo simulation. Finally, ref. [86] uses lattice results to express the critical value

Ref.	g_c	Method
This work	2.807(34)	Borel RPT
[84]	2.78(6)	HT
[80, 85]	2.76(3)	HT
[69]	2.769(2)	MPS I
[69]	2.7625(8)	MPS II
[66]	2.788(15)(8)	LMC
[86]	2.75(1)	LMC+Borel RPT

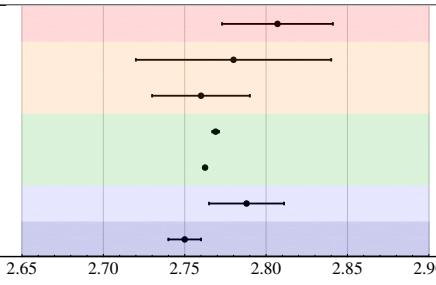

Table 5.5: Computation of g_c using Borel Resummed Perturbation Theory (RPT), Hamiltonian Truncation (HT), Matrix Product States (MPS) and Lattice Monte Carlo (LMC) methods.

of the renormalized coupling g_R, obtained by resumming the perturbative series in g_R [32, 33, 87] (see next section), in terms of the coupling g.

In table 5.6 we compare the values of Λ and M for three values of the coupling g with those obtained in refs. [80, 85]. At weak coupling $g = 0.2$, as probably expected, we get more accurate results but as the coupling increases (at $g = 1$ and at $g = 2$) the accuracy reached by refs. [80, 85] is better than ours. Overall, given also the statistical nature of our error, the results are in very good agreement between each other.

5.6.1 Comparison with Other Resummation Methods

As mentioned in the introduction, two different resummation methods have already been developed in the literature: resummation in the ϵ-expansion [88] and at fixed dimension [89]. The latter differs from our perturbative expansion in the renormalization scheme and the fact that the critical point is extracted from the vanishing of the β function (involving the 4-point function) instead of the mass gap (only involving the 2-point function), for this reason we denote such expansion $\mathrm{PT}_{4\mathrm{pt}}$, while ours will be called $\mathrm{PT}_{2\mathrm{pt}}$.

The ϵ-expansion is devised to study the critical theory as a function of the space-time dimensions. It is a well-known technique and has been used in a variety of contexts. Within applications to the 2d ϕ^4 theory, one first determines the value of the critical coupling g^* as a function of $\epsilon = 4 - d$ perturbatively from the β-function of the quartic coupling, computes critical exponents by resumming the corresponding series in $g^*(\epsilon)$ and then set $\epsilon = 2$ [90].

The fixed dimension coupling expansion of ref. [89] (see e.g. chapters 26 and 29 of ref. [91] for an introduction) is based on an expansion in terms of a renormalized dimensionless coupling g_R. As we mentioned, in the 2d ϕ^4 theory there is no need to introduce a wave function renormalization constant Z for the field ϕ or a coupling counterterm, since the bare coupling constant λ is finite. Nevertheless, one can define renormalized quantities in analogy to the 4d ϕ^4 renormalization conditions. Denoting by $\Gamma_R^{(n)}$ the 1-particle irreducible (1PI) n-point renormalized Schwinger functions, one defines m_R, Z and g_R by the following three conditions at zero momentum:[14]

$$\Gamma_R^{(2)}(p=0) = m_R^2\,, \quad \frac{d\Gamma_R^{(2)}(0)}{dp^2} = 1\,, \quad \Gamma_R^{(4)}(0) = m_R^2 g_R\,, \tag{5.56}$$

[14]Notice the different normalization of the coupling: $g_R = 4!g + \mathcal{O}(g^2)$.

Ref.	g	Λ	M
This work	0.2	$-0.00181641(8)$	0.9797313(4)
[80, 85]	0.2	$-0.0018166(5)$	0.979733(5)
This work	1	$-0.0392(3)$	0.7507(5)
[80, 85]	1	$-0.03941(2)$	0.7494(2)
This work	2	$-0.153(5)$	0.357(5)
[80, 85]	2	$-0.1581(1)$	0.345(2)

Table 5.6: The values Λ and M for different values of g and comparison with refs. [80, 85].

where as usual $\Gamma_R^{(n)}$ are related to the bare 1PI Schwinger functions $\Gamma^{(n)}$ as $\Gamma_R^{(n)} = \Gamma^{(n)} Z^{n/2}$. In the critical regime $m_R \to 0$ the $\Gamma_R^{(n)}$ are expected to satisfy an homogeneous Callan-Symanzik equation in terms of a β-function defined as

$$\beta(g_R) = m_R \frac{dg_R}{dm_R}\bigg|_\lambda . \tag{5.57}$$

In the proximity of a fixed point g_R^* where $\beta(g_R^*) = 0$, the Schwinger functions would satisfy the typical scaling behavior of a critical theory. In contrast to the ϵ-expansion case, the fixed point cannot be accessed perturbatively and is determined by Borel resumming the truncated expansion of $\beta(g_R)$. Once g_R^* is determined, critical exponents can be computed like in the ϵ-expansion by Borel resumming their series in g_R, setting $g_R = g_R^*$ after the resummation.

Using our perturbative coefficients of the 2-pt and 4-pt functions (see the Appendix) and the above procedure, the expansions for $\beta(g_R)$ and $\eta(g_R)$ read as follows:[15]

$$\begin{aligned}
\frac{\beta(v)}{2} =& -v + v^2 - 0.7161736 v^3 + 0.930768(3) v^4 - 1.5824(2) v^5 + 3.2591(9) v^6 - 7.711(5) v^7 \\
&+ 20.12(9) v^8 + \mathcal{O}(v^9)\,, \\
\eta(v) =& \; 0.0339661 v^2 - 0.0020226 v^3 + 0.0113932(2) v^4 - 0.013735(1) v^5 + 0.02823(1) v^6 \\
&- 0.06179(9) v^7 + 0.1475(8) v^8 + \mathcal{O}(v^9)\,,
\end{aligned} \tag{5.58}$$

where we have defined $v = 3g_R/(8\pi)$. The first 5(6) coefficients in $\beta(v)$ and the first 3(4) in $\eta(v)$ agree with the results obtained in ref. [33] ([92]), providing a consistency check on the determination of our coefficients up to $\mathcal{O}(g^5)$.[16] The other coefficients are new. We compare in table 5.7 our results for ν and η with those obtained with $\mathrm{PT}_{4\mathrm{pt}}$. We also include in the table the most recent results in the ϵ-expansion, based on a six loop (ϵ^6) resummation [73]. Under the column "Method" we also report the number of loop coefficients used. Resummation based on $\mathrm{PT}_{4\mathrm{pt}}$ is known to be not very accurate in $2d$, in contrast to the $3d$ case. In particular, as can be seen from table 5.7, the value of η significantly differs from its exact value $\eta = 1/4$. This problem seems to be related to possible non-analyticites in $\beta(g)$ that are not well captured by the Borel resummation [93]. This issue is not present in our way of extracting η directly from the two-point function, as explained in section 5.5. It does not seem to be present in the ϵ-expansion as well. On the other hand, our estimate for ν has not improved since ref. [35]. Using

[15] Using an appropriate Callan-Symanzik equation, the critical exponent ν could also be extracted from our perturbative coefficients. We thank Riccardo Guida for this observation.

[16] The v^3-coefficient of η in eq. (5) of ref. [92] is actually in disagreement with ref. [33] and our results, but we suspect this is simply due to a typo in that formula.

Ref., Year	ν	η	Method
[13], 1944	1	$\frac{1}{4}$	Exact
[11], 1978	0.92(30)	0.08(20)	PT_{4pt}, 4 loops
[12], 1980	0.97(8)	0.13(7)	PT_{4pt}, 4 loops
[19], 2000	0.966(?)	0.146(?)	PT_{4pt}, 5 loops
[38], 2017	0.952(14)	0.237(27)	ϵ-expansion, 6 loops
This work, 2018	0.96(6)	0.244(28)	PT_{2pt}, 8 loops (ν), 6 loops (η)

Table 5.7: Comparison of the critical exponents ν and η computed using different resummation techniques at different orders. See the main text for further details.

eqs. (5.58) and the PT_{4pt} scheme, we can determine v^* and $\eta = \eta(v^*)$, and compare our results with those in the literature. Consistency of the coupling expansion requires to keep terms up to $\mathcal{O}(v^{N+1})$ in β and to $\mathcal{O}(v^N)$ in η. With $N = 4$, the number of terms used in refs. [33, 35], we find $v^* = 1.84(5)$, $\eta = 0.13(5)$, in very good agreement with the values $v^* = 1.8(3)$, $\eta = 0.08(20)$ in ref. [33] and $v^* = 1.85(10)$, $\eta = 0.13(7)$ in ref. [35]. With $N = 5$, the number of terms used in ref. [92], we find $v^* = 1.82(5)$, $\eta = 0.13(3)$, in agreement with the values $v^* = 1.837(?)$, $\eta = 0.146(?)$ in ref. [92]. Taking $N = 6$, we find $v^* = 1.80(4)$ and $\eta = 0.15(3)$, while taking $N = 7$ we find $v^* = 1.82(4)$ and $\eta = 0.16(2)$. We see that the accuracy of the results grows very slowly as the order increases. In particular, the value of η at $N = 7$ is more than 4 standard deviations away from 1/4, confirming the poor accuracy of PT_{4pt} when applied to the 2d ϕ^4 theory.

Aside from a numerical comparison, the PT_{2pt} developed in our work has some advantages with respect to PT_{4pt}. First of all, the proofs in both ref. [16] and in section 5.1 about the Borel resummability in the 2d ϕ^4 theory apply for bare, and not renormalized, quartic coupling λ. Second, the definition of g_R requires the unavoidable computation of a 4-point function, $\Gamma^{(4)}$, while with PT_{2pt} such computation can be avoided. Typically the higher the Schwinger functions, the less accurate are the results based on numerical resummations. Finally, PT_{2pt} allows a direct comparison with intrinsically non-perturbative methods, such as lattice and Hamiltonian truncations, since their renormalization schemes coincide.

5.7 Perturbative Coefficients for the Broken Symmetry Phase

We start here the discussion of the broken-symmetry phase of the ϕ^4 theory which will appear in ref. [4]. For convenience of the reader, we write once again the Lagrangian describing the theory with negative squared mass:

$$\mathcal{L}' = \frac{1}{2}(\partial\phi)^2 - \frac{1}{4}\widetilde{m}^2\phi^2 + \lambda\phi^4 + \frac{1}{2}\delta\widetilde{m}^2\phi^2 + \delta\widetilde{\Lambda}\,, \tag{5.59}$$

where the counterterms are chosen in the normal ordering scheme as explained in Section 5.2. The potential in the Lagrangian above has two degenerate minima $\phi_\pm = \pm\widetilde{m}/(2\sqrt{2g})$. In the presence of an external source and in infinite volume, one of the two vacua is selected and the $\mathbb{Z}_2$ symmetry $\phi \to -\phi$ is spontaneously broken. This can be equivalently implemented by picking one of the two vacua and quantizing the theory around it.

Shifting the field $\phi \to \phi_+ + \phi$ and neglecting the vacuum energy terms, we get

$$\mathcal{L}' = \frac{1}{2}(\partial\phi)^2 + \frac{1}{2}\widetilde{m}^2\phi^2 + \lambda_3\,\phi^3 + \lambda\phi^4 + \delta J\,\phi + \frac{1}{2}\delta\widetilde{m}^2\phi^2\,, \tag{5.60}$$

where we defined

$$\lambda_3 \equiv \sqrt{2\lambda}\widetilde{m}\,, \qquad \delta J \equiv \frac{\lambda_3}{4\lambda}\delta\widetilde{m}^2\,. \tag{5.61}$$

The counterterm δJ thus obtained is such that it completely cancels the divergent 1-point tadpole term at one loop. The Lagrangian density (5.60) describes the theory we want to study with perturbation theory. Because of the presence of the cubic self-interaction, the perturbative expansion in the broken symmetry phase involves the computations of many more diagrams than in the symmetric phase. Moreover, diagrams with different number of cubic and quartic vertices contribute at each order in the effective coupling $\widetilde{g} = \lambda/\widetilde{m}^2$, making cancellations possible and lowering the numerical accuracy. The task of computing the perturbation series in this theory is for these reasons much more challenging. It should also be noted that the classical vacuum gets perturbative corrections at quantum level so that $\Gamma_1 \neq 0$. The computation of the n-point functions will then involve diagrams decorated with 1-point tadpole terms—i.e. sub-diagrams with zero net momentum flow. However we will show below that one can get rid of this set of diagrams using manipulations similar to those of Section 5.2. Consider the following Lagrangian density $\hat{\mathcal{L}}$, where, for simplicity, we neglect the vacuum energy terms,

$$\hat{\mathcal{L}} = \frac{1}{2}(\partial\phi)^2 + \frac{1}{2}\hat{m}^2\phi^2 + \hat{\lambda}_3\,\phi^3 + \lambda\phi^4 + (\delta\hat{J} + j)\,\phi + \frac{1}{2}\delta\hat{m}^2\phi^2\,, \tag{5.62}$$

$$\hat{\lambda}_3 \equiv \sqrt{2\lambda}\hat{m}\,, \qquad \delta\hat{J} \equiv \frac{\hat{\lambda}_3}{4\lambda}\delta\hat{m}^2\,. \tag{5.63}$$

The counterterms are defined as usual in the normal ordering scheme and the linear shift j is such to guarantee that $\Gamma_1 = 0$, i.e. in this theory the diagrams involving 1-point tadpole terms are vanishing. We will compute the perturbative series in this theory, as functions of λ, $\hat{\lambda}_3$ and $\hat{m}^2$.[17] The perturbative series for the theory described by eq. (5.60) can be obtained by the following method. We perform the shift $\phi \to \phi - v$ in the Lagrangian density (5.62) and match the obtained expression with eq. (5.60), i.e. we require that the linear term vanishes, that the quadratic term is equal to $(\widetilde{m}^2 + \delta\widetilde{m}^2)\phi^2/2$, and so on. The resulting equations relate the parameters $\hat{m}$, $\hat{\lambda}_3$ and v in the theory (5.62) to the parameters $\widetilde{m}$, λ_3 and λ of the original theory (5.60). Using eq. (5.14) for δm^2 and its analogous for $\delta\hat{m}$ we get the following system of equations

$$\begin{aligned} 0 &= \widetilde{m}^2 - \hat{m}^2 + 12\lambda Z + 6\lambda_3\,v + 12\lambda\,v^2\,, \\ 0 &= j - 3\lambda_3 Z - \hat{m}^2 v + 3\lambda_3\,v^2 + 8\lambda\,v^3\,, \\ 0 &= \lambda_3 - \hat{\lambda}_3 + 4\lambda\,v\,, \end{aligned} \tag{5.64}$$

where we defined

$$Z = \frac{1}{4\pi}\log\frac{\widetilde{m}^2}{\hat{m}^2}\,. \tag{5.65}$$

The system of equations (5.64) can be solved for

$$\hat{m}^2(\widetilde{m}^2, \lambda_3, \lambda)\,, \qquad v(\widetilde{m}^2, \lambda_3, \lambda)\,, \qquad \lambda_3(\widetilde{m}^2, \lambda_3, \lambda)\,, \tag{5.66}$$

[17] We keep the cubic coupling $\hat{\lambda}_3$ generic, in order to be able to apply EPT in this theory.

order by order in λ_3 and λ and the perturbative series of the theory described by eq. (5.60) are then obtained by re-expanding the corresponding series for the theory $\hat{\mathcal{L}}$.

The classification of the topologically distinct diagrams in the presence of cubic vertices, the computation of their multiplicities, and the evaluation of the corresponding integral is performed as in Section 5.4. We managed to compute the diagrams with up to 8 vertices (cubic and/or quartic) for the 1- 2- and 4-point functions. Therefore the series we obtain are at most of order $\widetilde{g}^4$ with $\widetilde{g}$ being the effective coupling of the theory $\widetilde{g} = \lambda/\widetilde{m}^2$. The case is different if we use EPT, since by redefining

$$\lambda_3 \xrightarrow{\text{EPT}} \lambda\sqrt{\frac{2}{\lambda_0}}\widetilde{m} \tag{5.67}$$

the cubic and quartic vertices are of the same order in λ and we can consistently keep all the terms up to $\mathcal{O}(\widetilde{g}^8)$.

5.7.1 Vacuum Expectation Value of ϕ

The vacuum expectation value $\langle\phi\rangle = v$ is computed from eq. (5.64) and requires the knowledge of j, which in turn is determined by the 1PI diagrams in the auxiliary theory $\hat{\mathcal{L}}$. We get

$$\langle\phi\rangle = -0.251893506(29)\,\widetilde{g}^{3/2} - 0.761006(23)\,\widetilde{g}^{5/2} - 2.3130(21)\,\widetilde{g}^{7/2} + \mathcal{O}(\widetilde{g}^{9/2})\,, \tag{5.68}$$

where the numbers in parenthesis indicate the error on the last two digits due to the numerical integration. In Appendix B.2 we report the coefficients for general cubic and quartic couplings λ_3 and λ.

5.7.2 Vacuum Energy

In order to get the perturbative series for the vacuum energy from the perturbation theory of the auxiliary theory, we need to keep track of the vacuum energy part which has been omitted from the discussion above. A more careful derivation shows that the vacuum energy is shifted by the following term

$$\Delta\hat{\Lambda} = \frac{1}{8\pi}(\hat{m}^2 - \widetilde{m}^2) + \frac{1}{2}\hat{m}^2 Z - 3\lambda Z^2 + (j - 3\hat{\lambda}_3 Z)v + \frac{1}{2}(\hat{m}^2 - 12\lambda Z)v^2 - \hat{\lambda}_3 v^3 + \lambda v^4\,. \tag{5.69}$$

The desired perturbative expression is then obtained by re-expanding the following quantity in the parameters of the original theory

$$\widetilde{\Lambda} = \Delta\hat{\Lambda} + \hat{m}^2 \sum_n \hat{c}_n \hat{g}^n\,, \tag{5.70}$$

where $\hat{c}_n$ are the perturbative coefficients for the vacuum energy of the auxiliary theory $\hat{\mathcal{L}}$. We obtain the following series for the vacuum energy

$$\frac{\widetilde{\Lambda}}{\widetilde{m}^2} = -\frac{3}{4\pi^{3/2}} G^{3,2}_{3,3}\Big(4\Big|\begin{matrix}0,0,\frac{1}{2}\\0,0,0\end{matrix}\Big)\widetilde{g} - 0.042182971(51)\widetilde{g}^2 - 0.0138715(74)\widetilde{g}^3 - 0.01158(19)\widetilde{g}^4 + \mathcal{O}(g^5)\,, \tag{5.71}$$

where the numbers in parenthesis indicate the error on the last two digits due to the numerical integration. The coefficients at order $\widetilde{g}$ has been computed analytically and it is expressed in terms of the Meijer G-function. Its numerical value is ≈ -0.0890578. In Appendix B.2 we report the coefficients for general cubic and quartic couplings λ_3 and λ which will allow us to use EPT as defined in eq. (5.67).

5.7.3 Physical Mass

The mass gap is computed from the smallest zero of the 1PI two-point function for complex values of the Euclidean momentum

$$\widetilde{\Gamma}_2(p^2 = -\widetilde{M}^2) \equiv 0\,, \tag{5.72}$$

using the perturbative expansions of $\widetilde{\Gamma}_2$ and its derivatives at $p^2 = -\widetilde{m}^2$ as explained in Subsection 5.4.2. We report here our preliminary result

$$\frac{\widetilde{M}^2}{\widetilde{m}^2} = 1 - 2\sqrt{3}\widetilde{g} - 4.1529(18)\widetilde{g}^2 - 14.886(30)\widetilde{g}^3 - 50.71(99)\widetilde{g}^4 + \mathcal{O}(\widetilde{g}^5)\,, \tag{5.73}$$

where the numbers in parenthesis indicate the error on the last two digits. The coefficient at order $\widetilde{g}^4$ is subject to a relatively high numerical uncertainty and will (hopefully) be improved in the future. In Appendix B.2 we report the coefficients for general cubic and quartic couplings λ_3 and λ.

5.7.4 Large Order Behavior

In Section 5.1 we proved that the theory with negative squared mass is Borel summable to the exact result (in a given phase of the theory), therefore the Borel function cannot have singularities on the real positive axis. The analysis of the semi-classical instanton configurations indeed shows that the leading singularities in the Borel plane are located at the complex points $t_\pm = \frac{1}{|a|}e^{\pm i\vartheta}$ with the following values of the parameters

$$|a| \approx 0.618002\,, \qquad \vartheta \approx 0.816714\,. \tag{5.74}$$

Notice that the value of $|a|$ is about of the same magnitude of the corresponding value in the symmetric phase (see eq. (5.39)). Thus we expect a similar growth of the absolute value of the coefficients at large orders, with the ones in the symmetric phase growing about 10% faster than the ones in the broken phase. Unfortunately we cannot test quantitatively this expectation, since the series we obtained are truncated at order $\widetilde{g}^4$, and the application of the large order estimate to the very first coefficients is not meaningful. The complex phase ϑ is instead telling us that the coefficients of the series should oscillate in sign about every $\pi/\vartheta \approx 4$ terms, which is consistent with not seeing oscillations in the perturbative series obtained above. The search for subleading instanton configurations shows that the next-to-leading singularities in the Borel plane are not aligned with the leading ones, having a smaller value of the complex phase θ. This means that the conformal mapping (2.21) will map those singularities inside the unit disk, reducing the radius of convergence of the series in the variable u and thus hindering the convergence of the method. However this hardly constitutes a problem since the series are truncated to the 4-th order and we can safely use the mapping to slightly extend the perturbative results into the non-perturbative region.

5.8 Preliminary Results in the Broken Symmetry Phase

We present here some preliminary results of about the resummation of the perturbative series in the broken symmetry phase. These results will appear in ref. [4], where a more careful analysis will be presented.

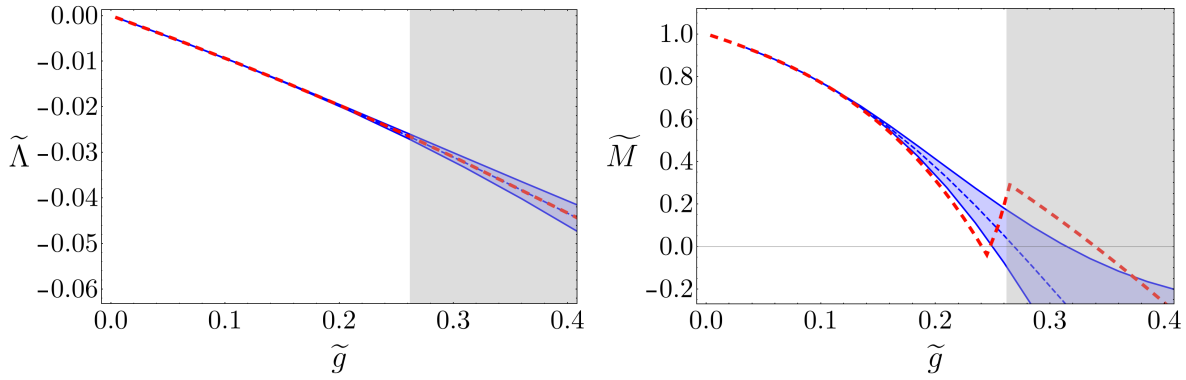

Figure 5.11: Preliminary results for the vacuum energy $\widetilde{\Lambda}$ (left panel) and the physical mass $\widetilde{M}$ (right panel) as functions of the coupling $\widetilde{g}$ (with $\widetilde{m} = 1$). The red dashed lines are obtained with optimal truncation; the blue bands are obtained using the general conformal map in eq. (2.21) with the parameters taken as (5.74). The region beyond the critical coupling $\widetilde{g}_c$ is shaded.

As mentioned at the beginning of the chapter, this theory undergoes two phase transitions at the critical couplings $\widetilde{g}_c$ and $\widetilde{g}'_c$ which are related to the critical coupling g_c through the Chang duality (5.19). Using the value of g_c as determined in eq. (5.47) we get

$$\widetilde{g}_c = 0.2620(44)\,, \qquad \widetilde{g}'_c = 1.287(36)\,. \tag{5.75}$$

We expect the results of perturbation theory to reproduce the exact behavior of the observables in the region $\widetilde{g} \leqslant \widetilde{g}_c$, while beyond the phase transition the resummations may not give the correct answers. In the following we set $\widetilde{m} = 1$ for simplicity.

The perturbative series obtained in the previous section are truncated at order $\widetilde{g}^4$ and one may wonder if there is any need to resum the series. Using optimal truncation we see that indeed for the vacuum energy $\widetilde{\Lambda}$ we can keep all the perturbative terms up to $\widetilde{g}_c$ while for the physical mass $\widetilde{M}$ we must discard the $\mathcal{O}(\widetilde{g}^4)$ term at $\widetilde{g} \approx 0.25$. Therefore for $\widetilde{M}$ we can hope to slightly improve the result by using the general conformal map in eq. (2.21) to resum the series. In Figure 5.11 we report the functions $\widetilde{\Lambda}$ and $\widetilde{M}$ obtained with the optimal truncation (red dashed lines) and with the conformal mapping (blue bands). The resummation of the vacuum energy $\widetilde{\Lambda}$ gives a very precise determination of the function up to the critical point $\widetilde{g}_c$ and we see that it is in very good agreement with the optimal truncation estimate. In the case of the physical mass $\widetilde{M}$ the resummation procedure gives bigger errors. Nevertheless, from the zero of the function we get an independent determination of the critical coupling $\widetilde{g}_c = 0.267(33)$, which is compatible with the value obtained in eq. (5.75) from Chang duality.

Even if the theory is Borel resummable from the beginning, we could have used EPT to improve the results, as we did for the tilted anharmonic oscillator in QM. However its use in QFT is hindered by the limited number of perturbative terms available. As a matter of fact EPT is expected to reproduce the correct results when the number of terms is $n \gg 1/\widetilde{g}^2$, thus with $n = 8$ we can only probe the region beyond the phase transition.

In ref. [4] we will show that the vacuum energy is sufficiently smooth across the phase transition so that the function $\widetilde{\Lambda}$ beyond $\widetilde{g}_c$ is mapped by Chang duality to a line which is consistent with the result in the unbroken phase. As a teaser we show in Figure 5.12 the plot for the dualized $\widetilde{\Lambda}$ in the weak branch (obtained with the conformal mapping for complex branches) and strong branch (obtained with the EPT defined in eq. (5.67)) on top of the result obtained in the symmetric phase.

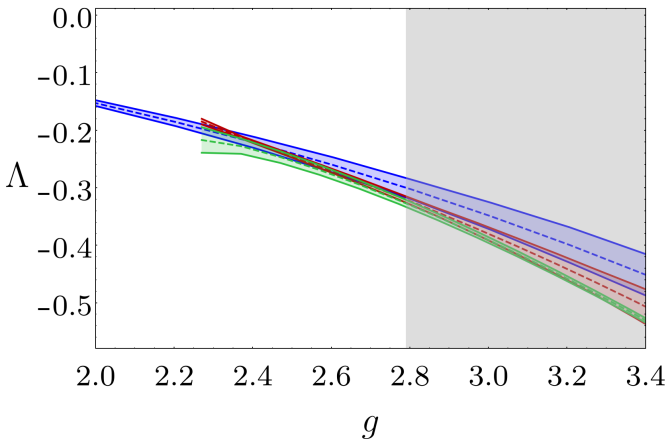

Figure 5.12: Preliminary check of the Chang duality. The blue band represents the vacuum energy Λ in the symmetric phase as showed in the left panel of Figure 5.4. It is expected to reproduce the exact result for $g < g_c \approx 2.8$. The green and red bands represent the dualized $\widetilde{\Lambda}$ for the weak and strong branch respectively. The weak branch is obtained with the conformal mapping for complex singularities and is expected to reproduce the exact result in the shaded region. The strong branch is obtained with the EPT defined in eq. (5.67). Despite the crossing of phase transitions the three bands appear to be consistent with each other.

Conclusions

In this thesis we have investigated the properties of the saddle point expansion of path integrals using results from Picard-Lefschetz theory. In Chapter 4 we focused on one-dimensional QM systems with bound-state potentials and discrete spectra. We characterized some of the conditions for the Borel summability of perturbation theory in QM. In particular when the potential admits only one critical point (minimum), we have shown that the loopwise expansion in the Euclidean path integral is Borel resummable and reproduces the full answer. Several known results in the literature about the Borel summability of certain QM systems are rederived and generalized in this new perspective. We also introduced EPT—a suitable modification of the perturbative expansion—which has allowed us to extend our result to systems with generic bound-state potentials, thus relaxing the requirement of a single critical point. Remarkably, EPT encodes all the non-perturbative corrections of SPT, the standard semi-classical expansion including instantons, providing the full answer for any value of the coupling constant. In particular, EPT works at its best at strong coupling, where the high accuracy obtained confirms its validity. All complications occurring in SPT, related to the need of a resurgence analysis to make sense of otherwise ambiguous results, or of a highly non-trivial Lefschetz thimble decomposition of the path integral, are bypassed when using EPT. These points have been illustrated in details with several examples.
In Chapter 5 we have extended the results to QFT showing that the Schwinger functions in a large class of Euclidean scalar field theories in $d < 4$ are Borel reconstructable from their loopwise expansion. Whenever phase transitions occur, care should be taken in selecting the appropriate vacuum in the other phase of the theory. In the context of the 2d ϕ^4 theory, we have argued that, in absence of a proper vacuum selection by means of an explicit symmetry breaking term, the Schwinger functions resummed from the unbroken phase might have a different analytic structure in the coupling constant g and the expected singularities associated to the phase transition at $g = g_c$ might not be visible. The resummed n-point functions for $g > g_c$ should be interpreted as n-point functions in the $\mathbb{Z}_2$ broken phase around a vacuum where cluster decomposition is violated. In the unbroken phase of the theory we have performed a detailed study of the 0- and 2-point functions with $0 \leq g \leq g_c$ and $m^2 > 0$. We have computed the perturbative series expansion for the vacuum energy and the physical mass up to order g^8 and Borel resummed the truncated series using known resummation techniques. In this way, for the first time, we accessed the strong coupling behavior of the 2d ϕ^4 theory away from criticality using Borel-resummed perturbative expansions. The renormalization scheme chosen allows us a direct comparison with other non-perturbative techniques, most notably Hamiltonian truncation methods. The overall very good agreement of the results can be seen as convincing numerical evidence of the Borel summability of the theory and of the effectiveness of the method. Finally we have started the investigation of the less known studied phase of the theory, computing for the first time the action of the complex semiclassical configurations that

determine the large order behavior of the perturbative coefficients. We have also numerically determined the perturbative expansion for the vacuum energy and the physical mass up to the 4-th order in the quartic coupling $\widetilde{g}$, and we have presented some preliminary analysis for the resummation of these observables. In addition, we have computed in this phase all the 0- 1- and 2-point diagrams involving up to 8 vertices (cubic plus quaritc) allowing us to use EPT in the 2d ϕ^4 theory.

Our results can be extended in various directions. It would be interesting to understand if and how they can be obtained directly in Minkowski space where, contrary to the Euclidean case, one would always expect an infinite number of saddles to contribute. Furthermore, the generality of our arguments in Section 5.1, suggest that our techniques should apply equally well to many other theories. Natural candidates to consider next include the 3d ϕ^4 theory and the $O(N)$ 3d vector models. More ambitious goals would be to extend our methods to QFT that are *not* Borel resummable, like gauge theories in $d = 4$. Any progress in this direction would be of great interest.

Appendix A

On the Finiteness of $\mathcal{B}^{(\infty)}_{-1/2}\mathcal{Z}$

In this appendix we report some checks we performed about the finiteness of the continuum limit of $\mathcal{B}^{(N)}_{-1/2}\mathcal{Z}(\lambda t)$. First of all, we consider the partition function of the harmonic oscillator. We discretize the path integral by cutting-off the real Fourier modes coefficients c_n of $x(\tau)$:

$$x(\tau) = \sum_{k=0}^{N} c_k \eta_k \cos\frac{2\pi k\tau}{\beta} + \sum_{k=1}^{N} c_{-k}\eta_k \sin\frac{2\pi k\tau}{\beta}\,, \quad \eta_k = \frac{\sqrt{2-\delta_{k,0}}}{\sqrt{\beta}}\,. \tag{A.1}$$

The discretized action reads

$$S^{(N)}[x] = \int_0^\beta d\tau\, \left[\frac{1}{2}\dot{x}^2 + \frac{1}{2}\omega^2 x^2\right] = \frac{1}{2}\sum_{k=-N}^{N} \mu_k c_k^2\,, \qquad \mu_k \equiv \omega^2 + \frac{(2\pi k)^2}{\beta^2}\,. \tag{A.2}$$

The path integral measure reads

$$\mathcal{D}^{(N)}x(\tau) = \prod_{k=-N}^{N} N_k\, dc_k\,, \qquad N_k \equiv \begin{cases} \frac{|k|}{\beta}\sqrt{\frac{2\pi}{\lambda}} & k \neq 0 \\ \frac{1}{\beta\sqrt{2\pi\lambda}} & k = 0 \end{cases}\,. \tag{A.3}$$

Introduce now a radial coordinate system defined as

$$c_k = \sqrt{\frac{2}{\mu_k}}\rho\,\hat{c}_k\,, \quad \sum_{k=-N}^{N}\hat{c}_k^2 = 1 \tag{A.4}$$

where ρ is the radius and the $\hat{c}_k$'s encode the standard parametrization of the unit $2N$-sphere in terms of its $2N$-angles, whose explicit form will not be needed. Using the expression (4.8) for the Borel-Le Roy function and the above results, we get

$$\begin{aligned}
\mathcal{B}^{(N)}_{-1/2}\mathcal{Z}_0(\lambda t) &= \frac{\sqrt{\lambda t}}{\beta}\prod_{k=1}^{N}\left[\frac{2\pi k}{\beta}\right]^2 \partial^N_{\lambda t}\int_0^\infty \frac{d\rho}{\rho}\,\Omega_{2N+1}\left[\prod_{k=-N}^{N}\frac{\rho}{\sqrt{\pi\mu_k}}\right]\delta(\rho^2 - t\lambda) \\
&= \frac{1}{\Gamma\left(N+\frac{1}{2}\right)}\sqrt{\lambda t}\,\partial^N_{\lambda t}(\lambda t)^{N-\frac{1}{2}}\frac{1}{\beta\omega}\prod_{k=1}^{N}\frac{1}{1+\left(\frac{\omega\beta}{2\pi k}\right)^2} \\
&= \frac{1}{\Gamma\left(\frac{1}{2}\right)}\frac{1}{\beta\omega}\prod_{k=1}^{N}\frac{1}{1+\left(\frac{\omega\beta}{2\pi k}\right)^2}\,,
\end{aligned} \tag{A.5}$$

where $\Omega_d = 2\pi^{d/2}/\Gamma(d/2)$ is the area of the unit $(d-1)$-dimensional sphere and we used the relation

$$\partial^N_{\lambda t}(\lambda t)^{N+p} = \frac{\Gamma(N+p+1)}{\Gamma(p+1)}(\lambda t)^p\,, \tag{A.6}$$

valid for any value of p. Notice how taking N derivatives with respect to λt gives rise to an N-dependent Gamma function that compensates the one coming from the area of the unit-sphere. As expected, the dependence on λt disappears and the continuum limit gives the finite answer

$$\lim_{N\to\infty}\mathcal{B}^{(N)}_{-1/2}\mathcal{Z}_0(\lambda t) \equiv \lim_{N\to\infty}\frac{\mathcal{Z}^{(N)}_0}{\Gamma(1/2)} = \frac{\mathcal{Z}_0}{\Gamma\left(\frac{1}{2}\right)}\,, \qquad \mathcal{Z}_0 = \frac{1}{2\sinh\left(\frac{\omega\beta}{2}\right)}\,, \tag{A.7}$$

which reproduces the known partition function $\mathcal{Z}_0$ of the harmonic oscillator after the integral over t is performed.

An exact computation of $\mathcal{B}^{(N)}_{-1/2}\mathcal{Z}(\lambda t)$ is clearly out of reach in interacting QM systems. Yet, we can show that $\mathcal{B}^{(\infty)}_{-1/2}\mathcal{Z}(\lambda t)$ is finite to all orders in perturbation theory for polynomial potentials. It is useful to work out in detail the first order term of $\mathcal{B}^{(N)}_{-1/2}\mathcal{Z}(\lambda t)$ for the quartic anharmonic oscillator $V(x) = \omega^2x^2/2 + x^4/4$. We have

$$\mathcal{B}^{(N)}_{-1/2}\mathcal{Z}(\lambda t) = \mathcal{Z}^{(N)}_0\frac{\sqrt{\lambda t}}{\pi^{N+\frac{1}{2}}}\partial^N_{\lambda t}\int_0^\infty d\rho\int d\Omega_{2N+1}\,\rho^{2N}\delta(\rho^2+\rho^4\xi - t\lambda)\,, \tag{A.8}$$

where $\mathcal{Z}^{(N)}_0$ is the discretized version of the harmonic oscillator partition function defined in eq.(A.7) and

$$\xi = \sum_{n,m,p,q=-N}^{N}\frac{\eta_n\eta_m\eta_p\eta_q}{\sqrt{\mu_n\mu_m\mu_p\mu_q}}\int_0^\beta d\tau(\hat{c}_nX_n)(\hat{c}_mX_m)(\hat{c}_pX_p)(\hat{c}_qX_q)\,, \quad X_n \equiv \begin{cases}\cos\frac{2\pi n\tau}{\beta}\,, & n\geq 0\\ \sin\frac{2\pi n\tau}{\beta}\,, & n<0\end{cases}\,. \tag{A.9}$$

At linear order in λt, once we expand the argument of the delta function, we get

$$\mathcal{B}^{(N)}_{-1/2}\mathcal{Z}(\lambda t) = \mathcal{Z}^{(N)}_0\frac{\sqrt{\lambda t}}{\pi^{N+\frac{1}{2}}}\partial^N_{\lambda t}\int_0^\infty d\rho\int d\Omega_{2N+1}\rho^{2N-1}(1-2\rho^2\xi)\delta[\rho-\sqrt{\lambda t}(1-\lambda t\xi/2)+\ldots]+\mathcal{O}(\lambda t)^2\,. \tag{A.10}$$

It is convenient to evaluate the integral over the angular variables $\hat{c}_n$ before the one in $d\tau$ appearing in eq. (A.9). This is easily obtained by using the following identity, valid in cartesian coordinates in any number of dimensions d:

$$\int d^dx\,x_nx_mx_px_qf(x^2) = \frac{(\delta_{nm}\delta_{pq}+\delta_{np}\delta_{mq}+\delta_{nq}\delta_{mp})}{d(d+2)}\int d^dx\,x^4f(x^2)\,, \quad x^2 = \sum_{k=1}^d x_kx_k\,, \tag{A.11}$$

from which it immediately follows, taking $d = 2N+1$,

$$\int d\Omega_{2N+1}\hat{c}_n\hat{c}_m\hat{c}_p\hat{c}_q = \frac{(\delta_{nm}\delta_{pq}+\delta_{np}\delta_{mq}+\delta_{nq}\delta_{mp})}{(2N+1)(2N+3)}\Omega_{2N+1} = \frac{\pi^{N+\frac{1}{2}}}{2\Gamma(N+\frac{5}{2})}(\delta_{nm}\delta_{pq}+\delta_{np}\delta_{mq}+\delta_{nq}\delta_{mp}). \tag{A.12}$$

The integral over $d\tau$ is straightforward and after a bit of algebra we get

$$\int d\Omega_{2N+1}\xi = \frac{3\beta}{2}\frac{\pi^{N+\frac{1}{2}}}{\Gamma(N+\frac{5}{2})}(\mathcal{G}^{(N)})^2\,, \quad \mathcal{G}^{(N)} \equiv \frac{1}{\beta}\sum_{k=-N}^{N}\frac{1}{\mu_k}\,. \tag{A.13}$$

Plugging eq. (A.13) in eq. (A.10) gives

$$\begin{aligned}\mathcal{B}^{(N)}_{-1/2}\mathcal{Z}(\lambda t) &= \mathcal{Z}^{(N)}_0\Big(\frac{1}{\Gamma(1/2)} - \frac{3\beta}{4}\sqrt{\lambda t}\partial^N_{\lambda t}(\lambda t)^{N+1/2}\frac{N+3/2}{\Gamma(N+\frac{5}{2})}(\mathcal{G}^{(N)})^2 + \mathcal{O}(\lambda t)^2\Big)\\ &= \mathcal{Z}^{(N)}_0\Big(\frac{1}{\Gamma(1/2)} - \frac{3\beta}{4}(\mathcal{G}^{(N)})^2\frac{\lambda t}{\Gamma(3/2)} + \mathcal{O}(\lambda t)^2\Big)\,.\end{aligned} \tag{A.14}$$

In the continuum limit we have

$$\lim_{N\to\infty}\mathcal{B}^{(N)}_{-1/2}\mathcal{Z}(\lambda t) = \mathcal{Z}_0\Big(\frac{1}{\Gamma(1/2)} - \frac{3}{4}\beta\mathcal{G}^2\frac{\lambda t}{\Gamma(3/2)} + \mathcal{O}(\lambda t)^2\Big)\,, \tag{A.15}$$

where

$$\mathcal{G} = \frac{1}{2\omega}\coth\frac{\beta\omega}{2} \tag{A.16}$$

is the particle propagator at $\tau = 0$. After integrating over t, eq. (A.15) reproduces the first order perturbative correction to the partition function of the quartic anharmonic oscillator.

Finiteness of $\mathcal{B}^{(N)}_{-1/2}\mathcal{Z}$ as $N\to\infty$ to all orders is easily shown. For simplicity, we just keep track of the factors of N, neglecting all other parameters. At order $(\lambda t)^k$, after expanding the argument of the delta function, we get

$$\mathcal{B}^{(N)}_{-1/2}\mathcal{Z}(\lambda t)|_{\lambda^k} \propto \mathcal{Z}^{(N)}_0\frac{\sqrt{\lambda t}}{\pi^{N+\frac{1}{2}}}\partial^N_{\lambda t}(\lambda t)^{N+k-1/2}N^k\int d\Omega_{2N+1}\xi^k\,. \tag{A.17}$$

The $4k$-generalization of eq. (A.11) gives

$$\int d\Omega_{2N+1}\xi^k \propto \frac{1}{N^{2k}}\Omega_{2N+1}\,. \tag{A.18}$$

Plugging eq. (A.18) in eq. (A.17) and using eq. (A.6) gives

$$\lim_{N\to\infty}\mathcal{B}^{(N)}_{-1/2}\mathcal{Z}(\lambda t)|_{\lambda^k} \propto \lim_{N\to\infty}\mathcal{Z}^{(N)}_0\frac{(\lambda t)^k}{\pi^{N+\frac{1}{2}}}\frac{\Gamma(N+k+1/2)}{\Gamma(k+1/2)}\frac{\Omega_{2N+1}}{N^k} \propto \mathcal{Z}_0\frac{(\lambda t)^k}{\Gamma(k+\frac{1}{2})}\,. \tag{A.19}$$

Similarly, we can prove the finiteness of the continuum limit to all orders in perturbation theory for any other interaction term of the form $g\,x^{2p}$. Recall that the loopwise parameter λ corresponds to a coupling constant $g = \lambda^{p-1}$ and hence, for $p\neq 2$, the two are not identical. Taking that into account, the scaling in N of $\mathcal{B}^{(N)}_{-1/2}\mathcal{Z}$ at order g^k reads

$$\lim_{N\to\infty}\mathcal{B}^{(N)}_{-1/2}\mathcal{Z}(\lambda t)|_{g^k} \propto \lim_{N\to\infty}\mathcal{Z}^{(N)}_0\frac{\sqrt{\lambda t}}{\pi^{N+\frac{1}{2}}}\partial^N_{\lambda t}(\lambda t)^{N+(p-1)k-\frac{1}{2}}N^k\frac{\Omega_{2N+1}}{N^{pk}} \propto \frac{g^k t^{k(p-1)}}{\Gamma\left[(p-1)k+\frac{1}{2}\right]}\,, \tag{A.20}$$

and is finite. q.e.d.

Finiteness of $\mathcal{B}^{(N)}_{-1/2}\mathcal{Z}$ to all orders in perturbation theory for any polynomial potential term easily follows from the above results.

Appendix B

Perturbative Coefficients of the 2d ϕ^4 Theory

B.1 The Symmetric Phase

We report here the coefficients for the series expansion of the 2 and 4 point functions obtained by integration of the Feynman diagrams as explained in Section 5.4. In Table B.1 (above), we list the coefficients $b_k^{(n)}$ of the nth-derivative of the 2-point function $\widetilde{\Gamma}_2^{(n)}$ at momentum $p^2 = -m^2$ that are relevant for the determination of the pole mass M up to g^8 order. Plugging the perturbative expansions of the derivatives $\widetilde{\Gamma}_2^{(n)}(-m^2)$ in eq. (5.34) and solving the equation order by order in g we get the series for M^2 as reported in eq. (5.37). In Table B.1 (middle) we list the coefficients for the two point function in configuration space $\langle\phi(x)\phi(0)\rangle$ up to order g^6 for some selected values of x. These coefficients have been used in subsection 5.5.3 to determine the critical exponent η. We consider values of x within the range $0.005 \leq x \leq 0.5$. The upper limit $x \leq 0.5$ is given by imposing $M(\Delta g)x \ll 1$, where Δg is the uncertainty in the determination of the critical coupling g_c. This condition is necessary for the residual exponential factor $\exp(-M(\Delta g)x)$ not to spoil the determination of η. The lower limit $x \geq 0.005$ is instead determined by the numerical accuracy we reach for the coefficients and the requirement that the coefficients must be statistically different between each other: this sets a lower bound on the possible Δx between two points which is numerically determined as $\Delta x \gtrsim 0.005$. In Table B.1 (below) we list the coefficients for the 2-point function $\widetilde{\Gamma}_2(p^2 = 0)$, its derivative $\partial_{p^2}\widetilde{\Gamma}_2(p^2 = 0)$ and the four point function $\widetilde{\Gamma}_4(\{p_i = 0\})$ that are needed in the determination of the series for $\beta(g_R)$ and $\eta(g_R)$ as reported in eq. (5.58).

B.2 The Broken Symmetry Phase

We report in Table B.2 the coefficients for the series expansions of $\langle\phi\rangle$, $\widetilde{\Lambda}$ and $\widetilde{M}$ for independent values of the couplings λ_3 (corresponding to the cubic coupling) and λ (corresponding to the quartic coupling), following the notation of eq. (5.60). We computed all the relevant Feynman diagrams containing up to 8 total vertices. By setting $\lambda_3 = \sqrt{2\lambda}\widetilde{m}$ and consistently truncating the series one recovers the series expansion reported in Section 5.7.

k	$b_k^{(0)}$	$b_k^{(1)}$	$b_k^{(2)}$	$b_k^{(3)}$
2	$-3/2$	0.0809453264	-0.0128046736	0.0035065405
3	$\frac{9}{\pi}+\frac{63\zeta(3)}{2\pi^3}$	$-0.341795194(75)$	0.079771437(20)	
4	$-14.777287(22)$	1.8559406(86)	$-0.5258941(27)$	
5	66.81651(43)	$-10.83118(19)$		
6	$-353.2405(28)$	68.3310(29)		
7	2111.715(36)			
8	$-13994.24(54)$			

$\lvert x\rvert$	g^2	g^3	g^4	g^5	g^6
0.005	0.10176449(22)	$-0.2637639(86)$	0.948600(25)	$-4.06456(43)$	20.0963(51)
0.010	0.10175903(21)	$-0.2637468(84)$	0.948552(29)	$-4.06308(71)$	20.1215(38)
0.020	0.10173618(21)	$-0.2636508(84)$	0.948322(26)	$-4.06241(72)$	20.0948(49)
0.050	0.10157963(21)	$-0.2631310(29)$	0.946740(29)	$-4.05581(70)$	20.0892(40)
0.100	0.10104318(21)	$-0.2615325(29)$	0.942048(29)	$-4.03942(76)$	20.0100(39)
0.200	0.09908619(21)	$-0.2562453(29)$	0.926197(25)	$-3.98035(64)$	19.7198(38)
0.300	0.09620711(21)	$-0.2488461(28)$	0.903417(23)	$-3.88874(53)$	19.3021(38)
0.500	0.08868032(20)	$-0.2299485(26)$	0.843591(23)	$-3.64994(65)$	18.1834(37)

order	$\widetilde{\Gamma}_2(p^2=0)$	$\partial_{p^2}\widetilde{\Gamma}_2(p^2=0)$	$\widetilde{\Gamma}_4(\{p_i=0\})$
0	1	1	0
1	0	0	24
2	$-\frac{12}{\pi^{3/2}}G^{3,2}_{3,3}\left(4\middle\vert \begin{matrix}0,0,\frac{1}{2}\\0,0,0\end{matrix}\right)$	$\frac{12}{\pi^{3/2}}G^{3,2}_{3,3}\left(4\middle\vert \begin{matrix}-1,-1,\frac{1}{2}\\0,0,0\end{matrix}\right)$	$-216/\pi$
3	3.7798975113	-0.27412237255	270.8452888
4	$-13.1529123(81)$	1.4204875(19)	$-1403.66817(58)$
5	57.50923(15)	$-7.983133(18)$	8341.758(61)
6	$-295.3633(20)$	48.89365(40)	$-54808.87(32)$
7	1723.533(29)	$-324.0971(70)$	392070.3(6.4)
8	$-11200.30(46)$	2312.97(19)	$-3.02573(45)\cdot 10^6$

Table B.1: (Above) Values of the coefficients $b_k^{(n)}$ for the series expansion of the nth-derivative of the two-point function $\widetilde{\Gamma}_2^{(n)}(-m^2)$ as defined in (5.36). These coefficients are the ones needed to get the series of the physical mass M^2 up to $\mathcal{O}(g^8)$ reported in eq. (5.37). The coefficients $b_2^{(1)}$, $b_2^{(2)}$, $b_2^{(3)}$ are determined numerically with arbitrary precision. (Middle) Series coefficients for the two point function $\langle\phi(x)\phi(0)\rangle$ up to order g^6 for some selected values of x. We omit here the tree level term–given by $G_0(x)$ defined in eq. (5.27)–and the $\mathcal{O}(g)$ term which is identically zero in the chosen scheme. (Below) Series coefficients for the two point function $\widetilde{\Gamma}_2$, its derivative $\partial_{p^2}\widetilde{\Gamma}_2$ and the four point function $\widetilde{\Gamma}_4$ at vanishing external momenta. At order 2 the coefficients of $\widetilde{\Gamma}_2$ and $\partial_{p^2}\widetilde{\Gamma}_2$ are expressed in terms of Meijer G-functions. At order 3 the coefficients are determined numerically with arbitrary precision.

$\langle\phi\rangle$	${\lambda_3}^1$	${\lambda_3}^3$	${\lambda_3}^5$	${\lambda_3}^7$
λ^0	0	−0.267173395(10)	−1.0631775(38)	−5.77322(83)
λ^1	$-\frac{3}{\pi^{3/2}}G^{3,2}_{3,3}\left(4\middle\vert \begin{matrix}0,0,\frac{1}{2}\\0,0,0\end{matrix}\right)$	2.3297864(28)	18.72732(33)	165.1097(38)
λ^2	−0.94497557(60)	−17.077459(80)	−235.4280(47)	
λ^3	3.795830(20)	123.0864(36)	2657.933(60)	
λ^4	−17.07032(12)	−916.534(44)		
λ^5	87.5081(29)	7168(13)		
λ^6	−501.799(48)			
λ^7	3182.8(3.6)			

$\widetilde{\Lambda}$	${\lambda_3}^0$	${\lambda_3}^2$	${\lambda_3}^4$	${\lambda_3}^6$	${\lambda_3}^8$
λ^0	0	$-\frac{3}{4\pi^{3/2}}G^{3,2}_{3,3}\left(4\middle\vert \begin{matrix}0,0,\frac{1}{2}\\0,0,0\end{matrix}\right)$	−0.037804619(13)	−0.14168986(85)	−0.7158909(36)
λ^1	0	0.079959370431	0.45728168(71)	3.0522(15)	
λ^2	-21$\zeta(3)/16\pi^3$	−0.37556393(34)	−4.103721(35)	−44.760(19)	
λ^3	27$\zeta(3)/8\pi^4$	1.7780406(30)	34.6608(25)		
λ^4	−0.116125964(91)	−9.413933(23)	−294.714(45)		
λ^5	0.3949534(18)	55.2353(57)			
λ^6	−1.629794(22)	−356.38(36)			
λ^7	7.85404(21)				
λ^8	−43.192(21)				

$\widetilde{M}$	${\lambda_3}^0$	${\lambda_3}^2$	${\lambda_3}^4$	${\lambda_3}^6$	${\lambda_3}^8$
λ^0	1	$-\sqrt{3}$	−6.01625(46)	−34.27524(61)	−259.922(52)
λ^1	0	10.70608065292	94.2044(74)	971.527(46)	
λ^2	−3/2	−60.79409(78)	−1099.716(99)	−17928(60)	
λ^3	$\frac{9}{\pi}+\frac{63\zeta(3)}{2\pi^3}$	374.676(23)	11671.1(1.4)		
λ^4	−14.655869(22)	−2493.24(11)	$-1.2079(11)\cdot 10^5$		
λ^5	65.97308(43)	17832.1(2.5)			
λ^6	−347.8881(28)	$-1.3632(15)\cdot 10^5$			
λ^7	2077.703(36)				
λ^8	−13771.04(54)				

Table B.2: Perturbative coefficients for $\langle\phi\rangle$ (above), $\widetilde{\Lambda}$ (middle) and $\widetilde{M}$ (below) with independent cubic and quartic coupling λ_3 and λ up to eight total vertices. The symmetric double-well case of eq. (5.60) is recovered for $\lambda_3=\sqrt{2\lambda}\widetilde{m}$ and by consistently truncating the series. In order to avoid clutter we fixed $\widetilde{m}=1$. The coefficients at order $\lambda{\lambda_3}^2$ for $\widetilde{\Lambda}$ and $\widetilde{M}$ are determined numerically with arbitrary precision.

Bibliography

[1] M. Serone, G. Spada, and G. Villadoro, "Instantons from Perturbation Theory", *Phys. Rev.*, vol. D96, no. 2, p. 021 701, 2017. DOI: 10.1103/PhysRevD.96.021701. arXiv: 1612.04376 [hep-th].

[2] M. Serone, G. Spada, and G. Villadoro, "The Power of Perturbation Theory", *JHEP*, vol. 05, p. 056, 2017. DOI: 10.1007/JHEP05(2017)056. arXiv: 1702.04148 [hep-th].

[3] M. Serone, G. Spada, and G. Villadoro, "$\lambda\phi^4$ Theory I: The Symmetric Phase Beyond NNNNNNNNLO", *JHEP*, vol. 08, p. 148, 2018. DOI: 10.1007/JHEP08(2018)148. arXiv: 1805.05882 [hep-th].

[4] M. Serone, G. Spada, and G. Villadoro, in preparation.

[5] F. J. Dyson, "Divergence of perturbation theory in quantum electrodynamics", *Phys. Rev.*, vol. 85, pp. 631–632, 1952. DOI: 10.1103/PhysRev.85.631.

[6] C. A. Hurst, "The Enumeration of Graphs in the Feynman-Dyson Technique", *Proc. Roy. Soc. Lond.*, vol. A214, p. 44, 1952. DOI: 10.1098/rspa.1952.0149.

[7] C. M. Bender and T. T. Wu, "Statistical Analysis of Feynman Diagrams", *Phys. Rev. Lett.*, vol. 37, pp. 117–120, 1976. DOI: 10.1103/PhysRevLett.37.117.

[8] L. N. Lipatov, "Divergence of the Perturbation Theory Series and the Quasiclassical Theory", *Sov. Phys. JETP*, vol. 45, pp. 216–223, 1977, [Zh. Eksp. Teor. Fiz.72,411(1977)].

[9] J. Zinn-Justin, "Perturbation Series at Large Orders in Quantum Mechanics and Field Theories: Application to the Problem of Resummation", *Phys. Rept.*, vol. 70, p. 109, 1981. DOI: 10.1016/0370-1573(81)90016-8.

[10] C. M. Bender and T. T. Wu, "Anharmonic oscillator. 2: A Study of perturbation theory in large order", *Phys. Rev.*, vol. D7, pp. 1620–1636, 1973. DOI: 10.1103/PhysRevD.7.1620.

[11] M. Marino, R. Schiappa, and M. Weiss, "Nonperturbative Effects and the Large-Order Behavior of Matrix Models and Topological Strings", *Commun. Num. Theor. Phys.*, vol. 2, pp. 349–419, 2008. DOI: 10.4310/CNTP.2008.v2.n2.a3. arXiv: 0711.1954 [hep-th].

[12] S. Pasquetti and R. Schiappa, "Borel and Stokes Nonperturbative Phenomena in Topological String Theory and c=1 Matrix Models", *Annales Henri Poincare*, vol. 11, pp. 351–431, 2010. DOI: 10.1007/s00023-010-0044-5. arXiv: 0907.4082 [hep-th].

[13] M. Marino, "Open string amplitudes and large order behavior in topological string theory", *JHEP*, vol. 03, p. 060, 2008. DOI: 10.1088/1126-6708/2008/03/060. arXiv: hep-th/0612127 [hep-th].

[14] J. J. Loeffel, A. Martin, B. Simon, and A. S. Wightman, "Pade approximants and the anharmonic oscillator", *Phys. Lett.*, vol. 30B, pp. 656–658, 1969. DOI: 10.1016/0370-2693(69)90087-2.

[15] B. Simon and A. Dicke, "Coupling constant analyticity for the anharmonic oscillator", *Annals Phys.*, vol. 58, pp. 76–136, 1970. DOI: 10.1016/0003-4916(70)90240-X.

[16] J.-P. Eckmann, J. Magnen, and R. Sénéor, "Decay properties and Borel summability for the Schwinger functions in $P(\Phi)_2$ theories", *Communications in Mathematical Physics*, vol. 39, no. 4, pp. 251–271, 1975. DOI: 10.1007/BF01705374.

[17] J. Magnen and R. Sénéor, "Phase Space Cell Expansion and Borel Summability for the Euclidean ϕ^4 in Three-Dimensions Theory", *Communications in Mathematical Physics*, vol. 56, no. 3, pp. 237–276, 1977.

[18] J. Ecalle, *Les fonctions résurgentes: Les algèbres de fonctions résurgentes*, ser. Les fonctions résurgentes: Université de Paris-Sud, Département de Mathématique, Bât. 425, 1981.

[19] M. Mariño, "Lectures on non-perturbative effects in large N gauge theories, matrix models and strings", *Fortsch. Phys.*, vol. 62, pp. 455–540, 2014. DOI: 10.1002/prop.201400005. arXiv: 1206.6272 [hep-th].

[20] D. Dorigoni, "An Introduction to Resurgence, Trans-Series and Alien Calculus", 2014. arXiv: 1411.3585 [hep-th].

[21] I. Aniceto, G. Basar, and R. Schiappa, "A Primer on Resurgent Transseries and Their Asymptotics", 2018. arXiv: 1802.10441 [hep-th].

[22] E. Brezin, J. C. Le Guillou, and J. Zinn-Justin, "Perturbation Theory at Large Order. 1. The φ^{2N} Interaction", *Phys. Rev.*, vol. D15, pp. 1544–1557, 1977. DOI: 10.1103/PhysRevD.15.1544.

[23] E. Brezin, J. C. Le Guillou, and J. Zinn-Justin, "Perturbation Theory at Large Order. 2. Role of the Vacuum Instability", *Phys. Rev.*, vol. D15, pp. 1558–1564, 1977. DOI: 10.1103/PhysRevD.15.1558.

[24] E. Brezin, G. Parisi, and J. Zinn-Justin, "Perturbation Theory at Large Orders for Potential with Degenerate Minima", *Phys. Rev.*, vol. D16, pp. 408–412, 1977. DOI: 10.1103/PhysRevD.16.408.

[25] E. Witten, "Analytic Continuation Of Chern-Simons Theory", *AMS/IP Stud. Adv. Math.*, vol. 50, pp. 347–446, 2011. arXiv: 1001.2933 [hep-th].

[26] E. Witten, "A New Look At The Path Integral Of Quantum Mechanics", 2010. arXiv: 1009.6032 [hep-th].

[27] D. Harlow, J. Maltz, and E. Witten, "Analytic Continuation of Liouville Theory", *JHEP*, vol. 12, p. 071, 2011. DOI: 10.1007/JHEP12(2011)071. arXiv: 1108.4417 [hep-th].

[28] Y. Tanizaki and T. Koike, "Real-time Feynman path integral with Picard–Lefschetz theory and its applications to quantum tunneling", *Annals Phys.*, vol. 351, pp. 250–274, 2014. DOI: 10.1016/j.aop.2014.09.003. arXiv: 1406.2386 [math-ph].

[29] G. Hardy, *Divergent Series*. Oxford University Press, 1949, ISBN: 0198533098.

[30] A. D. Sokal, "An improvement of watson's theorem on borel summability", *Journal of Mathematical Physics*, vol. 21, no. 2, pp. 261–263, 1980. DOI: 10.1063/1.524408.

[31] S. Graffi, V. Grecchi, and B. Simon, "Borel summability: Application to the anharmonic oscillator", *Phys. Lett.*, vol. 32B, pp. 631–634, 1970. DOI: 10.1016/0370-2693(70)90564-2.

[32] G. A. Baker, B. G. Nickel, M. S. Green, and D. I. Meiron, "Ising Model Critical Indices in Three-Dimensions from the Callan-Symanzik Equation", *Phys. Rev. Lett.*, vol. 36, pp. 1351–1354, 1976. DOI: 10.1103/PhysRevLett.36.1351.

[33] G. A. Baker Jr., B. G. Nickel, and D. I. Meiron, "Critical Indices from Perturbation Analysis of the Callan-Symanzik Equation", *Phys. Rev.*, vol. B17, pp. 1365–1374, 1978. DOI: 10.1103/PhysRevB.17.1365.

[34] J. J. Loeffel, Centre d'Etudes Nucléaires de Saclay, report Saclay DPhT/76-20, unpublished.

[35] J. C. Le Guillou and J. Zinn-Justin, "Critical Exponents from Field Theory", *Phys. Rev.*, vol. B21, pp. 3976–3998, 1980. DOI: 10.1103/PhysRevB.21.3976.

[36] G. Baker, *Essentials of Padé Approximants*. Elsevier Science, 1975, ISBN: 9780323156158.

[37] M. V. Berry and C. Howls, "Hyperasymptotics for integrals with saddles", *Proc. R. Soc. Lond. A*, vol. 434, no. 1892, pp. 657–675, 1991.

[38] C. Howls, "Hyperasymptotics for multidimensional integrals, exact remainder terms and the global connection problem", in *Proceedings of the Royal Society of London A: Mathematical, Physical and Engineering Sciences*, The Royal Society, vol. 453, 1997, pp. 2271–2294.

[39] A. I. Vainshtein, "Decaying systems and divergence of the series of perturbation theory", in *Continuous advances in QCD. Proceedings, Conference, Minneapolis, USA, May 17-23, 2002*, 1964, pp. 617–646.

[40] S. Gukov, M. Marino, and P. Putrov, "Resurgence in complex Chern-Simons theory", 2016. arXiv: 1605.07615 [hep-th].

[41] G. 't Hooft, "Can We Make Sense Out of Quantum Chromodynamics?", in *15th Erice School of Subnuclear Physics: The Why's of Subnuclear Physics Erice, Italy, July 23-August 10, 1977*, vol. 15, 1979, p. 943.

[42] J. Milnor, *Morse theory*, ser. Based on lecture notes by M. Spivak and R. Wells. Annals of Mathematics Studies, No. 51. Princeton, N.J.: Princeton University Press, 1963, pp. vi+153, ISBN: 0-691-08008-9.

[43] W. R. Inc., *Mathematica, Version 11.3*, Champaign, IL, 2018.

[44] T. Sulejmanpasic and M. Ünsal, "Aspects of perturbation theory in quantum mechanics: The BenderWu Mathematica package", *Comput. Phys. Commun.*, vol. 228, pp. 273–289, 2018. DOI: 10.1016/j.cpc.2017.11.018. arXiv: 1608.08256 [hep-th].

[45] C. M. Bender and T. T. Wu, "Large order behavior of Perturbation theory", *Phys. Rev. Lett.*, vol. 27, p. 461, 1971. DOI: 10.1103/PhysRevLett.27.461.

[46] P. Vieira, *Mathematica summer school on theoretical physics*, http://msstp.org, 2015.

[47] U. D. Jentschura and J. Zinn-Justin, "Higher order corrections to instantons", *J. Phys.*, vol. A34, pp. L253–L258, 2001. DOI: 10.1088/0305-4470/34/18/101. arXiv: math-ph/0103010 [math-ph].

[48] E. Witten, "Dynamical Breaking of Supersymmetry", *Nucl. Phys.*, vol. B188, p. 513, 1981. DOI: 10.1016/0550-3213(81)90006-7.

[49] I. I. Balitsky and A. V. Yung, "Instanton Molecular Vacuum in $N = 1$ Supersymmetric Quantum Mechanics", *Nucl. Phys.*, vol. B274, p. 475, 1986. DOI: 10.1016/0550-3213(86)90295-6.

[50] A. Behtash, G. V. Dunne, T. Schäfer, T. Sulejmanpasic, and M. Ünsal, "Complexified path integrals, exact saddles and supersymmetry", *Phys. Rev. Lett.*, vol. 116, no. 1, p. 011 601, 2016. DOI: 10.1103/PhysRevLett.116.011601. arXiv: 1510.00978 [hep-th].

[51] U. D. Jentschura and J. Zinn-Justin, "Instantons in quantum mechanics and resurgent expansions", *Phys. Lett.*, vol. B596, pp. 138–144, 2004. DOI: 10.1016/j.physletb.2004.06.077. arXiv: hep-ph/0405279 [hep-ph].

[52] J. Zinn-Justin, "Instantons in Quantum Mechanics: Numerical Evidence for a Conjecture", *J. Math. Phys.*, vol. 25, p. 549, 1984. DOI: 10.1063/1.526205.

[53] H. Taşeli, "Accurate computation of the energy spectrum for potentials with multiminima", *International journal of quantum chemistry*, vol. 46, no. 2, pp. 319–333, 1993.

[54] P. Dorey and R. Tateo, "Anharmonic oscillators, the thermodynamic Bethe ansatz, and nonlinear integral equations", *J. Phys.*, vol. A32, pp. L419–L425, 1999. DOI: 10.1088/0305-4470/32/38/102. arXiv: hep-th/9812211 [hep-th].

[55] R. Balian, G. Parisi, and A. Voros, "Discrepancies from asymptotic series and their relation to complex classical trajectories", *Physical Review Letters*, vol. 41, no. 17, p. 1141, 1978.

[56] A. Grassi, M. Marino, and S. Zakany, "Resumming the string perturbation series", *JHEP*, vol. 05, p. 038, 2015. DOI: 10.1007/JHEP05(2015)038. arXiv: 1405.4214 [hep-th].

[57] S.-J. Chang, "The Existence of a Second Order Phase Transition in the Two-Dimensional φ^4 Field Theory", *Phys. Rev.*, vol. D13, p. 2778, 1976, [Erratum: Phys. Rev.D16,1979(1977)]. DOI: 10.1103/PhysRevD.13.2778.

[58] B. Simon and R. B. Griffiths, "The $(\varphi_2)^4$ field theory as a classical ising model", *Commun. Math. Phys.*, vol. 33, pp. 145–164, 1973. DOI: 10.1007/BF01645626.

[59] G. H. Derrick, "Comments on nonlinear wave equations as models for elementary particles", *J. Math. Phys.*, vol. 5, pp. 1252–1254, 1964. DOI: 10.1063/1.1704233.

[60] J. Glimm and A. Jaffe, *Quantum physics: a functional integral point of view*. Springer Science & Business Media, 2012.

[61] J. Glimm, A. M. Jaffe, and T. Spencer, "Phase Transitions for phi**4 in Two-Dimensions Quantum Fields", *Commun. Math. Phys.*, vol. 45, p. 203, 1975. DOI: 10.1007/BF01608328.

[62] S. Weinberg, *The quantum theory of fields*. Cambridge university press, 1995, vol. 2.

[63] S. Rychkov and L. G. Vitale, "Hamiltonian truncation study of the ϕ^4 theory in two dimensions. II. The $\mathbb{Z}_2$ -broken phase and the Chang duality", *Phys. Rev.*, vol. D93, no. 6, p. 065 014, 2016. DOI: 10.1103/PhysRevD.93.065014. arXiv: 1512.00493 [hep-th].

[64] W. Loinaz and R. S. Willey, "Monte Carlo simulation calculation of critical coupling constant for continuum ϕ^4 in two-dimensions", *Phys. Rev.*, vol. D58, p. 076 003, 1998. DOI: 10.1103/PhysRevD.58.076003. arXiv: hep-lat/9712008 [hep-lat].

[65] D. Schaich and W. Loinaz, "An Improved lattice measurement of the critical coupling in ϕ^4_2 theory", *Phys. Rev.*, vol. D79, p. 056 008, 2009. DOI: 10.1103/PhysRevD.79.056008. arXiv: 0902.0045 [hep-lat].

[66] P. Bosetti, B. De Palma, and M. Guagnelli, "Monte Carlo determination of the critical coupling in ϕ_2^4 theory", *Phys. Rev.*, vol. D92, no. 3, p. 034 509, 2015. DOI: 10.1103/PhysRevD.92.034509. arXiv: 1506.08587 [hep-lat].

[67] A. Harindranath and J. P. Vary, "Solving two-dimensional φ^4 theory by discretized light-front quantization", *Phys. Rev.*, vol. D36, pp. 1141–1147, 1987. DOI: 10.1103/PhysRevD.36.1141.

[68] T. Sugihara, "Density matrix renormalization group in a two-dimensional $\lambda\phi^4$ Hamiltonian lattice model", *JHEP*, vol. 05, p. 007, 2004. DOI: 10.1088/1126-6708/2004/05/007. arXiv: hep-lat/0403008 [hep-lat].

[69] A. Milsted, J. Haegeman, and T. J. Osborne, "Matrix product states and variational methods applied to critical quantum field theory", *Phys. Rev.*, vol. D88, p. 085 030, 2013. DOI: 10.1103/PhysRevD.88.085030. arXiv: 1302.5582 [hep-lat].

[70] D. Lee, N. Salwen, and D. Lee, "The Diagonalization of quantum field Hamiltonians", *Phys. Lett.*, vol. B503, pp. 223–235, 2001. DOI: 10.1016/S0370-2693(01)00197-6. arXiv: hep-th/0002251 [hep-th].

[71] D. Lee, N. Salwen, and M. Windoloski, "Introduction to stochastic error correction methods", *Phys. Lett.*, vol. B502, pp. 329–337, 2001. DOI: 10.1016/S0370-2693(01)00198-8. arXiv: hep-lat/0010039 [hep-lat].

[72] S. Rychkov and L. G. Vitale, "Hamiltonian truncation study of the ϕ^4 theory in two dimensions", *Phys. Rev.*, vol. D91, p. 085 011, 2015. DOI: 10.1103/PhysRevD.91.085011. arXiv: 1412.3460 [hep-th].

[73] M. V. Kompaniets and E. Panzer, "Minimally subtracted six loop renormalization of $O(n)$-symmetric ϕ^4 theory and critical exponents", *Phys. Rev.*, vol. D96, no. 3, p. 036 016, 2017. DOI: 10.1103/PhysRevD.96.036016. arXiv: 1705.06483 [hep-th].

[74] D. I. Kazakov, D. V. Shirkov, and O. V. Tarasov, "Analytical Continuation of Perturbative Results of the $g\phi^4$ Model Into the Region g Is Greater Than or Equal to 1", *Theor. Math. Phys.*, vol. 38, pp. 9–16, 1979, [Teor. Mat. Fiz.38,15(1979)]. DOI: 10.1007/BF01030252.

[75] H. Kleinert, A. Pelster, B. M. Kastening, and M. Bachmann, "Recursive graphical construction of Feynman diagrams and their multiplicities in φ^4 theory and in $\varphi^2 A$ theory", *Phys. Rev.*, vol. E62, pp. 1537–1559, 2000. DOI: 10.1103/PhysRevE.62.1537. arXiv: hep-th/9907168 [hep-th].

[76] G. P. Lepage, "A New Algorithm for Adaptive Multidimensional Integration", *J. Comput. Phys.*, vol. 27, p. 192, 1978. DOI: 10.1016/0021-9991(78)90004-9.

[77] E. Brezin and G. Parisi, "Critical exponents and large order behavior of perturbation theory", pp. 269–292, 1992.

[78] E. M. Malatesta, G. Parisi, and T. Rizzo, "Two-loop corrections to large order behavior of φ^4 theory", *Nucl. Phys.*, vol. B922, pp. 293–318, 2017. DOI: 10.1016/j.nuclphysb.2017.07.011. arXiv: 1704.04458 [cond-mat.stat-mech].

[79] L. Onsager, "Crystal statistics. 1. A Two-dimensional model with an order disorder transition", *Phys. Rev.*, vol. 65, pp. 117–149, 1944. DOI: 10.1103/PhysRev.65.117.

[80] J. Elias-Miro, S. Rychkov, and L. G. Vitale, "High-Precision Calculations in Strongly Coupled Quantum Field Theory with Next-to-Leading-Order Renormalized Hamiltonian Truncation", *JHEP*, vol. 10, p. 213, 2017. DOI: 10.1007/JHEP10(2017)213. arXiv: 1706.06121 [hep-th].

[81] M. Burkardt, S. S. Chabysheva, and J. R. Hiller, "Two-dimensional light-front ϕ^4 theory in a symmetric polynomial basis", *Phys. Rev.*, vol. D94, no. 6, p. 065 006, 2016. DOI: 10.1103/PhysRevD.94.065006. arXiv: 1607.00026 [hep-th].

[82] N. Anand, V. X. Genest, E. Katz, Z. U. Khandker, and M. T. Walters, "RG flow from ϕ^4 theory to the 2D Ising model", *JHEP*, vol. 08, p. 056, 2017. DOI: 10.1007/JHEP08(2017)056. arXiv: 1704.04500 [hep-th].

[83] A. L. Fitzpatrick, J. Kaplan, E. Katz, L. G. Vitale, and M. T. Walters, "Lightcone Effective Hamiltonians and RG Flows", 2018. arXiv: 1803.10793 [hep-th].

[84] Z. Bajnok and M. Lajer, "Truncated Hilbert space approach to the 2d ϕ^4 theory", *JHEP*, vol. 10, p. 050, 2016. DOI: 10.1007/JHEP10(2016)050. arXiv: 1512.06901 [hep-th].

[85] J. Elias-Miro, S. Rychkov, and L. G. Vitale, "NLO Renormalization in the Hamiltonian Truncation", *Phys. Rev.*, vol. D96, no. 6, p. 065 024, 2017. DOI: 10.1103/PhysRevD.96.065024. arXiv: 1706.09929 [hep-th].

[86] A. Pelissetto and E. Vicari, "Critical mass renormalization in renormalized φ^4 theories in two and three dimensions", *Phys. Lett.*, vol. B751, pp. 532–534, 2015. DOI: 10.1016/j.physletb.2015.11.015. arXiv: 1508.00989 [hep-th].

[87] A. Pelissetto, P. Rossi, and E. Vicari, "Mean field expansion for spin models with medium range interactions", *Nucl. Phys.*, vol. B554, p. 552, 1999. DOI: 10.1016/S0550-3213(99)00311-9. arXiv: cond-mat/9903410 [cond-mat].

[88] K. G. Wilson and M. E. Fisher, "Critical exponents in 3.99 dimensions", *Phys. Rev. Lett.*, vol. 28, pp. 240–243, 1972. DOI: 10.1103/PhysRevLett.28.240.

[89] G. Parisi, "Field theoretic approach to second order phase transitions in two-dimensional and three-dimensional systems", pp. 7–40, 1993, [J. Stat. Phys.23,49(1980)]. DOI: 10.1007/BF01014429.

[90] J. Le Guillou and J. Zinn-Justin, "Accurate critical exponents from the ε-expansion", *Journal de Physique Lettres*, vol. 46, no. 4, pp. 137–141, 1985, reprinted in Le Guillou, J.C. (ed.), Zinn-Justin, J. (ed.): "Large-order behaviour of perturbation theory", 554-558.

[91] J. Zinn-Justin, *Quantum Field Theory and Critical Phenomena*, ser. International series of monographs on physics. Clarendon Press, 2002, ISBN: 9780198509233.

[92] E. V. Orlov and A. I. Sokolov, "Critical thermodynamics of the two-dimensional systems in five loop renormalization group approximation", *Submitted to: Sov. Phys. Solid State*, 2000. arXiv: hep-th/0003140 [hep-th].

[93] P. Calabrese, M. Caselle, A. Celi, A. Pelissetto, and E. Vicari, "Nonanalyticity of the Callan-Symanzik Beta function of two-dimensional O(N) models", *J. Phys.*, vol. A33, pp. 8155–8170, 2000. DOI: 10.1088/0305-4470/33/46/301. arXiv: hep-th/0005254 [hep-th].